AGARD

ADVISORY GROUP FOR AEROSPACE RESEARCH & DEVELOPMENT

7 RUE ANCELLE 92200 NEUILLY SUR SEINE FRANCE

AGARDograph No.303

Reynolds Number Effects in Transonic Flow

NORTH ATLANTIC TREATY ORGANIZATION

NORTH ATLANTIC TREATY ORGANIZATION

ADVISORY GROUP FOR AEROSPACE RESEARCH AND DEVELOPMENT

(ORGANISATION DU TRAITE DE L'ATLANTIQUE NORD)

AGARDograph No.303

REYNOLDS NUMBER EFFECTS IN TRANSONIC FLOW

by

A.Elsenaar
National Aerospace Laboratory NLR
Anthony Fokkerweg 2, 1059 CM Amsterdam
The Netherlands

T.W.Binion, Jr
Calspan Corporation/AEDC Operations
Arnold Air Force Base, TN 37389, USA

and

E.Stanewsky
Deutsche Forschungs- und Versuchsanstalt
für Luft- und Raumfahrt e.V.
Institut für Experimentelle Strömungsmechanik
D-3400 Göttingen, F.R. Germany

Edited by

H.G.Hornung
Graduate Aeronautical Laboratories
California Institute of Technology
Pasadena, CA 91125, USA

This AGARDograph has been produced at the request of the Fluid Dynamics Panel of AGARD.

THE MISSION OF AGARD

According to its Charter, the mission of AGARD is to bring together the leading personalities of the NATO nations in the fields of science and technology relating to aerospace for the following purposes:

- Recommending effective ways for the member nations to use their research and development capabilities for the common benefit of the NATO community;
- Providing scientific and technical advice and assistance to the Military Committee in the field of aerospace research and development (with particular regard to its military application);
- Continuously stimulating advances in the aerospace sciences relevant to strengthening the common defence posture;
- Improving the co-operation among member nations in aerospace research and development;
- Exchange of scientific and technical information;
- Providing assistance to member nations for the purpose of increasing their scientific and technical potential;
- Rendering scientific and technical assistance, as requested, to other NATO bodies and to member nations in connection with research and development problems in the aerospace field.

The highest authority within AGARD is the National Delegates Board consisting of officially appointed senior representatives from each member nation. The mission of AGARD is carried out through the Panels which are composed of experts appointed by the National Delegates, the Consultant and Exchange Programme and the Aerospace Applications Studies Programme. The results of AGARD work are reported to the member nations and the NATO Authorities through the AGARD series of publications of which this is one.

Participation in AGARD activities is by invitation only and is normally limited to citizens of the NATO nations.

Published December 1988

ISBN 92-835-0492-5

Printed by Specialised Printing Services Limited
40 Chigwell Lane, Loughton, Essex IG10 3TZ

PREFACE

Reynolds number effects in transonic flow are critically reviewed. In this review, the following geometries are considered: Airfoils and high aspect ratio wings typical of transport aircraft, fighter-type low aspect ratio delta wings, two- and three-dimensional bodies characteristic of missiles and combat aircraft fuselages, and afterbodies. Also discussed are "pseudo"-Reynolds number effects which may arise, for instance, due to the influence of the Reynolds number on the wind tunnel environment which may, in turn, affect the flow about a model. As an introduction to the AGARDograph, a brief retrospect of the "history" of Reynolds number effects is presented. There are two aspects closely related to viscous changes which are not discussed herein: the extrapolation of low Reynolds number wind tunnel results to flight conditions and fundamental Reynolds number effects, i.e., for instance, the influence of the Reynolds number on the boundary layer development and on basic viscous/inviscid interactions such as shock boundary layer interaction and trailing edge separation. Both topics are comprehensively treated in the report of the AGARD Working Group 09 "Boundary Layer Simulation and Control in Wind Tunnels" whose task it was to provide a methodology for transonic wind tunnel testing and the extrapolation of low Reynolds number wind tunnel results to flight conditions. The present AGARDograph, mainly concerned with a discussion of viscous effects actually observed on realistic configurations, can be considered a supplement to the report of AGARD WG 09.

Systematic study of Reynolds number (scale) effects, which obtained new impetus with the introduction of advanced transonic airfoils and wings, frequently revealed "anomalies" which could be traced to the wind tunnel environment and measuring techniques and their response to Reynolds number changes. These "anomalies", sometimes labelled "unit"-Reynolds number effects, are best described as "pseudo"-Reynolds number effects. Factors which have the potential of introducing pseudo-Reynolds number effects include: wall interference, tunnel Mach number calibration, noise, turbulence, humidity, non-uniform flow, flow contamination, side wall effects in two-dimensional tests, model deformation and transition fixing. True Reynolds number effects on transport-type airfoils and wings were found to be mainly related to two phenomena: transition point movement and the development of separation. Especially large variations in pressure distributions and corresponding force and moment coefficients were observed with varying Reynolds number when separation extended from the foot of the shock to the airfoil trailing edge and when the flow changed from a separated to an attached state as Reynolds number was increased (or vice versa). For conditions with attached or almost attached flow, Reynolds number effects appear to be smaller, though certainly not insignificant. Available data for low aspect ratio fighter-type configurations depicting Reynolds number effects are sparse. The data which are available, however, suggest for most of the flight regime of interest that Reynolds number effects are small.

The Reynolds number sensitivity of bodies is also strongly related to flow separation. Considering the classical body-related Reynolds number regimes — sub-critical, critical, supercritical and hypercritical — viscous effects are especially strong in the critical Reynolds number range, where large changes in the aerodynamic forces occur due to the sensitivity of transitional separation to viscous changes. The flow is not very sensitive to Reynolds number variations in the subcritical (laminar) and hypercritical (fully turbulent) Reynolds number domains in which separation is essentially fixed by pressure gradient. With increasing Mach number, the Reynolds number sensitivity also diminishes rapidly in the critical and supercritical domains due to the development of local supersonic regions with terminating shock waves strong enough to separate even the turbulent boundary layer. Significant changes in afterbody drag were consistently observed for subsonic Mach numbers above the transonic drag rise as result of the influence of viscous changes on the expansion around the shoulder of the afterbody and/or the pressure recovery downstream. The direction of the Reynolds number influence, i.e., increasing or decreasing boattail drag with Reynolds number, seems to be dependent on whether viscous changes predominantly alter the shoulder expansion or the pressure recovery, the latter being closely coupled with the development of separation over the rear of the afterbody.

* * *

Cette AGARDographie présente un examen des effets du nombre de Reynolds dans les écoulements transsoniques. Les géometries suivantes sont examinées: les profiles et les ailes à grande allongement caractéristiques des aéronefs de transport, les voilures en delta à faible allongement typiques des avions de chasse, les corps bi- et tri-dimensionnels caractéristiques des fuselages de missiles et d'aéronefs de combat, et les arrière-corps.

Les effets des "pseudo" nombres de Reynolds sont également examinés. Ces effets peuvent se produire, par exemple, en raison de l'influence du nombre de Reynolds sur le millieu ambiant de la soufflerie, ce qui risque, à son tour, de modifier les écoulements autour d'un modèle. Un bref résumé de "l'historique" des effets du nombre de Reynolds est présenté en préambule à l'AGARDographie.

Deux aspects étroitement liés aux changements de viscosité ne sont pas traités: il s'agit de l'extrapolation aux conditions de vol des résultats obtenus en soufflerie à des nombres de Reynolds peu élevés et des effets fondamentaux du nombre de Reynolds, c'est à dire, par exemple: l'influence du nombre de Reynolds sur ce développement de la couche limite et sur les interactions visqueuse/non visqueuse de base, telles que l'interaction choc/couche limite et le décollement au bord de fuite. Ces deux sujets sont traités de façon complète dans le rapport du groupe de travail 09, intitulé "La simulation et le contrôle de la couche limite en soufflerie" qui a pour objectif de fournir une méthodologie pour les essais en soufflerie transsonique et pour l'extrapolation au condition de vol des résultats obtenus en soufflerie, à des nombres de Reynolds peu élevés.

La présente AGARDographie, qui concerne principalement des effets visqueux examinés in-situ et produits par des configurations réelles, peut être considérée comme un supplément au rapport du groupe de travail AGARD 09.

L'étude systématique des effets du nombre de Reynolds (effets d'échelle qui a reçu une nouvelle impulsion avec l'arrivée de profils aérodynamiques et de voilures transsoniques avancées, a souvent révelé des "anomalies" parfois appelées des effets de nombre de Reynolds "unité" seraient mieux définies par le terme "effets de pseudo-nombre de Reynolds".

Les phénomènes susceptibles de créer des effets de pseudo-nombre de Reynolds sont les suivants: l'effet de paroi, l'étallonage du nombre de Mach de la soufflerie, le bruit, la turbulence, l'humidité, l'écoulement non-uniforme, la contamination de l'écoulement, les effets des parois latérales lors des essais bi-dimensionnels, les déformations de la maquette et le déclenchement de la transition.

Les effets des nombres de Reynolds réels sur les profils aérodynamiques et les voilures des aéronefs de transport, dépendent principalement de deux phénomènes: le déplacement du point de transition et le déclenchement de la séparation. Des écarts particulièrement importants de la répartition des pressions et des coéfficients de force et de moment ont été observés en fonction de la variation du nombre de Reynolds, lorsque le décollement s'étendait du pied du choc jusqu'au bord de fuite du profil aérodynamique et lorsqu'une écoulement détaché changeait d'état pour devenir un écoulement attaché au fur et à mesure de l'augmentation du nombre de Reynolds (ou vice-versa)

Dans le cas d'une écoulement attaché ou quasi-attaché, les effets du nombre de Reynolds semblent moins importants, sans être insignifiants pour autant.

Très peu de données sont disponibles concernant les configurations du type avion de chasse à faible allongement relatant les effets du nombre de Reynolds. Pourtant, les données existante indiquent que les effets du nombre de Reynolds sont peu marqués dans la majeur partie du régime de vol en question.

La réaction des corps au nombre de Reynolds est également étroitement liée au décollement. En considérant les régimes classiques du nombre de Reynolds associés au corps, soit, sous-critique, critique, surcritique et hypercritique, les effets visqueux sont particulièrement forts dans le domaine des nombres de Reynolds critiques, ou d'importantes transformations dans les forces aérodynamiques se produisent, en raison des effets du décollement en régime de transition provoqués par les changements de viscosité.

L'écoulement n'est que peu sensible à des variations du nombre de Reynolds dans les domaines Reynolds sous-critiques (laminaires) et hypercritiques (entièrement turbulents), ou le point de décollement est essentiellement regi par le gradient de pression. L'effet du nombre de Reynolds dans les domaines critiques et surcritiques diminue rapidement aussi, au fur et à mesure de l'augmentation du nombre de Mach, en raison de l'établissement de zones locales supersoniques, engendrant des ondes de choc terminales d'une puissance telle à provoquer même le décollement de la couche limite tourbillonnaire.

Des modifications non-negligeables de la trainée de l'arrière corps ont été observées de façon systématique, pour des nombres de Mach sub-soniques qui correspondent à l'accroissement de la trainée en régime transsonique, par suite de l'influence des changements de viscosité sur la détente de l'écoulement autour de l'épaulement de l'arrière corps et/ou la recupération de pression en aval. La direction de l'influence du nombre de Reynolds, c'est à dire, l'augmentation ou la diminution de la trainée de retreint en fonction du nombre de Reynolds, semble dépendre des changements de viscosité, qui modifient d'une maniére prédominante soit la détente de l'écoulement autour de l'épaulement, soit la récuperation de pression, cette dernière étant étroitement liée au développement du décollement sur la partie arrière de l'arrière corps.

CONTENTS

NOMENCLATURE

b	Wing span
$B_{1/2}$	Viscous flow parameter, see Ref. [79/1]
c, c_{av}	Average or mean aerodynamic chord
C_A	Axial-force coefficient
C, c, c_o	Aerodynamic chord
$\bar{C}_B$	Steady bending moment coefficient
C_B	*Unsteady bending moment coefficient*
C_D	Drag coefficient
$C_{D_{AP}}$	Afterbody pressure drag coefficient
C_{D_b}	Base drag coefficient
C_{D_i}	Induced drag coefficient
C_{D_o}	Zero lift drag coefficient
C_d	Section drag coefficient
CFF	Lockheed Compressible Flow Facility
$C_{d_{exp}}$	Experimental section drag coefficient
$C_{d_{FF}}$	Section drag coefficient based on form factor
C_f	Skin friction coefficient
C_L, CL	*Lift coefficient*
C_l, C_ℓ	Wing section lift coefficient
C_M, C_m	Pitching moment coefficient
C_n, C_N	Normal force coefficient
C_N'	Normal force coefficient based on fuselage plan area
C_{n_β}	Slope of normal force vs yaw angle curve
C_p^*	Pressure coefficient at local sonic velocity
C_p	Pressure coefficient
C_{p_b}	Base pressure coefficient
$C_{p_{te}}$, CPTE	Trailing edge pressure coefficient
C_Y	Side force coefficient
d	Porous wall hole diameter
D	Diameter of cylinder on body
f	Frequency
FF	Form factor
H, H	Shape factor
H_o	Total pressure
HST	NLR High Speed Tunnel
K_a	"Esch" factor
ℓ	Chord
ℓ_B	Shock induced separation bubble length
L	Lower, or length
L.E.	Leading edge
M	Mach number
M_a, M_o, M_∞	*Free stream Mach number*
M_D	Design Mach number
M_L, M_ℓ, M_{loc}	Local Mach number
M_{SH}	Mach number just upstream of shock
M_{∞_C}	Cross flow Mach number
p	Pressure
p_o, p_T	Total pressure
p_s'	Sound pressure
p_{cr}	Pressure coefficient at sonic velocity
q, q_∞	Free-stream dynamic pressure
R, Re, R_N	Reynolds number
R_D, Re_D	Reynolds number based on body diameter
Re_c, Re_c	Reynolds number based on chord

Re_{CN}	Reynolds number based on tunnel contraction and nozzle surface length
Re_{eff}	Effective Reynolds number, $ReD \cdot K_e$
Re_L	Reynolds number based on body length
Re_T	Reynolds number at the beginning of boundary-layer transition
$Re_{T_{aw}}$	Transition Reynolds number with adiabatic wall
Re/ℓ	Unit Reynolds number, ft^{-1}
Re_{δ^*}	Reynolds number based on displacement thickness
$Re_{\delta^*_o}$	Reynolds number based on displacement thickness at the beginning of the test section
Re_θ	Reynolds number based on momentum thickness
Re_{θ_a}	Reynolds number based on momentum thickness just upstream of shock
R_w	Reynolds number based on body width
R_{w_T}	Roughness height or corner radius of non-circular cylinder
S	Surface distance
S/C	Ratio of model reference area to tunnel cross-section area
S_T	Strouhal number
STN	Station
T.E.	Trailing edge
T_{aw}	Adiabatic wall temperature
T_T	Total temperature
T_w	Wall temperature
t	Thickness
u_e	Velocity at the edge of the boundary layer
U	Upper
u'	Fluctuating component of axial velocity
u_e	Boundary layer edge velocity
V	Velocity
X,x	Axial distance
X_T, X/C_{tr}	Transition location
XCSH, X/c_{SH}	Shock location in terms of chord
y	Spanwise coordinate
α	Angle of attack
α_{div}	Incidence angle for divergence of trailing edge pressure
α_f	Fuselage angle of attack
β	Compressibility factor
γ	Ratio of specific heats
Λ	Sweep angle
λ	Ratio of test section height to width
δ^*	Displacement thickness
δ_o	Lift interference factor
η	Semi-span ratio
θ_a	Momentum thickness just upstream of shock
θ	Momentum thickness
θ_s	Azimuth angle at separation
σ	Specific humidity
τ	Wall porosity or skin friction
ϕ	Flow angle at porous wall on roll angle

1. INTRODUCTION

by
A. Elsenaar
National Aerospace Laboratory NLR
Anthony Fokkerweg 2, 1059 CM Amsterdam
The Netherlands

1.1 Historical review

It is of considerable interest to examine the lines of thought with respect to Reynolds number effects in the past. This review, however, is not intended to be a complete coverage, the main intention being to highlight some of the more important events and related publications that increased the understanding or have changed the attitude of the scientific community towards what is called quite generally "Reynolds number effects". In this AGARDograph the discussion of Reynolds number effects is restricted to transonic flows. Thus, one should look for the earliest evidence at the end of the second world war when transonic flight became a topic of systematic scientific study.

Indeed, in the early fifties almost simultaneously a NACA [Ref. 52/2] and a RAE [Ref. 51/1] report were published that dealt with Reynolds number effects on swept wing configurations. Both studies had been initiated to investigate the cause of previously observed Reynolds number effects on lift and pitching moment of balance mounted models. These studies indicated, on the evidence of measured pressure distributions, that the region of shock-wave boundary layer interaction decreased with increasing Reynolds number. In the NACA report it was argued that the typical lambda shock pattern for laminar shock-wave boundary layer interaction as observed at a Reynolds number of 2 x 10**6 disappeared at a Reynolds number of 4 - 6 x 10**6 due to turbulent boundary layer flow. This was less clear in the RAE tests in which laminar boundary layer flow was still observed at the highest Reynolds number of 3.5 x 10**6. However, at that condition the size of the shock interaction region was much smaller as compared with the Re = 0.8 x 10**6 results (see fig. 1-1a). The resulting change in the pressure distribution significantly affected the section lift and pitching moment which was further amplified in the wing pitching moment due to the swept wing configuration. The prevailing thought at that time was that, since a laminar boundary was very susceptible to (pressure or shock induced) separation, the turbulent boundary layer development at higher Reynolds number would result in higher lift values. Instead, a decrease in lift was observed.
It was argued in the RAE report that fixing transition at low Reynolds number would remove the main problem caused by a thick laminar boundary layer. The results might then be comparable with the actual pressure distribution at flight Reynolds number. It was already indicated in the report, however, that forward fixation can produce premature trailing edge separation and a more forward shock (see fig. 1-1b). It is of interest to note here that the same figure shows a nice example of what is now called the "aft-fixation" technique.

In 1954 a review written by Pearcey and Holder [Ref. 54/1] was devoted to a discussion of adverse aerodynamic effects that severely limited flight handling qualities at transonic speeds, i.e. high speed buffet, aileron floating, wing-drop and pitch-up. It was argued that the effects were related to shock induced separation. The analysis is based largely on the interpretation of trailing edge pressures that appeared to rise quite suddenly for shock Mach numbers between 1.22 and 1.24. The problem of scale effect was not specifically addressed, although it was mentioned in a footnote that for a proper comparison with flight "the tunnel tests should, of course, be made with transition fixed". The case for transition fixing was discussed in much more detail at about the same by Haines, Holder and Pearcey [Ref. 54/2] who stated that "the major scale effects at highsubsonic and transonic speeds arise from differences between the conditions under which laminar and turbulent boundary layers separate, and in how they behave after separation".

As can be inferred from the "diagrammatic" sketch in figure 1-2 taken from Ref. (54/2), it was expected that scale effects were much less severe with turbulent boundary layer development and the resulting message was a clear one: fix the boundary layer in wind tunnel tests. Techniques discussed for doing so are distributed roughness (carborundum and ballotini), wires, adhesive tape and blowing, and remind us that there is nothing new today in this respect.

The noted difference between laminar and turbulent shock-wave boundary layer interactions was not at all unknown at that time as fundamental studies [see e.g. Ref. 46/1] had already indicated the phenomena years before. The new aspect was the notion that the differences could be related to adverse aerodynamic effects in high speed flight due to separation and scale effects. This notion stimulated basic research of shock-wave boundary layer interaction thereafter as reflected in a number of publications [e.g. Refs. 52/1, 55/1 and 55/2]. At the same time, control of the shock-wave formation on airfoils was attempted leading finally to the design of shock free supercritical airfoils [see e.g. Ref. 62/1]. The classical airfoil designs like the NACA 6-series with laminar flow (provided the wing surface was smooth enough) and without any appreciable rear loading, were replaced by designs of the "peaky" type (moving transition near the nose) and with a substantial amount of rear loading.

In 1966 a NASA report [Ref. 66/1] written by Loving was published that showed large differences between wind tunnel and flight data for the C-141 aircraft (fig. 1-3). As he wrote: "the purpose of the discussion is to caution experimenters concerning the use of wind-tunnel results in predicting flight loads and moments when supercritical separated flow is present". This event (or at least his figures, judged by the number of times they have been referenced) swept through the aerodynamic community like a shock wave, bringing a number of researchers and aircraft designers into a state of buffeting. Loving himself reported that "the results disclosed herein should not come as a surprise; they are merely additional evidence of the problem associated with separating flows". Scale effects had again become an area of considerable concern.

In a 1968 paper by Pearcey, Osborn and Haines [Ref. 68/2], a physical model was postulated that explained the aspect of the problem in more detail. The flows about the mid-fifties type airfoils were classified as type "A" separation, dominated by strong shock waves with separation rapidly developing from the shock to the trailing edge. This kind of flow was considered to be weakly Reynolds number dependent. However, the larger load carried by the aft part of modern airfoils could provoke "classical" (low speed) trailing edge separation even in the absence of shock waves which is considered to be Reynolds number dependent. They noted: "It is not surprising, therefore, to find these sensitivities carried over into flows in which rear separation and the local effects of the shock interact with one another, nor indeed to find them amplified by the interaction". They named this phenomenon type "B" separation. The publica-

tion was followed by a large numbers of papers that discussed scale effects [see e.g. Refs. 71/1, 71/3] most often related to shock-induced boundary layer separation. Some publications focussed attention on the means to calculate Reynolds number effects [e.g. Ref. 71/7], others to simulate Reynolds number effects in the wind-tunnel [e.g. Refs. 68/1, 71/4]. It was also argued that the final experimental answer could only be expected from wind tunnels which could achieve the full scale Reynolds number. In 1971, an AGARD meeting was organized in Goettingen specifically concerned with these problems ("Facilities and Techniques for Aerodynamic Testing at Transonic Speeds and High Reynolds number"). Therefrom plans were developed both in the US and in Europe, to build a high Reynolds number facility [Refs. 72/1, 72/4].

One other important change in judgement of the significance of Reynolds number effects should not be left unsaid in this review. Initially the interest was mainly concerned with the start and consequencies of flow separation. It was again Haines who noted in 1976 [Ref. 76/2] that "uncertainties (due to Reynolds number effects) not only affect the flow separation characteristics but also the drag in conditions where the flow is attached". Its significance is that scale effects are not only of interest for off-design conditions but also for performance prediction at the design condition. The argument was even carried one step further by Haines in Ref. [79/2] where it was argued that the optimisation of the aircraft design is greatly hampered by the Reynolds number gap of the present day windtunnels (figs. 1-4).

In the absence of a flight Reynolds number facility and stimulated by the aircraft industry that simply can not afford a major design change or a short-fall in aerodynamic performance due to uncertain scale effects, the study of Reynolds number effects is still continuing today. The most systematic information in this respect is obtained from existing [e.g. Ref. 78/1] or newly developed [e.g. Ref. 82/1] windtunnels in which the Reynolds number can be varied over a considerable range. This basic research has not been restricted to airfoils or high aspect ratio wings but has also widened to other configurations like slender bodies, afterbodies and delta wings.

Partly as a result of anomalies from these systematic Reynolds number studies, but also in its own right, a considerable interest exists with respect to the tunnel environmental and measuring technique effects (like wall interference, tunnel noise and flow quality, transition tripping devices, etc.) in relation to Reynolds number effects. As already indicated by Holder et al in 1955 [Ref. 55/1], flow quality might have a substantial impact on the pressure distributions as measured in the wind tunnel (see fig. 1-5 and compare with fig. 1-1). The influence of the tunnel environment on the transition location appeared to be a hot item in the sixties in connection with what was called a "unit Reynolds number effect" [Ref. 69/2]. The problem was more or less settled by Dougherty and Fisher [Ref. 80/4] in 1980. They were able to correlate transition Reynolds number on a 10 degree cone in both wind tunnel and flight with aerodynamic noise. Conflicting results of drag measurements with the AGARD Nozzle Afterbody [Ref. 75/1] could largely be explained when the Reynolds number effect on tunnel calibration was taken into account as pointed out by Aulehla and Besigk [Ref. 74/2]. Many more examples of this kind give as many warnings that the "observed Reynolds number effects" are, in some cases, attributable to measurement error or the wind tunnel (and/or flight) environment rather than Reynolds number per se.

This historical introduction has shown how the way of thinking with respect to Reynolds number effects has changed, not because of the physics changed but primarily because the frontiers of aerodynamic design have been widened. To quote Haines once more: "evidence (from the past) has to be judged in the context of the wing designs in the future" [Ref. 76/2]. And that is the intention of this AGARDograph.

1.2 Scope of report

1.2.1 Classification

Some kind of classification is needed for the description of Reynolds number effects. However, it should be emphasized that not all of the phenomena that are loosely called Reynolds number effects, are necessarily related to the "change in flow development with Reynolds number for a particular configuration in free air". Some of the observed Reynolds number effects in wind tunnels or unexplained differences between wind tunnel and flight happen to be caused by deficiencies in aerodynamic testing in ground based facilities. These effects, named hereafter "pseudo Reynolds number effects" have sometimes hampered the understanding of Reynolds number effects and, as is to be expected, will continue to do so even after high Reynolds number facilities become available. These effects are considered to be of so much importance that they are dealt with separately in Chapter 7.

If we now restrict ourselves to "true" as opposite to "pseudo" Reynolds number effects, they can be discussed either in a fundamental way by isolating one particular aspect or flow phenomenon or as changes in aerodynamic characteristics as observed on certain classes of aerodynamic shapes (Chapter 3 and 4). For the latter, a more precise classification is possible, according to the particular flow characteristics:

- airfoils and high aspect ratio wings with flows that are essentially two-dimensional or very weakly three-dimensional (such that local strip theory still applies);
- low aspect ratio wings with a highly three-dimensional flow development characterized by free vortex flow, highly skewed shock waves and/or three-dimensional separated regions;
- slender bodies with free-vortex flow development and/or base flow interacting with a jet or plume.

It is the purpose of this AGARDograph to review some of the evidence on Reynolds number effects and to provide a kind of more general frame work that might assist in the understanding of the observed effects. The Reynolds number enters into the fluid dynamic equations through the viscous terms of the Navier-Stokes equations. In other words, viscous effects constitute a necessary condition for the occurence of Reynolds number effects. But not all flows with embedded viscous regions are necessarily Reynolds number dependent. In a still most relevant review by Hall [Ref. 71/5], scale effects were defined as "the complex of interactions between the boundary layer development and the external inviscid flow". This distinction between a viscous shear layer and the outer inviscid flow field can conveniently be used to define two kinds of Reynolds number effects (see fig. 1-6):

- direct Reynolds number effects which occur as a consequence of a change in boundary layer development with Reynolds number for a fixed ("frozen") pressure distribution and
- indirect Reybolds number effects which appear as variations in the pressure distribution and hence in the aerodynamic characteristics due to a change in the boundary layer and wake development with Reynolds number.

This distinction is very useful in a practical, operational sense as will be discussed next.

1.2.2 Direct versus indirect Reynolds number effects

According to its definition direct Reynolds number effects can be calculated or estimated with the help of boundary layer calculation methods and/or semi-empirical correlations. However, the so calculated direct Reynolds number effects are only relevant for the prediction of scale effects in so far as the indirect Reynolds number effects are absent or negligible small. This is to some extent true for attached flow conditions but as soon as local effects of separation (e.g. near the trailing edge or at the foot of a shock wave) are present significant changes in pressure distribution might result. For larger separated flow regions the distinction is even less relevant: direct and indirect Reynolds number effects are essentially coupled.

This is all very similar to the distinction between weak and strong interactions as used by Hall in the above referenced paper. More recently this classification is also used in computational fluid dynamics to describe the mathematical approach of the coupling of viscous and inviscid fluid flow [see e.g. Ref. 83/2]. Basically, the strong interaction approach removes the so called Goldstein singularity for separated flows and involves a (quasi-)simultaneous solution of outer (inviscid) and inner (viscous) flow fields. In other words: for separated flows the direct and indirect Reynolds number effects are formaly coupled.

The most simple and very regular direct Reynolds number effect is related to the change in boundary layer development for a well developed laminar or turbulent boundary layer. The boundary layer properties generally vary as $Re^{-1/n}$ with $n = 2$ for laminar and $n \approx 5$ for turbulent flow. Skin friction drag, being the best observable example of a direct Reynolds number effect, varies accordingly. Equally important is the change in displacement thickness with Reynolds number. This change modifies the external inviscid flow field and is therefore, by definition, the cause of indirect Reynolds number effects. It is to be expected that a regular and continuous change in displacement thickness results in comparable smooth changes in the outer flow field.

A very significant and irregular direct Reynolds number effect stems from the transition from laminar to turbulent boundary layer flow. For swept wings the attachment line flow can be either laminar or turbulent, depending on Reynolds number, sweep angle and leading edge shape. For flat plate (subsonic or transonic) flow, a situation somewhat similar to the boundary layer development ahead of the shock on transport-type wings, the transition Reynolds number varies between 2×10^6 and 5×10^6 depending on noise level and free-stream turbulence. The corresponding chord Reynolds number is often just in between the Reynolds numbers of the wind tunnel model and the flying aircraft. These variations in transition location may interact with the outer field in a highly non-linear way. They are very often clearly discernable in the development of the aerodynamic characteristics. Even more important: laminar boundary layers fundamentally behave differently compared with turbulent boundary layers. As a typical example, a much smaller pressure gradient is needed for a laminar boundary layer to separate than for a turbulent boundary layer. Consequently, transition point changes might trigger significant changes in boundary layer separation as will be discussed next.

The most important direct Reynolds number effect is the Reynolds number influence on the start of separation (separation onset or incipient separation) and the subsequent separation development. Vortex burst or wake-stall are similar, but probably less critical phenomena in this respect. In all these cases one deals essentially with an interaction between the vicous flow development and the inviscid outer flow field, with large consequences for the pressure distribution. They are, for that reason, the cause of significant indirect Reynolds number effects. The onset of separation is very often described in terms of a viscous flow parameter (shape factor, Reynolds number based on displacement thickness etc.), although strictly speaking, locally a strong interaction approach may be more appropriate. When separations are confined to a small part of the flow field (e.g. a leading edge separation bubble or a local trailing edge separation) the effects on the outer flow field are only felt by a change in Kutta condition. This in turn affects the circulation and hence the overall flow field. In some cases, the resulting flow developes continuously, though sometimes highly non-linearly from the attached to partly separated flow conditions. In other cases, however, the separation might set-off a chain of reactions, leading finally to a complete and sudden break down of the flow field.

The direct Reynolds number effects will not be discussed in great depth in this AGARDograph. A very thorough discussion of these effects can be found in the report of the Research Committee of the AGARD working group 09 "Wind Tunnel Boundary Layer Simulation and Control" [Ref. 88/1].

1.2.3 The sensitivity to Reynolds number: A matter of definition?

Some configurations or types of flow are reported to be highly sensitive to changes in Reynolds number. But what precisely is meant with such a qualification?

Reynolds number sensitivity can be defined as the variation in aerodynamic characteristics (like lift, drag, pitching moment, pressure distribution ...) with Reynolds number for a particular configuration (shape) at constant flow conditions (like Mach, alpha ...). This sensitivity can in principle be obtained by plotting the particular aerodynamic characteristic versus Reynolds number. Unfortunately, it is not an easy matter to do an experiment in which only the Reynolds number is varied and all other flow conditions are kept constant. Even apart from tunnel environmental effects, that might introduce the "pseudo" Reynolds number effects to be discussed in chapter 2, the nominal flow conditions in Mach and incidence are rarely reproduced exactly. Also, in wind tunnel flight comparisons small configuration differences are almost inevitable. For these reasons the analysis of Reynolds number effects often requires some kind of interpolation or, at least, an estimation of the involved accuracies.

If it is assumed that the derivative with respect to Reynolds number can be defined for a particular aerodynamic characteristic, it still remains to be judged if the Reynolds number sensitivity is large or small. A very pragmatic criteria is: Reynolds number effects are large when they affect significantly the design (performance) of an aircraft as derived from sub-scale wind tunnel testing. Three drag-counts variation in drag-creep will be significant for a transport type aircraft, but irrelevant for a manoeuvring condition of a fighter configuration. An other, slightly different view is that Reynolds number effects should be considered large when the indirect Reynolds number effects are large. Most direct Reynolds number effects (like skin-friction) follow well established rules. One should only worry when the indirect Reynolds number effects are significant. Indeed, very often changes in pressure distribution are presented to emphasize that a particular kind of flow is Reynolds number sensitive. Unfortunately, such a proof is not sufficient since some pressure distributions are sensitive to changes in other flow conditions as well. A typical example is the design condition of certain supercritical airfoils that are known to be very sensitive to small Mach number and angle of incidence changes (see fig. 1-7; note that these results have been obtained in an adaptive wall wind tunnel where flow conditions are exceptionally well defined [Ref. 85/1]).

The quantification of Reynolds number sensitivity from the change in pressure distribution is clearly not applicable when the particular aerodynamic characteristic is not a continuous funtion of the flow conditions. Such situations typically occur when the flow changes from one type to the other, connected with events like:

- the onset of vortex formation on a delta-wing
- the maximum lift boundary
- lift divergence
- vortex break-down
- etc.

A typical example is presented in figure 1-8. At alpha = 2° the pressure distribution hardly changes with Reynolds number whereas near the maximum lift boundary at alpha = 3° large differences can be observed (note that this figure has some similarity with the classical Reynolds number case presented in fig. 1-3). An other example [Ref. 80/1] is given in figure 1-9 where pressure distributions on a delta wing are presented just before (high Reynolds) and beyond (low Reynolds) vortex formation. These examples do not really prove that a particular type of flow is highly Reynolds number sensitive. Instead, when such discontinuous changes are present in the flow development, the Reynolds number effect should be expressed as the variation in the boundary between two flow regimes, rather than comparing pressure distributions from two basically different flow regimes. Only when this variation is significant (e.g. in terms of the flight envelope) one can speak of a large Reynolds number sensistivity.

In view of these arguments it might be advantageous to consider the Reynolds number effects in the lift-Mach number plane (fig. 1-10). In this plane (mapping the flight envelope) typical flight conditions like cruise, maximum lift, drag-rise, etc. are defined. Off-design boundaries (very often related to discontinuities in flow development) are also defined in this plane and the aircraft designer actually wants to know how these boundaries change with Reynolds number. Also, the aircraft is designed for a particular lift at a chosen Mach number and the aircraft designer wants to know how the pressure distribution, the drag, the pitching moment, etc. changes with Reynolds number for that particular lift/Mach number combination. He will be only indirectly interested in the change of angle of attack for constant lift. He is most likely not interested in the change in pressure distribution at constant angle of attack although this is very conveniently measured in the wind tunnel. For these reasons the analysis and interpretation of Reynolds number effects is often preferably done in the lift-Mach number plane, at constant lift, constant Mach number or a combination of both.

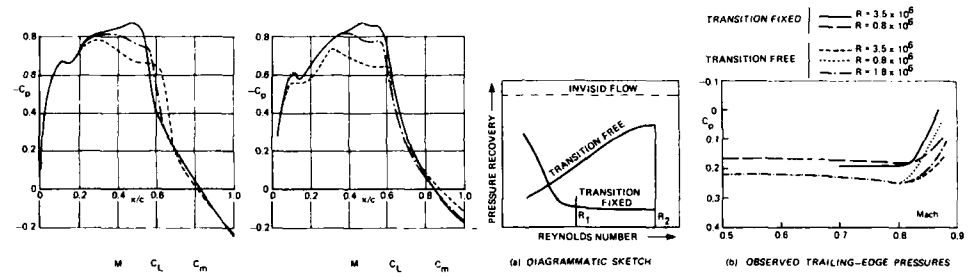

Fig. 1-2 The effect of Reynolds number and the state of the boundary layer on the pressure recovery over an airfoil when boundary-layer separation occurs at the shock waves (from ref. 54/2)

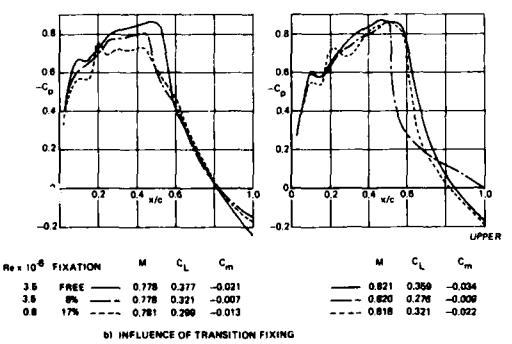

Fig. 1-1 Early evidence of the effects of Reynolds number on the pressure distribution (from ref. 51/1)

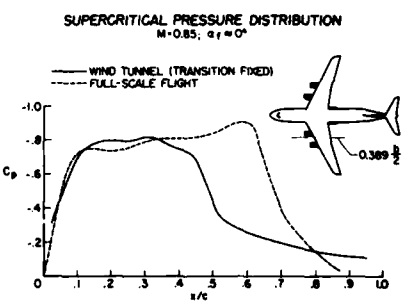

Fig. 1-3 The "classical" example of the effect of Reynolds number on the pressure distribution: the C-141 aircraft (from ref. 66/1)

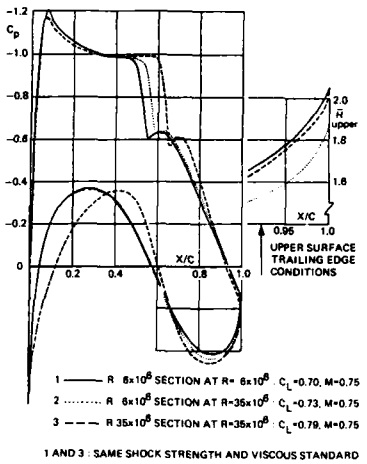

Fig. 1-4 Example of the achievable gain in design lift through design for a higher Reynolds number (from ref. 79/2)

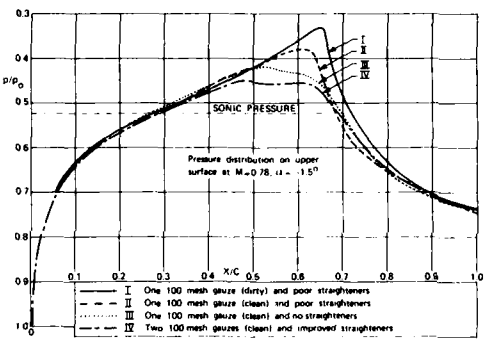

Fig. 1-5 Early example of the effect of flow quality on the pressure distribution (from ref. 55/1)

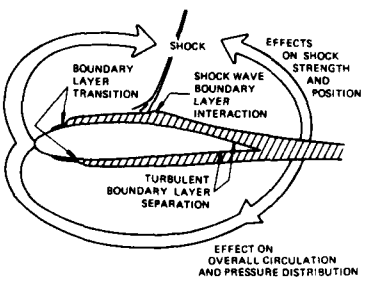

→ DIRECT REYNOLDS NUMBER EFFECT

⇨ INDIRECT REYNOLDS NUMBER EFFECT

DOMINANT RE-NUMBER EFFECT		
CHARACTERISTIC	DIRECT	INDIRECT
LIFT AND PITCHING MOMENT		x
VISCOUS DRAG	x	
WAVE DRAG		x
DRAG DIVERGENCE		x
BOUNDARY LAYER SEPARATION	x	
BUFFET BOUNDARY	x	x

Fig. 1-6 Schematic representation of direct and indirect Reynolds number effects

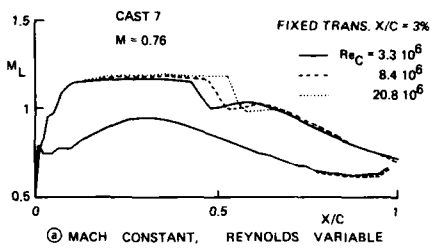

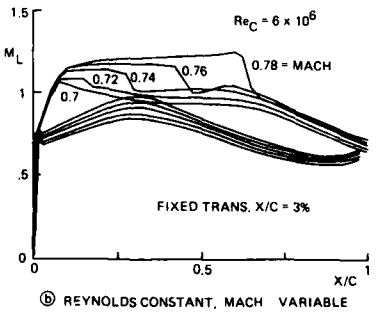

Fig. 1-7 Example of the sensitivity of a supercritical airfoil at the design condition for variations in flow conditions (from ref. 85/1)

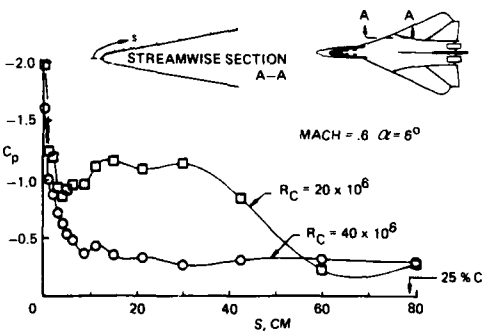

Fig. 1-9 Reynolds number effect on the pressure distribution prior to and beyond vortex formation illustrating large differences due to a Reynolds number effect on the boundary for vortex formation (from ref. 80/1)

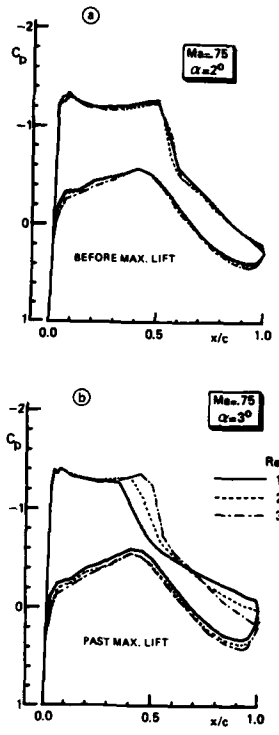

Fig. 1-8a Reynolds number effect on the pressure distribution prior to and beyond maximum lift illustrating large differences due to a Reynolds number effect on the maximum lift boundary (from ref. 83/3)

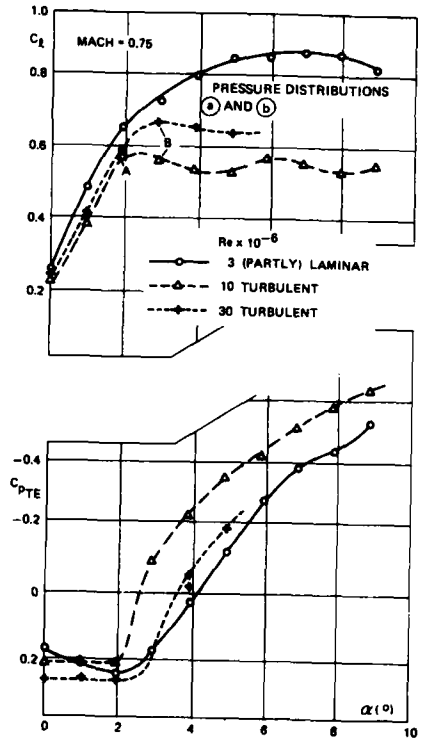

Fig. 1-8b Reynolds number effect on lift and trailing edge pressure near the maximum lift boundary (from ref. 83/3)

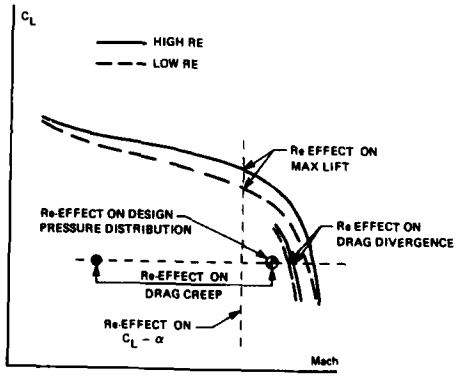

Fig. 1-10a Example of evaluation of Reynolds number effects at constant lift

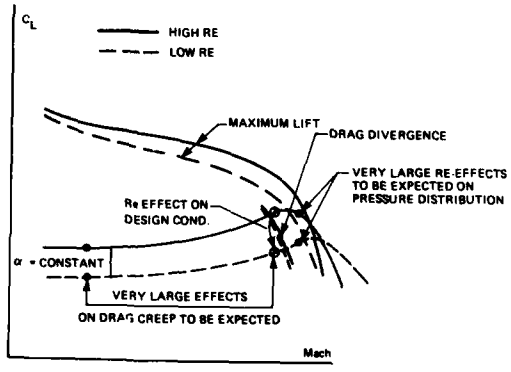

Fig. 1-10b Example of evaluation of Reynolds number effects at constant incidence

2.0 POTENTIALS FOR PSEUDO-REYNOLDS NUMBER EFFECTS

by
T. W. Binion, Jr.
Calspan Corporation/AEDC Operations
Arnold Air Force Base, TN 37389

2.1 INTRODUCTION

Reynolds number effects have been traditionally determined by testing a given model in a variable Reynolds number tunnel, testing a given model in several wind tunnels with different Reynolds number capabilities, testing similar models of different scale in a given or different wind tunnels, or a combination of the three. The data are then extrapolated to flight using various semi-empirical correction techniques. Almost every parameter which can introduce spurious effects into wind tunnel data has the potential to vary from tunnel to tunnel at the same nominal test condition or from one Reynolds number to another in a given tunnel. Factors which have the potential of introducing pseudo-Reynolds number effects include wall interference, tunnel Mach number calibration, noise, turbulence, humidity, nonuniform flow (flow angle, tem-perature and pressure gradients), flow contamination, sidewall effects in two-dimensional tests, thermal non-equilibrium, model deformation, and transition fixing. In some instances not only are the effects of the parameters not well understood, their influences may be coupled and not easily separated by experimental techniques. At present, the theoretical capability does not exist to evaluate the individual effects of the above factors with confidence much less their potential coupling. Thus, some of the discussion below is somewhat speculative. Nevertheless, the evidence presented is strong enough to elicit a degree of caution in ascribing the cause of variations of data with Reynolds number solely to Reynolds number.

2.2 WALL INTERFERENCE[1]

Attempts to experimentally assess the effects of wall interference have been careful to keep as many parameters constant as possible, e.g., model support, instrumentation, transition location, test conditions, etc. Therefore, there is not much direct evidence of wall interference varying with tunnel Reynolds number. J. Smith (NLR) has calculated the wall interference for two Reynolds numbers from boundary conditions measured between the slots of the NLR High Speed Tunnel with a 50-cm chord full span 2D airfoil. Although the changes in interference are small as a function of Reynolds number, Fig. 2-1, "they are still substantial when compared with some observed Reynolds number effects", Ref. [83/4].

For porous walls it has been established in experiments by Jacocks, Ref. [76/5], and Chan, Ref. [82/6], that the wall crossflow characteristics are a function of the local wall boundary-layer characteristics. Thus, not only does this imply that wall interference is a function of tunnel Reynolds number but also the model imposed pressure distribution on the wall as it affects the displacement thickness. Subsequent to Ref. [76/5], Jacocks, has correlated the classical wall porosity parameter, $dC_p/d\theta$, with a nondimensional wall parameter, $(\tau t/d)^2 Re_{\delta_*}$, where τ is the wall porosity, t the wall thickness, d the hole diameter, and $Re\delta_*$ the Reynolds number based on the porous wall boundary-layer displacement thickness. The correlation shown in Fig. 2-2 clearly demonstrates the porous wall boundary condition, hence wall interference, varies with Reynolds number. It should also be noted that, particularly with a ventilated wall, Re_{δ_*} varies with the pressure distribution over a given wall which is a function of test conditions, model and support configuration, and model attitude. Theory does not yet allow a detailed computation of the local wall boundary condition, nor has it been established that such a detailed specification is necessary. However, for the AEDC tunnels, Jacocks also has correlated Re_{δ}^* at the tunnel nozzle exit with Reynolds number based on the contraction nozzle length, Fig. 2-3. If one accepts the variation of $Re_{\delta}^*{}_o$ as an indication of the variation of the wall boundary condition with tunnel Reynolds number, then combining the equations in Figs. 2-2 and 2-3 yields

$$\frac{dC_p}{d\theta} = 53.4 \frac{d}{u} \left(Re_{C_N} \right)^{-2.5} \tag{2-1}$$

at least for the AEDC tunnels.

---

[1]The analysis presented draws upon an unpublished document by Dr. E. M. Kraft, Calspan Corporation/AEDC Operations.

The potential effect of Re on wall interference may be estimated from the classical theory of Ref. [69/1]. Shown in Fig. 2-4 is the variation of the lift interference factor with the wall porosity parameter, Q, defined for incompressible flow[1] as

$$Q = \left| 1 + \frac{1}{R} \right|^{-1} \tag{2-2}$$

where

$$\frac{1}{R} = 1/2\, dC_p/d\phi.$$

The change in the lift interference factor caused by variations in unit Reynolds number for Tunnel 4T is indicated in the figure and accompanying table. The tunnel Reynolds number effects are substantial.

Experiments conducted on an A-10 aircraft model, Fig. 2-5, in Tunnels 16T and 4T by J. M. Whoric, yielded some information on the effect of Reynolds number on wall interference. The model blockage was 0.13 and 2.11 percent in 16T and 4T, respectively. Because of the small blockage ratio, the 16T data are considered wall interference free. The two tests were conducted with the same instrumentation, support sting, and test conditions. The difference between the 16T and 4T angle of attack, pitching moment, and induced drag at constant lift is shown in Fig. 2-6 for two unit Reynolds and Mach numbers. Even though the tests were conducted transition free, the transition Reynolds numbers based on Dougherty's cone data, Ref. [82/7], at the conditions of the comparison are almost identical in the two tunnels. Furthermore, the A-10 data from 16T exhibited no Reynolds number effects. Thus, the data variations with Reynolds number are the result of phenomena in 4T. The $\Delta\alpha$ is not zero at $C_L = 0$ because the tail incidence is 6 deg with respect to the wing. Therefore, both the wing and tail are lifting, albeit in opposite directions at $C_L = 0$, which causes lift interference in Tunnel 4T resulting in an effective angle change for zero lift. The classical lift interference applicable to the A-10 was shown in the table accompanying Fig. 2-4. While classical theory would not be expected to produce accurate results for such a large and complicated model or even necessarily the correct trends at transonic Mach numbers, the theoretical lift interference slopes, $d\alpha/dC_L$, agree rather well with the data in Fig. 2-6a, particularly at low lift. Theory aside, if wall interference is the dominant variable between the two data sets, then the data in Fig. 2-6 strongly suggest that wall interference is a function of Reynolds number for both Mach numbers since the variation of the coefficient differences is considerably different for each Reynolds number. Furthermore, the fact that $\Delta\alpha$ is not linear with C_L suggests that the wall interference boundary condition is not constant with C_L which is not inconsistent with the hypothesis that the boundary condition is a function of the model imposed pressure distribution.

2.3 NOISE AND TURBULENCE

Pate and Schueler, Ref. [69/2], and Dougherty, Ref. [82/7], have shown that the location of boundary-layer transition is influenced by aerodynamic noise. Dougherty devised a correlation function between transition Reynolds number and root-mean-square pressure fluctuation shown in Fig. 2-7. Recently, however, Murthy and Steinle, Ref. [86/2], have re-examined Dougherty's and other data and suggested that at transonic speeds, if the tunnel noise is less than about 1% rms C_p, noise may not affect transition at all, the real mechanism being turbulence. For Tollmien-Schlichting type transition, the spectral content of the disturbances in relation to the laminar instability frequency is probably the factor in producing premature transition [87-3]. While it is difficult to decouple the effects of noise and turbulence in wind tunnel data, free-stream turbulence by itself can exert a substantial influence on transition location. For example, Mignosi, Ref. [85/7], has calculated the effects of free-stream turbulence on the skin friction distribution for a supercritical airfoil, Fig. 2-8. The calculations indicate that transition location on the upper surface is a strong function of rather small variations in turbulence. The laminar boundary layer on the lower surface separates at about 60% chord and transition occurs at the end of the separation zone. In a given non-cryogenic wind tunnel, the amplitude and spectra of the noise and turbulence, hence transition location, is a function of unit Reynolds number, i.e., tunnel power. For models with free transition, variation of free-stream noise and/or turbulence with tunnel power could produce a pseudo-Reynolds number effect by causing transition location to be a function

[1]Even though the theories in Ref. [69/1] claim applicability to compressible flow, experience does not substantiate such a claim.

of tunnel Reynolds number rather than model Reynolds number. Such effects can be partially avoided by fixing transition forward of the free transition location.

There is no known clear evidence that noise affects boundary-layer properties other than transition location. However, several investigators have obtained experimental evidence of the effect of free-stream turbulence on boundary-layer properties. Green, Ref. [73/2], working with low-speed zero-pressure-gradient data and taking Re_θ as a characteristic parameter showed that "not only is the effective Reynolds number highly sensitive to turbulence - the fractional increment in Re_θ is 60 times that in u'/ue . . . - but also this sensitivity increases with increasing Reynolds number." Raghunathan and McAdams also found a strong influence of turbulence on attached zero-pressure-gradient turbulent boundary layers up to 0.8 Mach number and Re_θ from 3- to 10-thousand, Ref. [82/8]. They conducted further experiments using a 9% thick circular-arc tunnel-wall bump at Mach numbers from 0.65 to 0.78, Refs. [83/5] and [83/6]. Transition was fixed upstream of the bump. The variation they obtained of trailing-edge separation length, shock location, and the ratios of boundary-layer momentum thickness, shape factor, and displacement thickness upstream and downstream of the shock are shown in Fig. 2-9. The major conclusions of those experiments were: (1) increasing turbulence intensity causes the shock position to move downstream, (2) while free-stream turbulence affects Re_θ and δ^* upstream of the shock, it also appears to have a direct effect on the shock boundary-layer interaction and hence shock position, and (3) increasing turbulence intensity produces a decrease in the length of the trailing-edge separation region and hence an increase in pressure recovery.

The data which Green analyzed did not contain any information below turbulence values of 1%. The values of turbulence intensity on the Raghunthan and McAdams experiments, 0.3 to 6%, were also larger than encountered in many wind tunnels. Mr. Peter Bradshaw, has argued, as discussed in Ref. [23/2], that the variation of gross boundary-layer properties with turbulence should be parabolic such that the effects at low values of turbulence (< 1%) would be diminished and negligible. Further experiments by Raghunthan and McAdams, Ref. [85/9], while not specifically confirming Bradshaw's hypothesis, do show that for fixed transition the effects of turbulence below 1% are small at least for the 18% circular arc airfoil. With free transition there is, of course, a coupling between the well-known effects of turbulence on transition location and the effects depicted in Fig. 2-9. The experimental configurations used in each of the above cited experiments are not particularly sensitive to small changes in any parameter relative to a supercritical airfoil for example, Fig. 2-8. Therefore, the results should not be discounted merely because the turbulence values were large. It seems logical to conclude that if the flow over the model being tested is sensitive to small changes in boundary-layer properties and if turbulence intensity varies with tunnel Reynolds number (power), then even with fixed transition location a pseudo-Reynolds number effect is possible.

2.4 HUMIDITY EFFECTS

The effects of water vapor condensation in the free-stream flow at supersonic Mach numbers have been recognized for many years. In 1979 preliminary data were obtained in Tunnel 16T during the tunnel drying process which indicated lift, pitching moment, and axial force all varied significantly as a function of specific humidity at subsonic Mach numbers, provided a portion of the flow over the model was supercritical. Typical data acquired with two scale models of the same configuration are shown in Fig. 2-10. Note that the effects begin with the dewpoint temperature 10° below the static temperature. Other, although rather crude, data were obtained which indicated the aerodynamic coefficient variation, both in magnitude and form, was a function of model configuration. It is hypothesized that the variations were caused by water vapor condensation in the supercritical portion of the flow field and hence are potentially a function of Mach number, temperature, pressure, model attitude, configuration and, because of condensation rate kinetics, model size.

A computer program has been devised which solves the Euler equations along with the energy and specie conservation equations for two and three-dimensional transonic flows, Ref. [85/8]. The code has been verified with almost exact replication of condensation data from a 10-cm-diam supersonic nozzle, Ref. [63/1], and unpublished calibration data from Tunnel 16S nozzle (4.9-meter exit diameter). Therefore, the code appears to have wide ranging applicability. Results from the code applied to the two- dimensional, 200-mm chord, CAST 10 airfoil tested by Stanewsky, Ref. [83/7], is presented in Fig. 2-11 for two Reynolds numbers obtained by changing the tunnel total pressure. The value of specific humidity at which the dewpoint temperature equals the free-stream static temperature is 0.07 and 0.018 for the 3- and 1-atm total pressure condition,

respectively. Thus, the effects occur at humidity values much below the saturation value. Three conclusions are obvious:

1. There is a significant variation in each coefficient with specific humidity.

2. There is a significant effect of Reynolds number at a constant humidity.

3. The higher the total pressure the lower the value of specific humidity at which the effect begins and the greater the effect. The effect is a consequence of the thermodynamic relationship between saturation specific humidity and pressure and of the higher energy release per unit weight of air as pressure is increased.

As shown in Fig. 2-12, the humidity effect is manifested first as an increase in pressure on the airfoil upper surface and, as specific humidity increases, by a forward movement of the shock position. In each instance, the change in the sign of the axial-force slope corresponds to the beginning of the forward movement of the shock.

The conclusions expressed in this subsection only apply to the specific conditions of the calculations. There is not yet enough experience nor experimental variation to generalize. However, the calculation results are sufficiently compelling to warrant the measurement of humidity as a parameter which defines the test conditions and an assessment of its influence when trying to define true Reynolds number effects.

2.5 TUNNEL CONTAMINATION

The contamination of tunnel flow by particles small enough to be airborne and simultaneously hard enough to cause pitting of model surfaces in stagnation point regions will lead to premature boundary-layer transition. Aluminum models are particularly susceptible to such damage. From a Reynolds number effect viewpoint, roughness at the leading edge would mask any true transition movement with Reynolds number effect, negate the effectiveness of transition trips which would normally be downstream of the stagnation region and could conceivably produce an unrealistic variation of transition location with angle of attack, Mach number and Reynolds number. In all but the most severe instances, the effects of tunnel contamination can be avoided by using hardened steel models.

2.6 TUNNEL CALIBRATION

All aerodynamic data exhibit some sensitivity to tunnel calibration parameters. It has been shown that the calibration of perforated tunnels is a function of Reynolds number, Ref. [78/3]. Aulehla and Eberle, Ref. [82/9], using computational results, argue that calibration of a solid wall tunnel is a function of Reynolds number which, if not corrected, will produce an erroneous variation of shock position with Reynolds number. Perhaps the parameter most sensitive to errors in tunnel calibration is afterbody drag whose sensitivity near zero can be shown to be

$$\Delta C_D = \frac{2A}{A_W} \cdot \frac{\Delta M}{M\left(1 + 0.2M^2\right)} \qquad (2\text{-}3)$$

where A is the cross-sectional area, A_w the wing area, and M the tunnel Mach number. The afterbody drag error is equal to the error in free-stream pressure acting on the model cross-sectional area. For a typical fighter aircraft an error of 1 count in afterbody drag is produced by the Mach number error shown in Fig. 2-13. Such extreme sensitivity to small errors requires not only very careful calibrations, but also that all factors which affect the tunnel calibration are properly considered.

One example of the effects of calibration error is shown in Fig. 2-14 wherein the integrated pressure drag on a body of revolution is presented with and without the Reynolds number correction to the tunnel calibration, Ref. [80/8]. The fact that the slopes of the uncorrected forebody and afterbody curves are of opposite sign is caused by the free-stream pressure-area term acting in the opposite direction for the two integrations. Proper application of the tunnel calibration essentially eliminates the variation of pressure drag with Reynolds number. There is still a small error in free-stream pressure at the lowest Re in Fig. 2-14 which was not properly removed in the calibration.

Other examples and an extensive discussion of the effects of not calibrating variable density wind tunnels as a function of Reynolds number has been published by Aulehla in Ref. [87/1].

2.7 SIDEWALL EFFECTS IN 2-D TESTS

There has been a lot of attention paid to the effect of the sidewall boundary layer on two-dimensional test data, Refs. [82/10] and [83/8] for example. However, no one seems to have considered the effect tunnel Reynolds number has on the sidewall boundary layer and hence its influence on the model data. The effect the sidewall boundary layer can have is illustrated in Fig. 2-15, which presents data with "adequate" sidewall boundary layer removal (according to the authors of Ref. [83/8]) and none. The effects are obviously large, leading to the hypothesis that unless the boundary layer receives the proper conditioning or the aspect ratio is large (greater than 2.5), tests defining the variation of two-dimensional data with Reynolds number contain large pseudo-Reynolds number effects. The definition of what constitutes proper conditioning has not been totally agreed upon by the testing community and may vary from facility to facility. However, the procedures summarized in Ref. [87/2], which are being used in the Langley 0.3m TCT Facility, significantly improve data comparisons.

2.8 NON-UNIFORM FLOW

Obviously a tunnel-empty spatial gradient of any free-stream flow property can affect model data depending upon its magnitude and the model configuration. There is little information known which indicates if the gradient of parameters normally considered in this category, pressure, temperature, and flow angle vary with tunnel Reynolds number. Considering the mechanisms which could cause gradients to vary with Reynolds number, only the variation of the wall boundary layer influencing buoyancy appears plausible. Such is possible in a solid wall wind tunnel but not likely in a ventilated test section. Unpublished data from a porous tunnel indicate buoyancy is not a function of Reynolds number. Also, there is no reason to expect either tunnel temperature or flow angle is a function of Reynolds number. It should be noted that buoyancy-like gradients in x, y, and z due to wall interference can exist and be a function of Reynolds number.

2.9 THERMAL NONEQUILIBRIUM

Although not as severe a problem in a continuous flow tunnel as in a short duration facility, heat transfer into or out of the model can produce spurious effects on data which are sensitive to the boundary-layer properties. In short duration facilities significant differences are likely to arise between the temperature of the model and the recovery temperature of the stream. Since the temperature of the stream is influenced by throttling the flow from the reservoir to tunnel total pressure, the stream temperature is generally a function of tunnel Reynolds number, i.e., of the throttling pressure ratio. Unless provisions are made to cool the model prior to each test, the stream will be appreciably cooler than the model. The resulting heat transfer will significantly alter the boundary-layer properties and appear as a spurious scale effect. A brief study of this phenomena, Ref. [72/6], concluded that an increase of 1% in model-to-free-stream temperature ratio would produce an effect roughly equivalent to a 3½% reduction in Reynolds number. For Reynolds number variations within a given tunnel, the problem may not be significant. For example, expanding air from a 300-atm pressure reservoir at 300°K to 50 atm reduces the stagnation temperature to about 270°K; whereas, expanding to 1 atm reduces the temperature another 10°K. At a constant Mach number the real gas effects between conditions at 50 atm and 1 atm would be equivalent to a 13% Reynolds number change within the tunnel. However, if the data from a blowdown facility with the model at room temperature were compared to a similar condition wherein the model was in thermal equilibrium, the data at 1 atm would contain an effect equivalent to a 53% change in Reynolds number because of the effect of heat transfer on the boundary layer of the model in thermal non-equilibrium. While the numbers given are very approximate, the effects are significant and should be considered when comparing Reynolds number data from short-duration facilities.

Dougherty and Fisher, Ref. [80/4], deduced the effect of non-adiabatic wall temperature on transition Reynolds number measured on a 10-deg cone both in flight and the AEDC Tunnel 4T. The empirical relationship derived from their data

$$Re_T/Re_{T_{aw}} = \left(T_w/T_{aw}\right)^7 \qquad (2\text{-}4)$$

encompasses at least a Mach number range from 0.55 to 2.0 and temperature ratios from 0.95 to 1.08. Such a large sensitivity could introduce pseudo Reynolds number effects depending upon how a particular test was conducted and the sequential relationship between Re, T_{aw}, and time.

It has long been recognized that temperature changes in continuous tunnels can manifest as balance shifts. Strain gages have been temperature compensated to minimize the effect. However, work by Ewald and Krenz, Ref. [86/6], has shown significant sensitivity (80 μv) of axial-force gages to moderate thermal gradients (8°C) within the balance structure. Since the mechanism producing the effect is heat transfer into one end of an internal balance, the time constant is measured in hours requiring long times to reach thermal equilibrium. Such effects will be very pronounced in cryogenic facilities. If the tunnel temperature is varied systematically as a function of Reynolds number, the data from an internal balance may well contain a pseudo-Reynolds number effect.

2.10 MODEL DEFORMATION

While it is recognized that wind tunnel model support systems deflect under load, the models themselves are generally considered to be rigid. However, to comply with the present day accuracy requirements such assumptions may not be valid. As an example, the deflections of the two-dimensional model reported in Ref. [83/7] were computed. The model has a 200-mm chord and a 510-mm span. It was assumed to be rigidly constrained at the tunnel walls and made of solid steel. The calculated change in the mid-span angle of attack caused by torsional bending for Re = 30 x 10^6 and 2-deg incidence varied between 0.07 and 0.10 deg in the Mach number range 0.6 to 0.8. The effect of such changes is shown in Fig. 2-16. The data at 30 x 10^6 Reynolds number have been corrected to account for the computed torsional deflection of the airfoil. The correction reduces the difference between the 10 x 10^6 and 30 x 10^6 curves by more than a factor of two except at Mach number 0.8 at which the wing is almost completely stalled and there is little variation of lift with incidence. Model deformation does not significantly influence the data at the 10 x 10^6 and 4 x 10^6 Reynolds number since the loads are relatively low.

As another example, the wing torsional bending of the ONERA calibration model M5, Fig. 2-17, was also calculated. A solid steel wing was assumed although the wing does contain pressure orifices. The change in incidence as a function of semi-span location is shown in Fig. 2-18 for Mach number 0.84, lift coefficient 0.4, and various Reynolds numbers. The deflections at the higher values are large enough to cause variations which could be interpreted erroneously as Reynolds number effects. In this instance, the wing dihedral also changes with Reynolds number. However, the dihedral effects should be less than those caused by the change in wing twist.

2.11 TRANSITION FIXING

A final word is needed on transition fixing as it relates to Reynolds number effects. A boundary-layer trip is sized for a particular Reynolds number, Mach number, pressure gradient condition. Substantial deviation from that condition results in either an over- or under-fixed boundary layer. The necessary variable range for the deviation to be substantial is not very well defined. A systematic study has not been published. Nevertheless, the necessary range seems to be several times less than the range of most test condition variables. Most studies have indicated one must change grit size with Re. The consequences of overfixing is that the turbulent boundary layer may be thicker than desired and the drag higher because of grit drag. The consequences of under-fixing are that the transition zone is either longer than for a just adequate trip height or the transition is downstream of the desired location. In each situation consequences can accrue in all aerodynamic parameters. An example of the consequences of over-, under-fixing is given in Fig. 2-18 taken from Ref. [84/6]. Obviously, if Reynolds number is varied with fixed transition without changing grit size appropriately with Re or with a non-hydraulically smooth surface, the resulting variation in aerodynamic coefficients with Reynolds number is not a true scale effect.

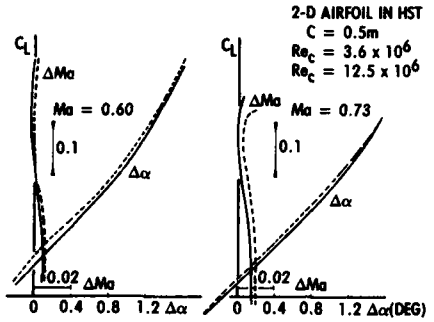

Fig 2-1. Blockage (ΔMach) and incidence (Δα) corrections calculated from measured top and bottom wall pressure distributions, [84/3].

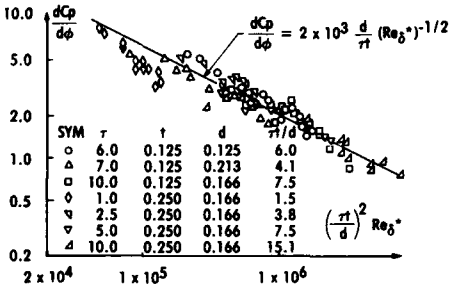

Fig. 2-2. Correlation of porous wall characteristics with displacement thickness Reynolds numbers.

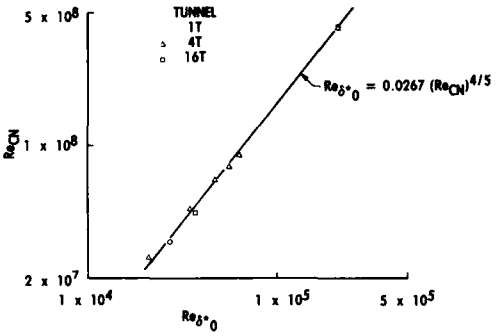

Fig. 2-3. Correlation of nozzle exit displacement thickness Reynolds number with tunnel contraction-nozzle Reynolds number.

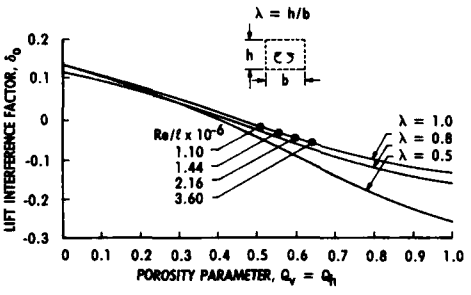

A-10, M = 0.3, τ = 5%

$Re/\ell \times 10^{-6}$	$dC_p/d\theta$	Q	δ_o	$\Delta\alpha = 57.3\,(S/C)\delta_o C_L$
1.10	1.90	0.51	-0.020	-0.090 C_L
1.44	1.59	0.56	-0.035	-0.159 C_L
2.16	1.35	0.60	-0.050	-0.227 C_L
3.60	1.10	0.64	-0.065	-0.295 C_L

Fig. 2-4. Variation of the upwash interference with changes in unit Reynolds number.

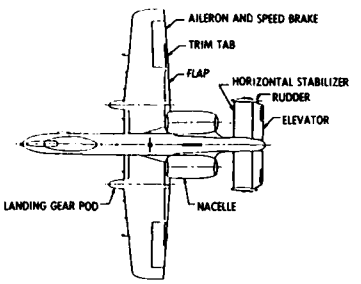

Fig. 2-5. The A-10 model.

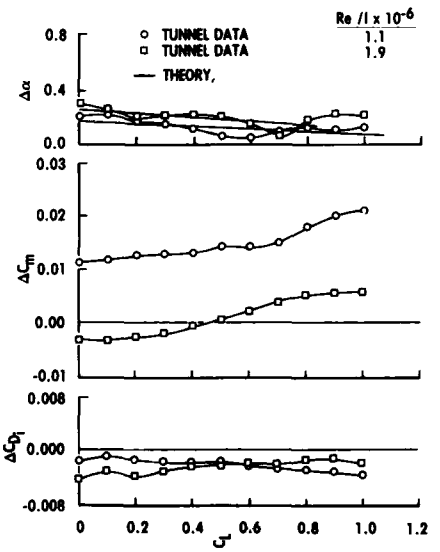

a. M = 0.3

Fig. 2-6. Comparison of theoretical and experimental results for the A-10 model.

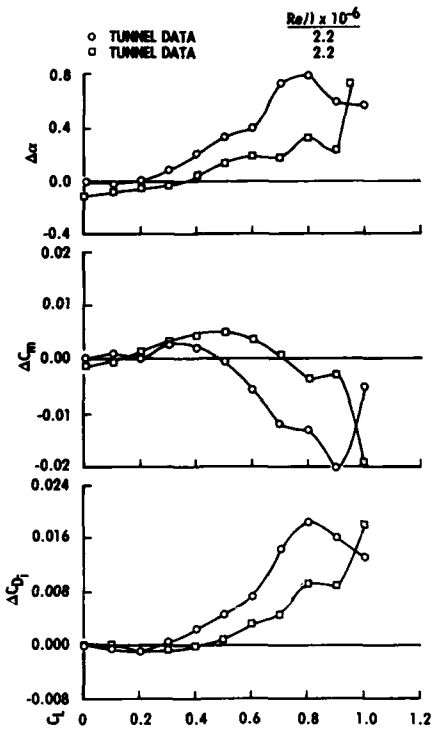

b. M = 0.75
Fig. 2-6. Continued.

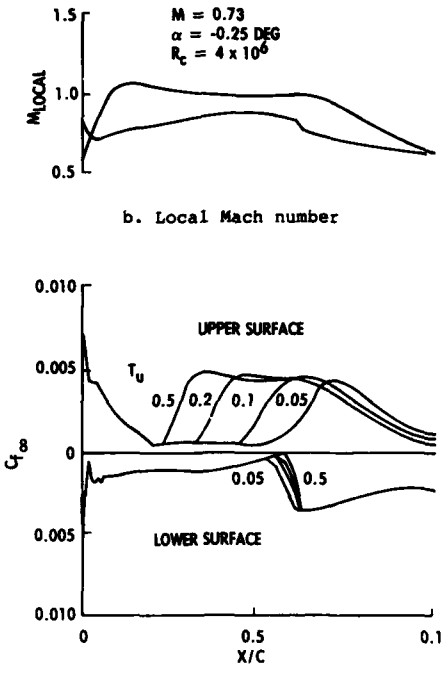

a. Skin friction
Fig. 2-8. Effect of free-stream turbulence on skin friction distribution, [85/7].

SYM	TUNNEL
○	AEDC TUNNEL 16T
◔	AEDC TUNNEL 16T (WALLS TAPED)
△	AEDC TUNNEL 4T
✱	AEDC TUNNEL 4T (WALLS WITH TAPE OR SCREEN)
◇	ONERA 6 X 6 S-2 MODANE
▽	NASA/AMES 11 TWT
◤	NASA/AMES 11 TWT (WALLS TAPED)
▷	NASA/AMES 14 TWT
◣	NASA/AMES 14 TWT (WALLS TAPED)
▫	CALSPAN 8 TWT
○	ARA, LTD. BEDFORD 9 X 8

SYM	TUNNEL	
◐	NASA/AMES 12 PT	
▽	RAE BEDFORD 8 X 8 SWT	
■	NASA/LANGLEY 16 TT	FREON TEST MEDIUM
▲	NASA/LANGLEY 16 TDT*	
◆	NASA/LANGLEY 8 TPT	
●	NSR&DC 7 X 10 T	
▷	NASA/LANGLEY 4 SPT	
◇	RAE BEDFORD 3 X 4 HSST	
▫	NASA/AMES 9 X 7 SWT	
◿	NASA/LANGLEY 4 SUPWT (TS NO. 1)	
▯	FLIGHT DATA, FIG. 18	

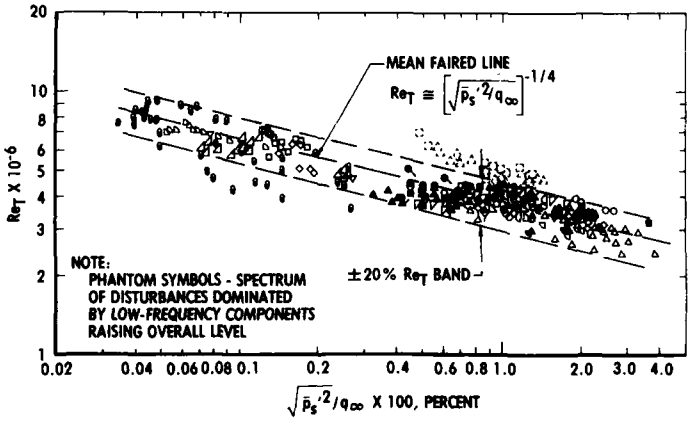

Fig. 2-7. Correlation between Re_T and cone surface disturbance measurements, [82/7].

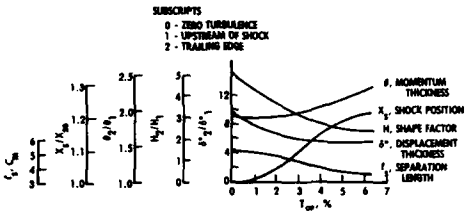

Fig. 2-9. Effects of free-stream turbulence on shock and boundary-layer properties on a 9%-thick circular airfoil, fixed transition location, [83/5, 83/6].

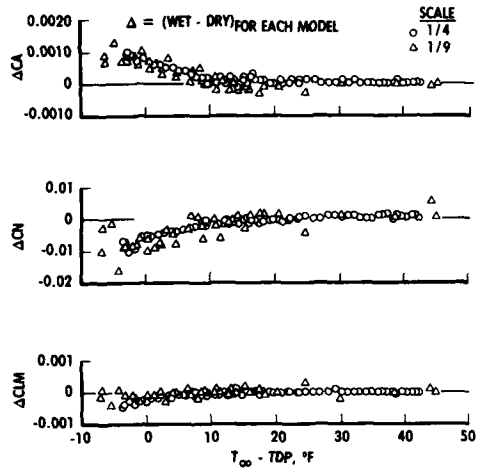

Fig. 2-10. Effect of moisture content on model aerodynamic coefficient, M = 0.9, α = 6 deg.

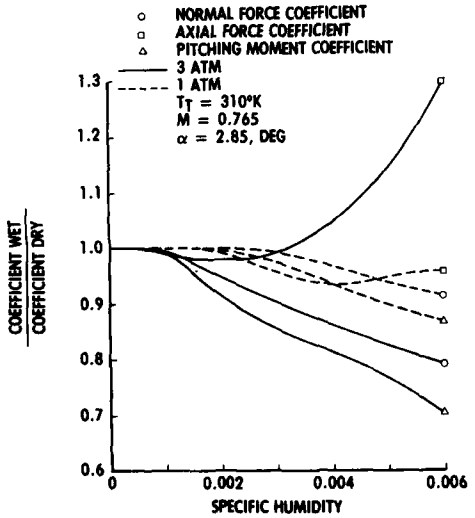

Fig. 2-11. Effect of the humidity on aerodynamic coefficients, two-dimensional CAST-10 airfoil.

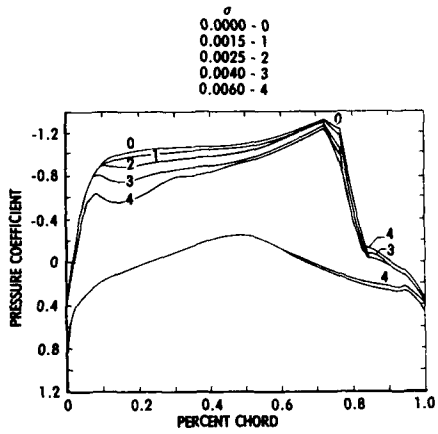

Fig. 2-12. Effect of humidity variation on CAST-10 pressure distribution.

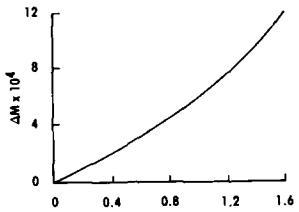

Fig. 2-13. Error in Mach number to produce a 1-count error in afterbody drag for a typical fighter aircraft.

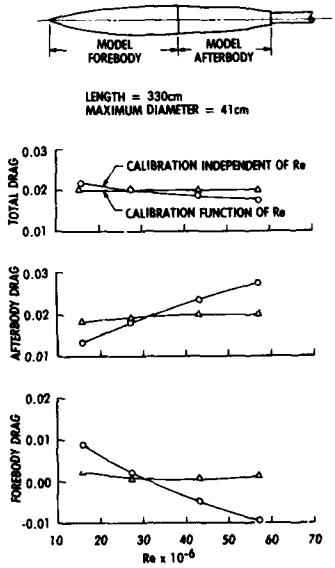

Fig. 2-14. Comparison of pressure-drag coefficient calculated with and without Reynolds number corrections to the tunnel calibration, [80/8].

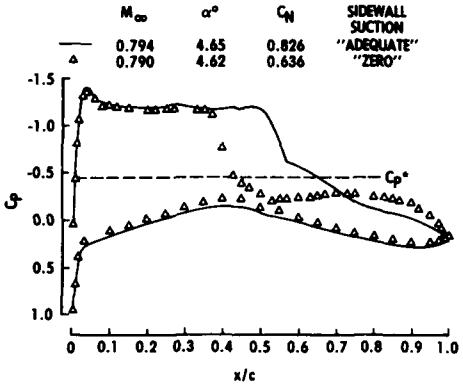

Fig. 2-15. Effect of sidewall boundary-layer removal on two-dimensional airfoil pressure distribution, [83/8].

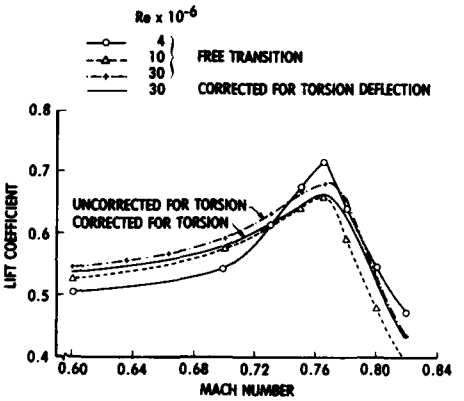

Fig. 2-16. Variation of lift coefficient with Mach number at 2-deg incidence and various Reynolds numbers, 2D CAST-10 airfoil in 20-in. span wind tunnel.

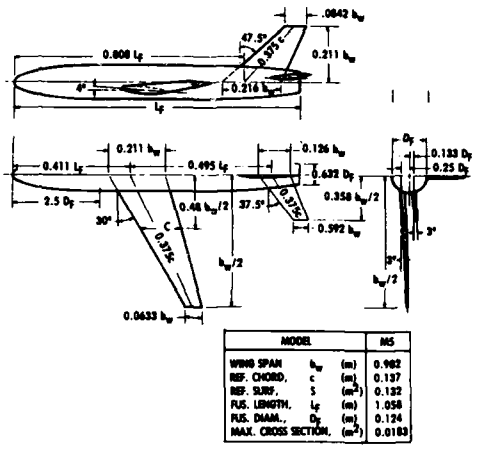

Fig. 2-17. Onera M-5 model.

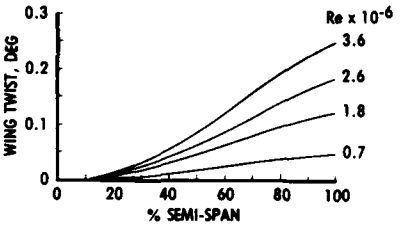

Fig. 2-18. Wing twist, ONERA M-5 model, Mach number 0.84, C_L = 0.4.

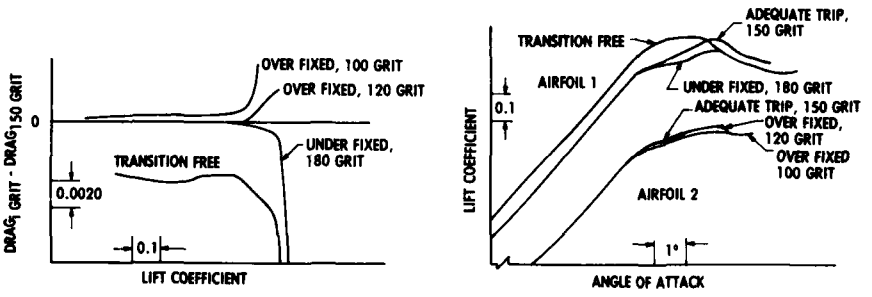

Fig. 2-19. Effect of over, under fixing boundary layer, cruise Mach number, grit a 7% chord, [84/6].

3. OBSERVED REYNOLDS NUMBER EFFECTS: AIRFOILS AND HIGH ASPECT RATIO WINGS

by
A. Elsenaar
National Aerospace Laboratory NLR
Anthony Fokkerweg 2, 1059 CM Amsterdam
The Netherlands

3.1 Introduction

After the preceding discussion of the pseudo-Reynolds number effect, this and the following chapters are concerned with the Reynolds number effects as actually observed on various aerodynamic configurations. In doing this, the classification as discussed in section 1.2.1 will be followed. The experimental information has been selected from the open literature and from unpublished results of the National Aerospace Laboratory NLR in the Netherlands. As far as possible results that were part of a larger systematic study have been used. In this way the internal consistency of the data could be checked to some extend. Moreover, only results with transition close to the leading edge have been used (with the exception, of course, of section 3.2). But it can not be excluded completely that part of the data still contain some measurement error or "pseudo-Reynolds number effects", as discussed in chapter 2.

The flow about two-dimensional airfoils has drawn a lot of attention in respect to Reynolds number effects. The attention is caused by the fact that the first high Reynolds number facilities were, because of their size, mainly used for two-dimensional testing. But also two-dimensional flow is relevant for high aspect ratio wings. Thus two-dimensional and high aspect ratio configurations are discussed together in one chapter.

To obtain a better understanding of the problems involved, this chapter has been sub-divided into a number of sections. As a first distinction the state of the boundary layer is used. Flows with a substantial amount of laminar boundary layer development are discussed separately from flows with a fully turbulent boundary layer. The reason is that transition location variations, laminar shock-wave boundary layer interactions and, in some cases, laminar separation bubbles introduce typical flow phenomena that are absent in flight where normally well developed turbulent boundary layers are found. Helicopter blades and the flow on propeller blades are an exception (due to the low chord Reynolds number), but they can be tested at their full scale Reynolds number in ground based facilities and do not represent an extrapolation problem. One other class of airfoils is excluded: the (either forced or natural) laminar flow airfoil. They deserve a very special attention from the point of view of Reynolds number effects which is beyond the scope of this AGARDograph. In section 3.2 a number of examples related to drag, maximum lift and pitching moment will be discussed to illustrate the point that tests with free transition behave qualitatively different from flows with mostly turbulent boundary layer development (whether caused by natural transition close to the leading edge or by artificial means such as fixation). Free transition results can even by very misleading for flight conditions.

The next two sections are only concerned with Reynolds number effects observed on configurations with fully turbulent boundary layer flow. This allows a systematic discussion of the problem. Use will also be made of the distinction (as discussed in section 1.2) between direct Reynolds number effects (resulting from changes in boundary layer development) and indirect Reynolds number effects (that appear as changes in pressure distribution). In section 3.5 the question how relevant two-dimensional flows are to high aspect ratio wings will be addressed. It will be argued that certain conditions must be met before one can speak of a good correspondence between two- and three-dimensional flows.

The last section of this chapter summarizes the preceding discussions especially in view of the usefulness of wind tunnel tests for flight prediction. The AGARD working group WG-09 addresses this topic specifically and for more information their final report should be consulted (see ref.00/1). However, the analysis presented in this chapter is hopefully useful in reducing the uncertainty implied in the full scale prediction on the basis of sub-scale wind tunnel tests.

3.2 Effects related to partly laminar boundary layer flow

3.2.1 *The direct effect on drag*

Boundary layer transition appears to be a function of Reynolds number, pressure distribution, sweep angle, flow quality, etc. On the basis of empirical criteria, it can be determined in principle if the boundary layer will be laminar or turbulent in the wind tunnel or in flight. For a smooth flat plate boundary layer the transition Reynolds number is 2 to 5×10^6 depending on noise level and turbulence intensity. This indicates that an airfoil with a flat pressure distribution might experience substantial regions of laminar flow for chord Reynolds numbers below 10×10^6. This will be even more true for laminar flow airfoils (like the NACA 6-series). For "peaky"-type pressure distributions the pressure gradient near the nose will trigger transition, almost independent of Reynolds number. Leading edge contamination complicates the situation even more for wings with an appreciable wing sweep. Therefore, at tunnel Reynolds numbers of the order of 3×10^6 laminar or turbulent boundary layer flow will be found, depending on wing geometry and flow conditions. For the same reason appreciable transition location variations might be found on wind tunnel models as the Mach number or the incidence is changed. On the other hand it is generally assumed that the boundary layer will be predominantly turbulent at flight Reynolds numbers (say in excess of 20×10^6) unless the airfoil has been designed specifically for laminar flow. By and large, appreciable differences in transition location are possible between wind tunnel and flight.

The skin fraction drag of a laminar boundary layer is significantly less than that of a turbulent boundary layer. Therefore, transition location variations have a very pronounced effect on drag. As a rule of the thumb one can state that a 1% chord transition point variation corresponds roughly with half a drag count. Consequently, transition point variations play a dominant role in the variation of drag with Reynolds number as is well illustrated when comparing test results with fixed and free transition (Fig. 3.2-1). Along the laminar lower-left branch of the drag curve in this figure transition moves closer to the airfoil nose till a Reynolds number of about 10×10^6. In this case the transition variation has been caused by a Reynolds number increase either in a direct way or by an increase in noise level or turbulence intensity. At constant Reynolds number the transition point might move as a result of a changing pressure distribution, e.g. with Mach number. This is typically observed on the upper surface of supercritical airfoils with a roof-type pressure distribution. A rather extreme case (18% thick supercritical airfoil) is presented in figure 3.2-2. The transition movement is coupled with the rearward movement of the shock (Fig. 3.2-3). The resulting effect on drag is strongly felt at Mach numbers in excess of 0.7

and shows up as a very deep drag bucket around the design Mach number. In this particular case the effect has been amplified by the fact that the turbulent boundary layer in combination with the shock causes a trailing edge separation below Mach = 0.7 as the trailing edge pressure development indicates. Less extreme examples for two other airfoils are presented in figure 3.2-4. Transition fixing near the nose completely eliminates the drag bucket near the design condition. The figure is also included to show how transition variations on the lower surface can easily be interpreted as a significant difference in drag creep between these two airfoils that have identical upper surface pressure distributions and differ only in the lower surface airfoil geometry. All these examples illustrate the necessity to measure and/or control the transition location on airfoils for accurate drag assessment.

3.2.2 Indirect effects on the pressure distribution

It could be argued that the change in airfoil contour through the relatively thin (either laminar or turbulent) boundary layer will have only a minor effect as far as the pressure distribution is concerned. This is, however, not entirely true. The Kutta condition is directly influenced by the boundary layers near the trailing edge. And the Kutta condition in turn affects significantly the overall circulation in addition to the effect of the boundary layer displacement thickness on the effective airfoil thickness and camber. Moreover, when boundary layer separations are present (e.g. a leading edge bubble, a separation underneath the shock or at the trailing edge) the interaction with the outer flow is an essential feature with substantial local or even overall effects on the pressure distribution. The difference between laminar, transitional or turbulent shock-wave boundary layer interactions is particularly important. The dominant effect appears to be a variation of the interaction length as discussed in more detail by Green (Ref. [71/2]; see also fig. 3.2-5). The extent of the interaction appears to decrease with increasing Reynolds number (apart from an anomaly at the lower turbulent Reynolds number range). This is all very well reflected in the pressure distributions as presented in the figures 3.2-6 and 3.2-7. Note that in the last example hardly any changes are noticeable in the pressure distribution with fixed boundary layer transition. These cases are very typical for the laminar-type airfoils of the 1950's as discussed in section 1.1.

The elimination of the high Mach number peak (as found with a turbulent boundary layer) due to the laminar shock-wave boundary layer interaction as shown in the preceding figures appears to be generally less pronounced for modern supercritical airfoils with a characteristic "roof-type" pressure distribution. The interaction region can still be recognized in the form of a pressure plateau ahead of the shock, but the dominant effect appears to be an upstream movement of the shock itself as indicated for two different airfoils presented in the figures 3.2-8 and 3.2-9. In both examples a change in pressure distribution can be noticed when the transition point is moved artificially (in an attempt to simulate Reynolds number changes) at constant Reynolds number. The very large effect on the shock position (as much as 30% chord for airfoil NLR 7301) is due to the interaction of the (almost) separated boundary layer at the trailing edge with the outer flow field, as can be observed from the trailing edge pressures. The upstream movement of transition thickens the boundary layer over the aft part of the airfoil, thereby hastening separation in addition to the already noted local effect of a laminar versus a turbulent shock-wave/boundary-layer interaction.

Figure 3.2.9 also shows a typical effect on the lower surface in the rear loading region. Just behind 50% chord, a laminar separation bubble can be observed in the case with natural transition. This bubble disappears with fixed transition but the very thick turbulent boundary layer causes a substantial reduction in rear-loading, especially with 7% and 15% fixation positions (where the turbulent boundary layer is possibly separated).

A final example, presented in fig. 3.2-10, is related to the nose region of an airfoil. Such a situation might occur at intermediate Mach numbers and high angles of attack. In this case transition fixation near the leading edge suppresses the formation of a laminar separation bubble at the lower Mach numbers. The appearance of a shock at higher Mach numbers complicates the situation further with possible effects on maximum lift development as argued in the report. This type of flow, however, is still not well understood (see also [Ref. 76/1]).

In all these cases large differences in pressure distribution between laminar and turbulent boundary layer development could be observed. Its significance in the context of Reynolds number effects is that the transition from a laminar to a turbulent boundary layer depends critically on the Reynolds number. Moreover, the flow quality in the wind tunnel is of considerable importance as well as discussed in chapter 2. Therefore similar effects as the ones shown here might be observed between wind tunnel and flight without any artificial boundary layer transition fixation. This can have serious consequencies for an evaluation of the overall wing characteristics.

3.2.3 Effects on lift and pitching moment

The variation of the pressure distribution with the extent of the laminar flow region as discussed in the previous section will of course also be reflected in the overall airfoil characteristics. Figure 3.2-11 (unpublished results of NLR) shows a selection of lift curves of a supercritical airfoil at one Reynolds number. In addition to the free transition case, the transition point has been changed artificially. It appears that with free transition the approximate linear relation between lift and incidence is lost, most notably for the highest Mach number. At Mach = .75 and c_l = .25 the natural transition location at the upper surface is close to the leading edge. It moves rapidly downstream, both with decreasing and increasing angle of incidence. In the latter case the transition point movement is coupled with the downstream movement of the shock, particularly at the higher Mach numbers and similar to that in figure 3.2-2 and 3.2-3. The transition variations are the cause of significant variations in the local lift curve slope, as compared with the turbulent case. Very similar effects have also been observed on other supercritical airfoils like the one presented in figure 3.2-13.

The effect on the pitching moment, figure 3.2-12, is even more dramatic, especially at the higher Mach numbers. At constant lift the pitching moment variation results from a redistribution of lift over the airfoil chord. For that reason variations in shock position give rise to significant pitching moment variations at the higher Mach numbers. But also small variations in the rear loading region at the lower surface (due to changes in the local boundary layer thickness) result in a significant but now almost constant shift over the complete Mach number range. Again, the non-linearities around a lift of .25 at Mach = .75 are eliminated completely with fixed transition.

The variation of maximum lift resulting from different transition point locations is also of some interest as the figures 3.2-11 and 3.2-13 indicate. With free transition, the more favourable boundary layer condition ahead of the shock and the improved boundary layer development downstream retards the separation as compared with the fixed transition case and leads to higher maximum lift values. It is also worth noting that the c_l-max development is qualitatively different for the higher Mach numbers: with natural transition the lift loss is much more gradual which is most likely caused by local effects of the laminar shock-wave/boundary-layer interaction. It is generally observed that transition fixation reduces the maximum lift value at the higher Mach numbers, or more specifically, at conditions where the pressure distribution shows a plateau region terminated by a shock further aft on the airfoil. In the lower Mach number range the situation is less clear. The local interaction of the shock with a laminar separation bubble, as discussed in section 3.2.2 (fig. 3.2-10) seems to result in a slightly higher maximum lift as compared with a turbulent boundary layer (fig. 3.2-14, related to the same airfoil). In another case however (fig. 3.2-12) a slightly lower maximum lift is observed in the case of free transition. As was already noted in Ref. [71/8] the local effects near the nose, and the way in which they interact with the boundary layer development further downstream, are less clear as compared with a flow which has the shock wave further downstream. Fortunately, the differences in maximum lift are also appreciable smaller at the lower Mach numbers.

All these examples illustrate that the state of the boundary layer (laminar or turbulent) significantly affects aerodynamic characteristics like drag, maximum lift or pitching moment. This is even more so when the transition location varies within a set of experimental results. These variations can be due to changes in pressure distribution (Mach or angle of attack) but they can also result from Reynolds number changes or unknown and uncontrolable wind tunnel environmental effects. Generally, such transition variations will be absent at flight conditions due to the high Reynolds number and surface roughness. For the evaluation of wind tunnel test results it is advisable to either control transition or measure its location.

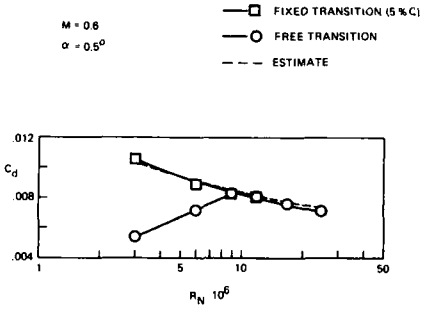

Fig. 3.2-1 Variation of subsonic airfoil drag with Reynolds number (from ref. 68/1)

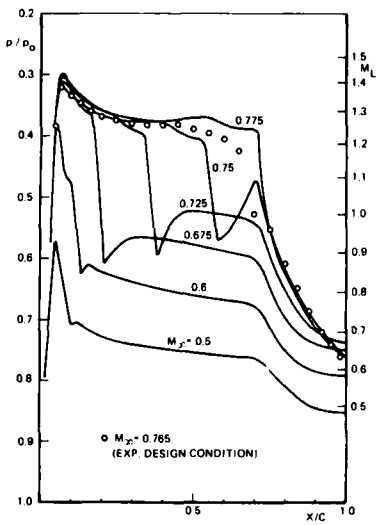

Fig. 3.2-2 Development of the pressure distribution in the transonic regime indicating the development of a pressure plateau with laminar boundary layer flow (from ref. 78/2)

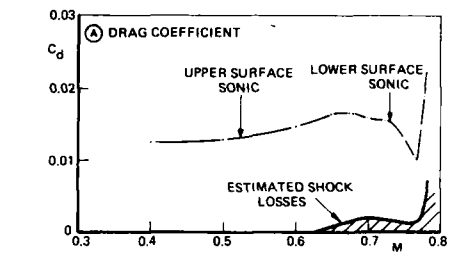

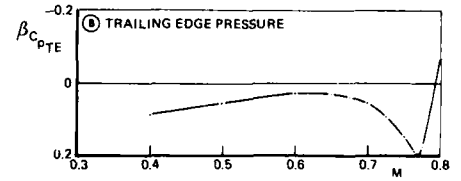

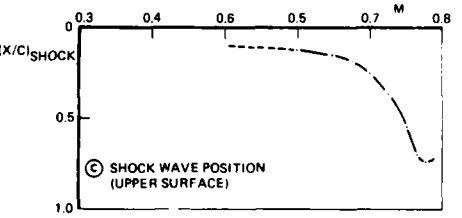

Fig. 3.2-3 Variations in drag and trailing edge pressure due to transition point movement coupled to the shock wave displacement (see figure 3.2-2)

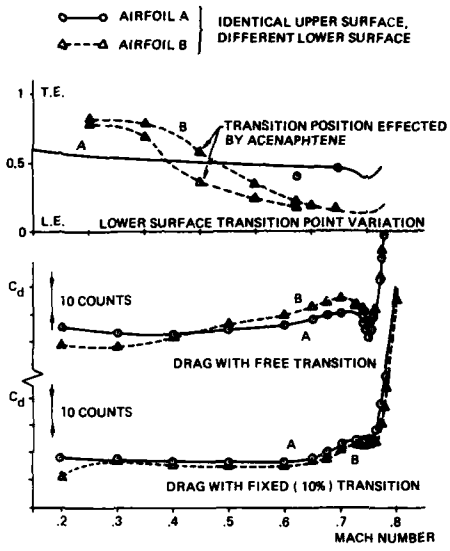

Fig. 3.2-4 The effects of transition point variations on drag creep (from ref. 84/2)

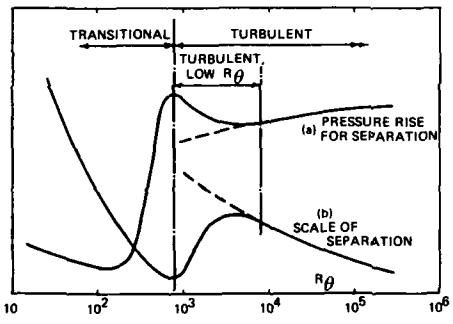

Fig. 3.2-5 Effect of Reynolds number on some properties of shock-induced separation at Mach = 1.5 (conjectural; ref. 71/2)

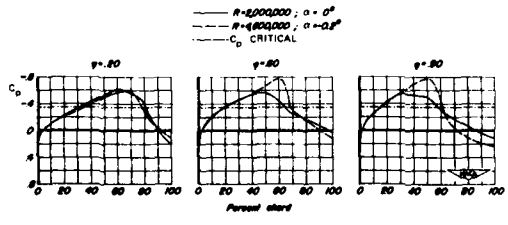

Fig. 3.2-6 Effect of a Reynolds number increase on the pressure distribution presumably caused be a change from laminar to turbulent shock-wave/boundary-layer interaction (from ref. 52/2)

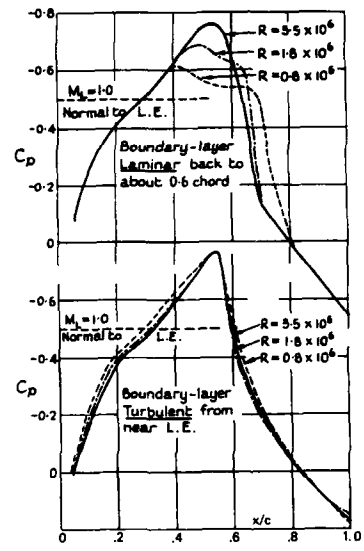

Fig. 3.2-7 Effect of Reynolds number and artificial boundary layer fixation on the pressure distribution (from ref. 55/1)

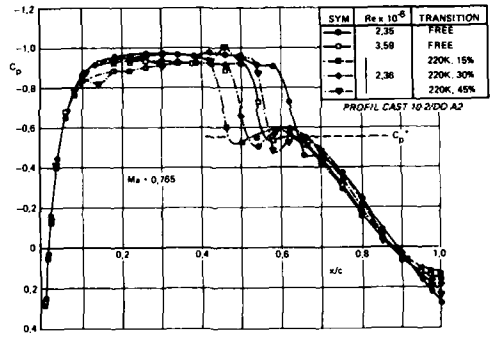

Fig. 3.2-8 Effect of transition point changes on the pressure distribution of a supercritical airfoil (from ref. 81/1)

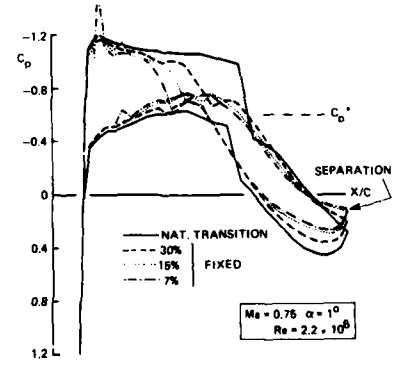

Fig. 3.2-9 Effect of transition point changes on the pressure distribution of a supercritical airfoil (from ref. 84/2)

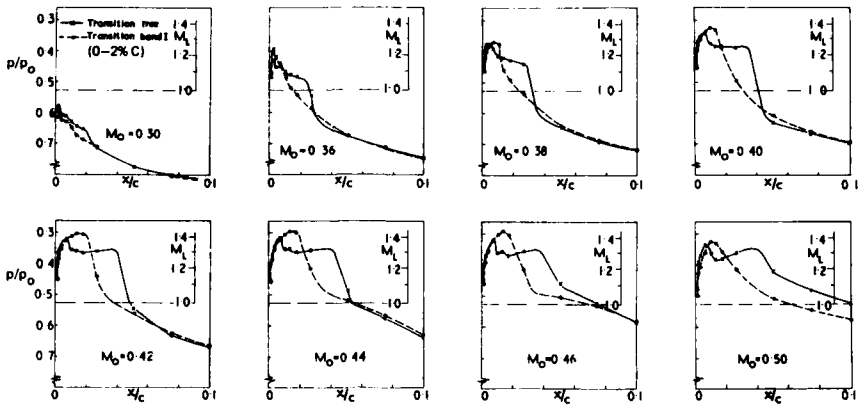

Fig. 3.2-10 Effect of transition fixation near the leading edge at intermediate Mach numbers (from ref. 71/8)

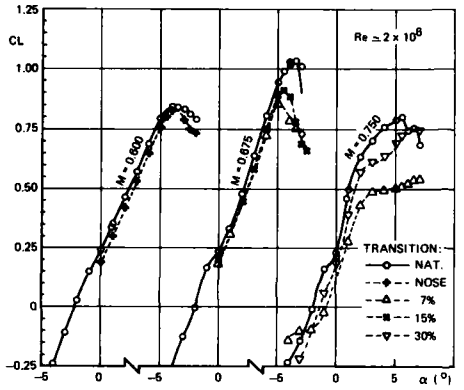

Fig. 3.2-11 Effect of transition fixation on lift development of a supercritical airfoil for various Mach numbers

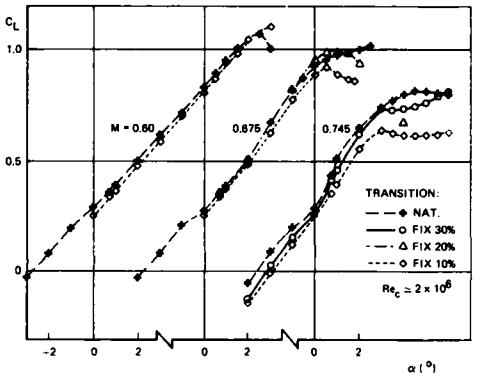

Fig. 3.2-13 Effect of transition fixation on lift development of a supercritical airfoil for various Mach numbers

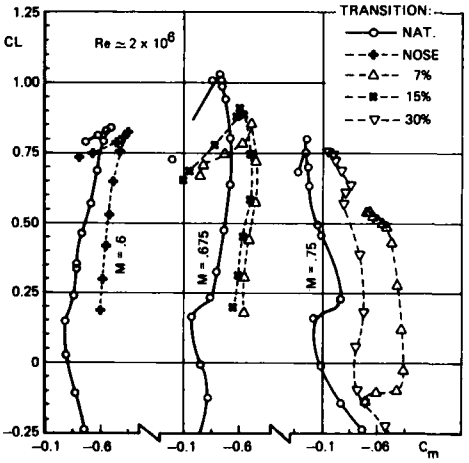

Fig. 3.2-12 Effect of transition fixation on pitching moment development of a supercritical airfoil for various Mach numbers

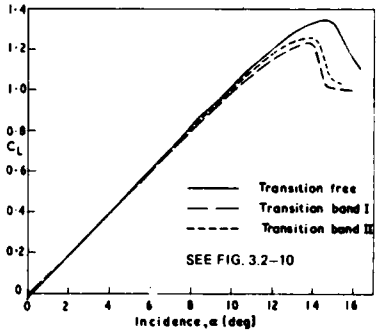

Fig. 3.2-14 Effect of transition fixation on maximum lift at an intermediate Mach number (see also fig. 3.2-10)

3.3 Flows with (almost) attached turbulent boundary layers

3.3.1 The pressure distribution - overall effects

In this and the following sections only results with turbulent boundary layer flow (either natural or artificially tripped) will be considered. They constitute a class of flows with a Reynolds number effect in the most pure way. A very obvious, but unfortunately not so easy, comparison can be made between wind tunnel and flight. Some examples are shown in the figures 3.3-1, (a) to (e) taken from the references [66/1], [68/2] and [72/3]. In the subcritical case (a) and the supercritical cases (c) and (d) the differences in pressure distribution are small with, for the latter cases, variations in shock position of 5% chord at most. The cases (b) and (e) seem to indicate a separation in the wind tunnel that was not observed in flight and vica-versa. In case (b) this separation is connected with a large shift in shock wave position: this case is the almost classical example how Reynolds number can change the pressure distribution. In case (e) the shock position remains virtually unchanged. In reference [72/3] it was reported that interference effects from the pressure tubing as used in flight were believed to have influenced the pressure readings here, although three-dimensional separation effects (see section 3.5) were not excluded. This may be another example (see chapter 2) that Reynolds number effects and measuring problems are not always easy to separate. Case (b) seems to suggest that separation of the boundary layer is of importance. Separation effects will be discussed more extensively in the next section. In this section we will be concerned mainly with attached or almost attached (only local trailing edge separation) flow conditions.

The example (e) illustrates that wind tunnel/flight comparison is not always an easy matter. Fortunately, pressurized wind tunnels provide the means for systematic studies and some typical results are presented on the figure 3.3-2 to 3.3-7. They are mainly taken from unpublished work at NLR, studies made by Stanewsky at DFVLR [Ref. 81/1] and studies made by Blackwell [Ref. 76/4]. Reynolds number effects as reflected in the pressure distribution are (by definition: see section 1.2.1) "indirect Reynolds number effects": the change in pressure distribution due to a variation in the (turbulent) boundary layer development. The "regular" part of the pressure distribution change is due to the thinning of the boundary layer with increasing Reynolds number (the displacement thickness being roughly proportional to $Re^{-1/5}$). Consequently the effective airfoil thickness decreases and the effective camber increases. Of these two effects, the latter appears to be the most important, especially over the rear part of the airfoil, resulting in a local load increase. For a comparison at constant lift, as shown in figure 3.3-2, the increase in load over the aft part of the airfoil must be compensated by a decrease in load over the front of the airfoil, that is realized by a decrease in angle of incidence. This feature is common to all pressure distributions of figure 3.3-2. The shock wave movement appears to be less consistent. With the lessening of viscous effects over the rear of the airfoil the shock wave moves downstream (in the limiting case of inviscid flow the shock will be farthest downstream). The decrease in angle of incidence (to keep the lift the same) moves the shock, in general, more upstream. The final outcome of these opposite effects will depend on their relative strength: a downstream movement in the figures 3.3-2 (b) and (d), an upstream movement in case (c). The change from an upstream to a downstream shock movement is very regular as figure 3.3-3 (b) indicates. In this case the variations in shock position at constant lift appear to be rather small. Near the design condition, however, larger differences can be observed as discussed in section 1.2.3 (figure 1-7). It is due to the fact that the flow is often sensitive to any small change near the design condition. Figure 3.3-2 (a) provides an other example: a similar change from a double to a single shock can be obtained at constant Reynolds number with a small increase in angle of incidence. These moderate changes in pressure distribution (except for the design condition) are also reflected in the small decrease in shock strength at constant lift (fig. 3.3-3 (a)). Is the airfoil of figure 3.3-2 possibly a not so extreme case from the point of view of aerodynamic loading? The pressure distribution reveals a moderate amount of rear loading and the airfoil does not show appreciable variations in trailing edge pressure with Reynolds number. Such variations do appear to be much larger for another supercritical airfoil, CAST-10, as reported in [Ref. 81/1] and corresponding with the pressure distribution as already presented in figure 3.2-8. However, when the variation of shock wave strength and position is plotted for the two airfoils as a function of lift and/or Mach number, rather similar variations are observed (see fig. 3.3-3 and 3.3-4). Also the results of other airfoils (this time at constant incidence) as given in the figures 3.3-5 to 3.3-7 and reported by Blackwell [Ref. 76/4] reflect rather small changes in pressure distribution. Note also that the Reynolds number effect on the NACA airfoil at high lift is similar to those observed on the two supercritical airfoils.

These moderate variations in pressure distribution should not come as a surprise. All the examples are related to attached, or almost attached (limited trailing edge separation at most) flow conditions. When separations are present the variations in pressure distribution are considerably larger as was already illustrated with figure 3.3-1b. Moreover, variations with Reynolds number at constant angle of incidence may be a little bit larger.

3.3.2 The pressure distribution - local effects

In combination with the rather regular and global Reynolds number effect on the pressure distribution due to effective thickness and camber variations a number of local effects should be noted.

* Local separation underneath the shock

The interaction between the shock wave and the (turbulent) boundary layer will depend on Reynolds number. A very good review is given by Delery and Marvin [Ref. 85/12] and they indicate that incipient separation occurs at a shock Mach number close to 1.3 almost independent of Reynolds number. However, beyond incipient separation a local separation at the foot of the shock is sometimes clearly visible in the pressure distribution (see e.g. figure 3.4-4). Extensive correlations made by Fulker and Ashill [Ref. 85/4] indicate that the length of the separation bubble roughly scales with the thickness of the incoming boundary layer and will therefore be Reynolds number dependent. The development of this separation bubble is of prime importance for defining the location of the separation boundaries in the C_l-Mach plane (see 3.4).

* Second expansion behind the shock

In some cases, depending on the local curvature of the airfoil, the second expansion behind the shock can be so strong that locally a second shock is generated. A thick turbulent boundary layer in this region will reduce the local surface curvature, but at higher Reynolds numbers this second shock may very

well increase in strength, possibly with significant consequencies for the drag development; see fig. 3.3-9 taken from Ref. [76/2] as a typical example. (It was noted later that some of the high Reynolds number data are invalid because of inadequate side-wall suction). The effect might be important when large variations in surface curvature occur just downstream of the shock position as measured in the wind tunnel.

* Lower surface separation

A third local effect in the pressure distribution, already mentioned in section 3.3.2 (fig. 3.2-9), can be noted on the lower surface of the airfoil in the rear loading region as typically found on modern supercritical airfoils. The steep local pressure gradient might provoke boundary layer separation at lower Reynolds numbers. In the concave airfoil contour this separated boundary layer will most likely reattach a bit further downstream. For this reason this kind of separation is sometimes hardly visible in the pressure distribution and difficult to detect. In more extreme cases it will cause an appreciable loss of lift in the lower surface rear loading region. In that case the effect on drag can be considerable, in a direct way through lower surface separation drag and in an indirect way through increased shock strength at the upper surface to keep the total lift constant. The effect can be assessed experimentally by comparing drag of a forward and rear fixation position after a correction for the length of the laminar boundary layer.

* Local trailing edge separation

The last and most important local effect on the pressure distribution is a limited or local separation near the trailing edge. When the "load" on the boundary layer increases (higher lift or Mach number, lower Reynolds number) a small separation will start to develop at the trailing edge and will gradually move upstream. The term "local" is used here to distinguish this separation from one that extends from shock to trailing edge as will be discussed later. The extent of this separation is difficult to establish both experimentally and theoretically. In fact one might argue that there is hardly any difference between a locally separated boundary layer and a thick turbulent boundary layer in this region. This is partly due to a stabilizing effect of the interaction with the outer flow: the thick turbulent boundary layer over the rear of the airfoil decreases the trailing edge pressure and reliefs the severity of the pressure gradient. This separation will modify the Kutta condition and hence the circulation around the airfoil. It is to be expected that the local separation will therefore contribute to some loss of lift at constant angle of incidence with decreasing Reynolds number. As long as the separation is restricted to a small part of the chord (say 10% of chord), the effects will be gradual. However, at a certain stage in the separation development a sudden and complete flow break-down can occur as indicated by a rapid increase in trailing edge pressure. This situation is complicated further by the interaction between the trailing edge separation and the bubble underneath the shock. This process will be discussed in more detail in section 3.4. Here only conditions with a small and localized separation (either underneath the shock or at the trailing edge) will be considered. It is believed, and to some extend justified by the evidence presented till now and still to come, that such local separations will have, in general, a minor and gradual effect on the pressure distribution. Some indication of local trailing edge separation can be obtained by plotting trailing edge pressure versus lift or Mach number as illustrated in the figures 3.3-10, 11 and 12. The low trailing edge pressures seem to indicate that the NACA airfoil at 3° angle of attack (fig. 3.3-10) has developed a trailing edge separation at low Reynolds number that disappears at higher Reynolds number. This is also the case for the CAST-10 airfoil (fig. 3.3-12) at the lowest Reynolds number (and prior to flow break-down as indicated by the rapid decrease on trailing edge pressure). It is believed that these local separations are of particular significance for the evaluation of drag and pitching moment as will be presented in the next sections.

3.3.3 Lift and pitching moment

The lift curves related to the two supercritical airfoils as discussed in the previous section (see fig. 3.3-2 to 3.3-4) are presented in the figures 3.3-13 and 3.3-14. The decrease in angle of incidence for constant lift is more pronounced when the viscous effects are stronger e.g. at higher lift and Mach numbers. This appears as a shift and a rotation of the c_l-alpha curves. Note also that the largest variations in α with Reynolds number are found at low Reynolds numbers. The results of airfoil CAST-10 and model "A" are similar in this respect.

The variation of lift, pitching moment and trailing edge pressure with Mach number (this time at constant incidence) for both airfoils is presented in the figures 3.3-11 and 3.3-12. Both lift and pitching moment show an appreciable variation with Reynolds number, this being the most extreme for CAST 10-2. This is only partly due to the indirect Reynolds number effect on shock wave position. An equally important contribution arises from a loss of lift with decreasing Reynolds number over the aft part of the airfoil due to the local decambering effect of the thick boundary layer. As discussed before, the trailing edge pressure development might be viewed as an indicator for the severity of the viscous effects. A comparison of its development for the two airfoils is therefore of interest. In both cases a very regular variation of trailing edge pressure with Mach number is observed. The CAST-10 airfoil, being closer to separation at the design condition as boundary layer calculations reveal, shows at the lowest Reynolds number even a decrease in trailing edge pressure with increasing Mach number (where the Prandtl-Glauert rule would suggest an increase), a situation that is often indicative of local trailing edge separation. It is of interest to note here that the lift and pitching moment variations correlate well with the trailing edge pressure development before as well as after flow breakdown as indicated by the rapid decrease in trailing edge pressure.

The increase in lift at constant incidence with Reynolds number has already been discussed. With respect to its variation with Mach number, theory suggests a development that follows approximately the Prandtl-Glauert rule. The results as presented in the top of figures 3.3-11 and 3.3-12 illustrate very well that viscous effects modify this development in a Reynolds dependent way and for the CAST-10 airfoil (low Re) even to such an extent that an almost constant lift is found. Also the pitching moment (up to lift-divergence) is in this case almost constant. One can conclude that the viscous effects appear to be stronger on the CAST-10 airfoil. Nevertheless, the two airfoils behave qualitatively very similar.

The study of Blackwell [Ref. 76/4] supports this view as the figures 3.3-6 and 3.3-7 and 3.3-10 indicate. In all cases the lift and pitching moment varies very regular with Reynolds number. The largest changes with Reynolds number are observed at higher lift or Mach number conditions and at the lowest Reynolds number range where viscous effects are more pronounced.

3.3.4 Drag and drag-divergence

In the analysis of drag it is useful to distinguish between flat-plate skin friction drag, subsonic minimum airfoil drag, subsonic lift dependent drag, compressibility drag and drag-divergence.

* Flat plate skin friction drag

There are many expressions for the Reynolds number dependence of flat plate skin friction drag as indicated in fig. 3.3-15. Skin friction is approximately proportional to $Re^{-1/n}$ with n = 2 for a laminar and n 5 for a turbulent boundary layer. As a result of this large difference in Reynolds number dependence, the transition location must be accurately known for drag evaluation as already discussed in section 3.2. All results presented in this section are obtained with artificial fixation near the nose or for conditions at which the Reynolds number was so high that natural transition could be expected in the nose region. When necessary corrections for a (small) region of laminar flow have been made.

* Subsonic minimum airfoil drag

It is common practice in drag evaluation studies to split-up the subsonic drag in a zero lift and a lift-dependent (viscous and induced drag) contribution. However, modern airfoils are designed for a particular lift and for that reason far from symmetric. Consequently, zero-lift drag is not necessarily minimum drag. The airfoil might even show separation at zero lift! Also the induced drag of a wing of finite span is not necessarily zero at zero lift. For that reason the term subsonic minimum airfoil drag is used in a rather pragmatic way.

Minimum airfoil drag is often estimated with so-called form factor methods. They express essentially the airfoil drag as the flat plate skin friction drag multiplied by the form factor that depends on the airfoil thickness. The form factor accounts, in fact, for some kind of average of the flow velocity over the airfoil. Typical examples of the variation of experimentally observed drag values are presented in figure 3.3-16. Although drag is not accurately predicted, the variation with Reynolds number follows closely a skin friction law.

* Subsonic lift dependent drag

A summary of some lift dependent drag values is presented in figure 3.3-17. In this figure the minimum drag as estimated with a form factor method has been subtracted from the experimental values. Moreover, the results have been divided into a low and a (moderately) high Reynolds number range. This particular representation has been chosen to show the much larger variation in lift dependent drag for the low Reynolds number cases. It should also be noted that the most "extreme" airfoils (CAST-10 and model "B", as established from boundary layer calculations) show the largest deviations. For that reason it is suggested that local trailing edge separation (or at least a very thick boundary layer) increases the drag significantly. This is of some practical importance when low Reynolds number wind tunnel data have to be extrapolated to flight values on the basis of a well established skin friction trend; the drag might then be over-estimated by as much as 10%. Also, a particular airfoil, disregarded since it had a relatively high drag at the tunnel Reynolds number might very well be acceptable or even superior to other airfoils that apparently performed much better in the tunnel. This is another illustration of the point raised by Haines [Ref. 79/2] in his plea that high Reynolds number facilities are important for aircraft design and drag optimization. Although trailing edge separation can be detected in the wind tunnel or (approximately) calculated from boundary layer theory, it seems hardly possible, at present, to either correct or predict the resulting drag penalty of such a local separation.

* Compressibility drag

The compressibility drag is often defined as the drag increase at constant lift relative to a subsonic condition. Compressibility drag is partly the result of a (slight) decrease in flat plate skin friction drag with increasing Mach number and an adverse effect on the boundary layer development due to substantial changes in the pressure distribution as a result of transonic effects. Both effects are represented rather crudely in some form factor methods (by a compressible skin friction law and by Prandtl- Glauert scaling of the airfoil thickness). This drag creep contribution can be calculated more accurately from a boundary layer calculation. However, when the boundary layer is separated or close to separation (as is very often the case) such a simple calculation will under-estimate the drag and hence also its Reynolds number dependence due to the pressure gradient "relief" of the thick boundary layer. Only more recently, calculation methods that model in a fundamental way the interaction between the boundary layer (including separation) and the outer flow field (so called strong interaction) are able to give good quantitative results for not so strong shock waves [see Ref. 85/10 and 85/11]. The other major contribution to compressibility drag results from the shock wave development and the interaction with the boundary layer. The Reynolds number effect on the shock wave development is by definition an indirect Reynolds number effect. In the figures 3.3-2 to 3.3-7 it was already noted that the Reynolds number effect on shock wave strength at constant lift is small. Nevertheless, in view of the large sensitivity of the wave drag to the shock Mach number, quite small changes in pressure distribution may lead to a substantial increase or decrease in compressibility drag. The existing evidence does not indicate that such large variations in compressibility drag are generally found as the figures 3.3-5, -7, -8, -18, -19 illustrate. Supercritical airfoils are designed for a low drag creep by restricting through design the shock wave development with Mach number. Figure 3.3-18 suggests that the drag creep closely follows the form factor estimate for lift values slightly below the design lift, with little room for wave drag. The wave drag contribution increases with lift, but even then the Reynolds number dependence appears to be almost nil for airfoil "A". The CAST-10 airfoil on the other hand (fig. 3.3-19) reveals a much larger dependence on Reynolds number. Since, however, the shock wave development is not to different for these two airfoils (see fig. 3.3-3 and 3.3-4) it is suggested that local trailing edge separation is also of importance for this different behaviour. Like the lift dependent subsonic drag, the effect is most pronounced for the lowest Reynolds number.

The drag creep results as presented in the figures 3.3-5 up to 3.3-8 generally seem to confirm this view. The variation with Reynolds number is small except for the 21% thick airfoil of figure 3.3-7. Note however that for this extreme thick airfoil a subsonic (below Mach = .5) drag increase of 10 counts (relative to a form factor estimate) is observed when the Reynolds number is changed. This is somewhat similar to the observations of the lift dependent drag for the CAST-10 airfoil.

Although these results seem to indicate a rather consistent view with respect to compressibility drag, one should be careful in generalizing these findings. The airfoil discussed in section 3.3.2 and for which the pressure distribution is presented in figure 3.3-9 experiences an unfavourable Reynolds number effect on drag creep due to a very pronounced secondary expansion at higher Reynolds numbers. An other extreme case is presented in the figures 3.3-20 to -22. This airfoil (the same one as shown in figure 1-8) shows a dramatic increase in drag with Reynolds number when evaluated at constant incidence (α = 1.3°), whereas a favourable development is found at constant lift (fig. 3.3-20). This behaviour can be understood from the development of the pressure distributions (fig. 3.3-21 and -22). Due to trailing edge separation at the lowest Reynolds number the shock moves aft when the Reynolds number is increased. This is accompanied with a pronounced increase in shock strength at constant incidence leading to an increase in wave drag that, at the highest lift values, more than compensates the decrease in viscous drag. At constant lift, however, the shock still moves aft, but the lower incidence (to keep the lift constant) reduces the shock strength such that the total drag decreases (note the revised trend in suction peak level with increasing Reynolds number). The example nicely illustrates the importance of evaluating Reynolds number effects, especially as far as drag is concerned, at constant lift as discussed in section 1.2.3. (fig. 1-10). In all cases a very careful examination of the pressure distribution is required before a high Reynolds number estimate can be made with some confidence.

* Drag divergence

The sharp rise in drag with increasing Mach number as experienced in the transonic regime is often called drag divergence. Its boundary in the C_L-Mach number plane limits the region of economic flight. Drag divergence is distinct from drag creep: the gradual increase of drag prior to drag divergence and also due to compressibility effects. The drag divergence boundary can be derived from plots similar to figure 3.3-18. Various definitions are possible here like d C_D/d Mach (at constant lift) = 0.1 as used in figure 3.3-23. Drag divergence is basically an inviscid flow phenomenon caused by a rapid, non-linear increase in shock strength. Viscous effects will modify the drag divergence boundary to the extent that they modify the pressure distribution. For that reason Reynolds number effects on drag divergence will be small when the indirect Reynolds number effects (changes in pressure distribution due to Reynolds number) are small. Figure 3.3-23 shows some typical examples of the Reynolds number effect on drag divergence in addition to the drag results as shown in the figures 3.3-5, -7 and -8. In general, the effects appear to be very small. Only the results of the CAST-10 airfoil show a much stronger effect. This is not well understood, but it is possible that local trailing edge separation is also to blame.

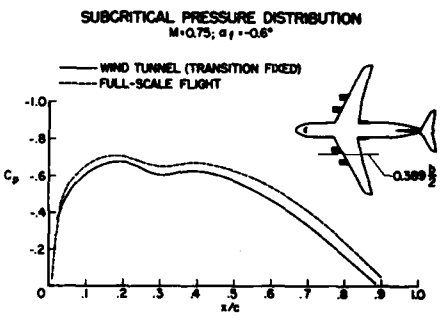

Fig. 3.3-1a Comparisons of pressure distributions for wind tunnel and flight - C-141, subcritical -

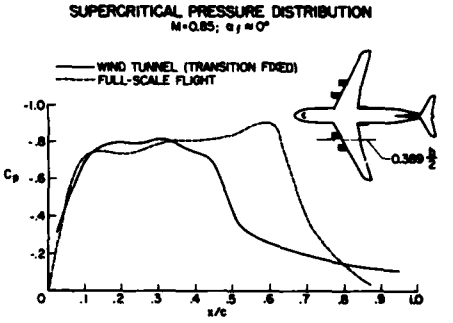

Fig. 3.3-1b Comparisons of pressure distributions for wind tunnel and flight - C-141, supercritical -

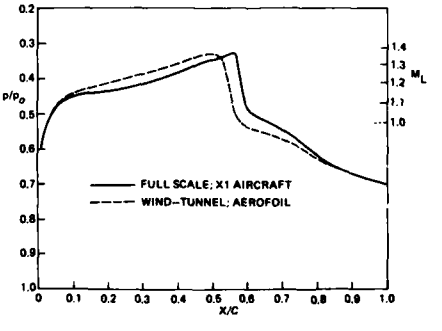

Fig. 3.3-1c Comparisons of pressure distributions for wind tunnel and flight - X-1 aircraft -

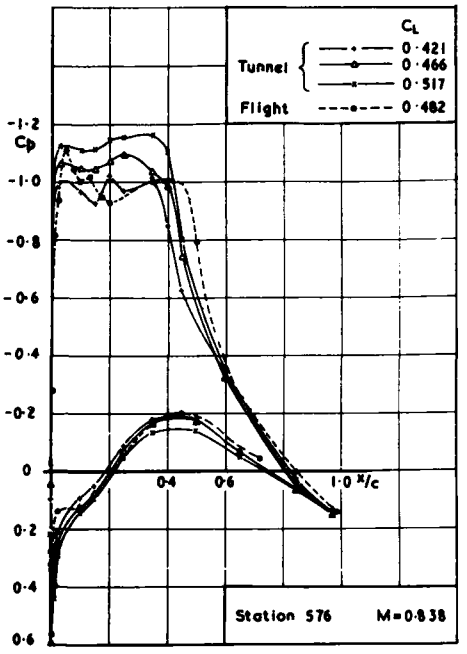

Fig. 3.3-1d Comparisons of pressure distributions for wind tunnel and flight - VC-10 -

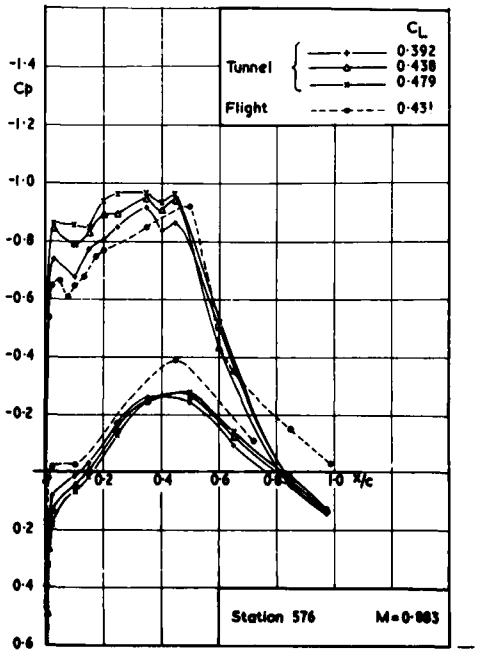

Fig. 3.3-1e Comparisons of pressure distributions for wind tunnel and flight - VC-10 -

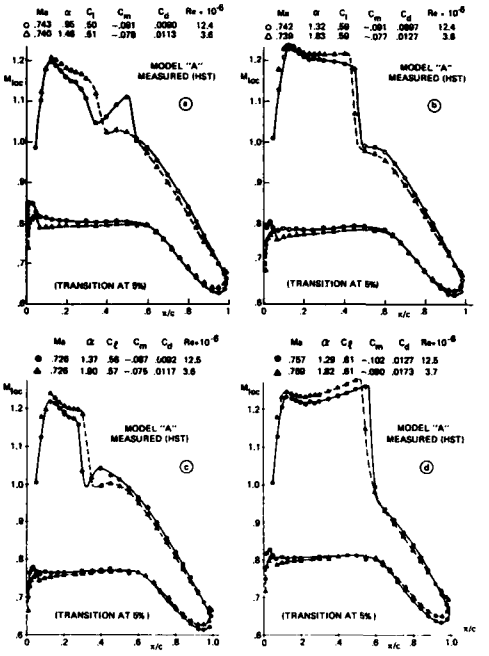

Fig. 3.3-2 Example of indirect Reynolds number effects on a supercritical airfoil

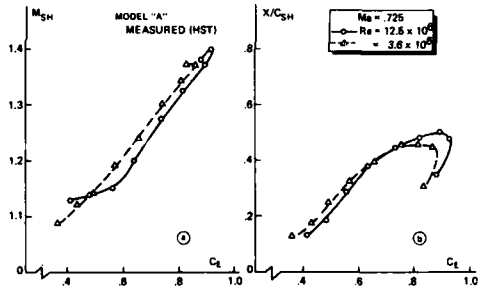

Fig. 3.3-3 Development of shock strength and position with lift for two Reynolds numbers (unpublished results of NLR/HST, model "A")

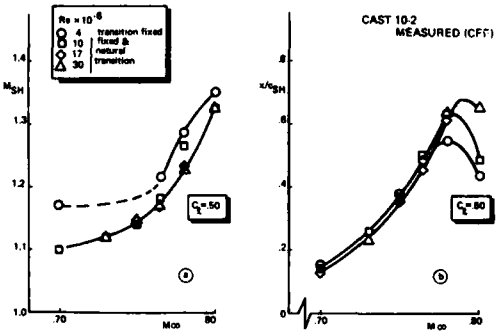

Fig. 3.3-4 Development of shock strength and position with Mach number (CAST 10-2 airfoil)

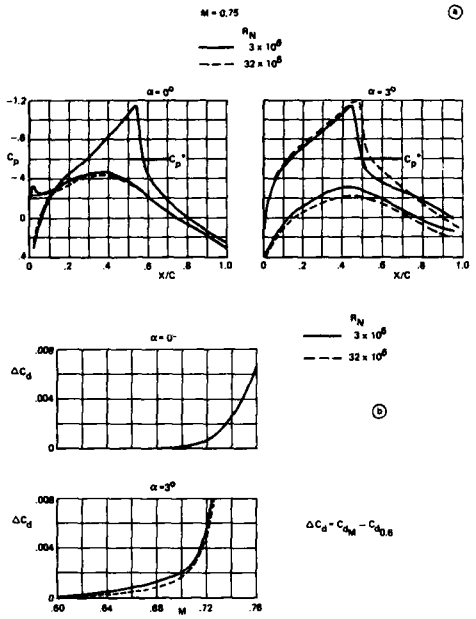

Fig. 3.3-5 Reynolds number effects for a conventional (NACA 65,- 213) airfoil (from ref. 76/4)

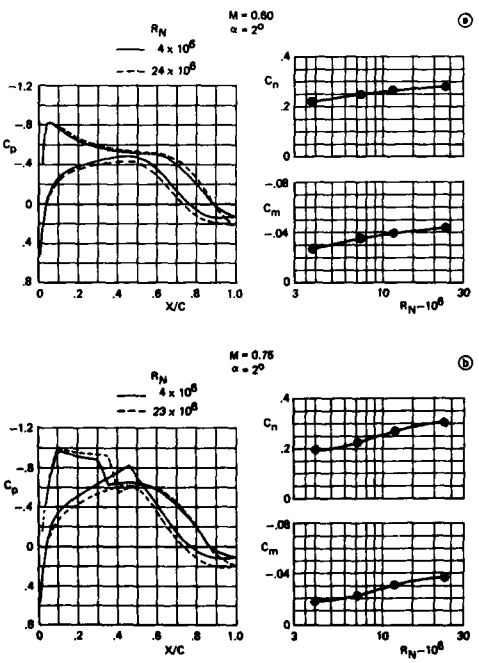

Fig. 3.3-6 Reynolds number effect for a supercritical airfoil (from ref. 76/4)

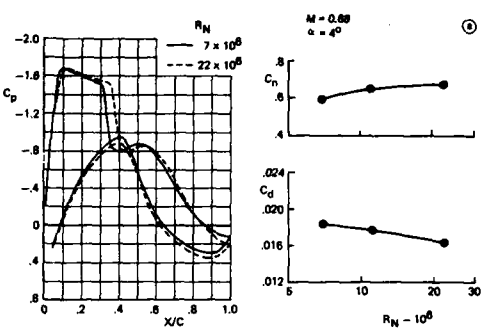

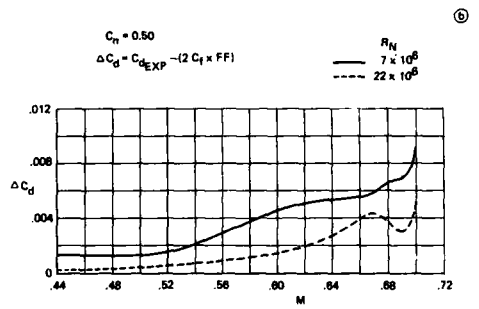

Fig. 3.3-7 Reynolds number effect for a thick supercritical airfoil (from ref. 76/4)

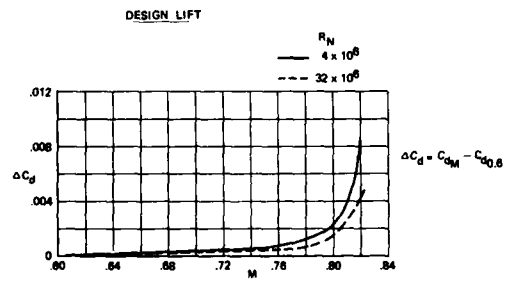

Fig. 3.3-8 Reynolds number effect on compressibility drag for a supercritical airfoil (from ref. 76/4)

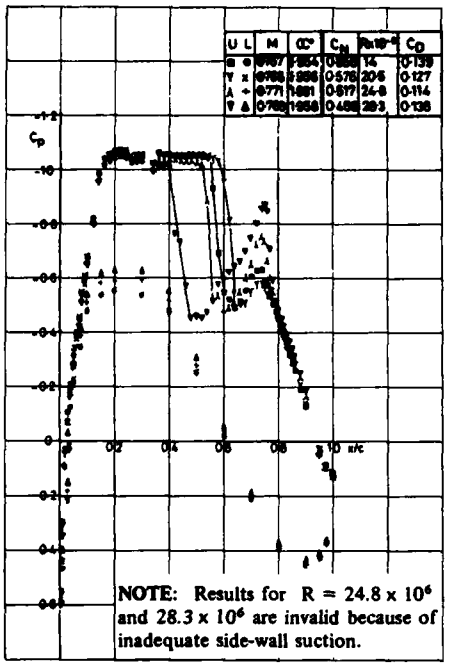

ⓐ BEFORE DRAGRISE

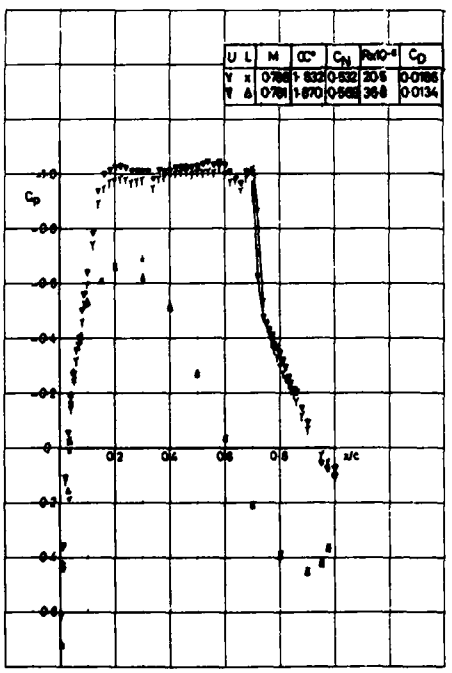

ⓑ AFTER DRAG RISE

Fig. 3.3-9 Example of Reynolds number effect on second expansion behind the shock (from ref. 76/2)

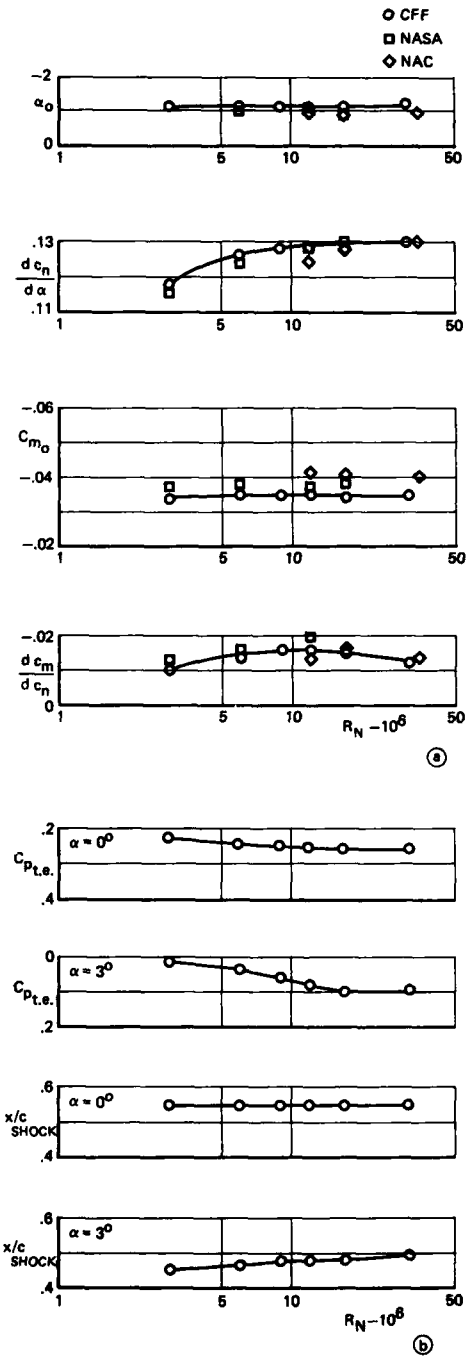

Fig. 3.3-10 Reynolds number effect of some aerodynamic characteristics for a conventional (NACA 65,- 213) airfoil (from ref. 75/3)

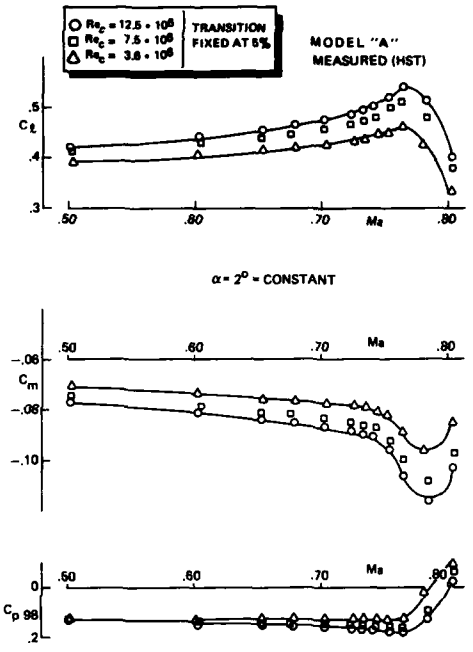

Fig. 3.3-11 Development of lift, pitching moment and trailing edge pressure with Mach number for a supercritical airfoil (unpublished results of NLR/HST Model "A")

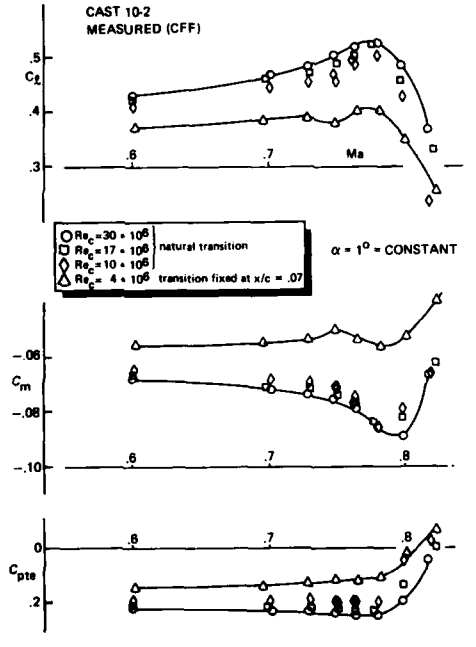

Fig. 3.3-12 Development of lift, pitching moment and trailing edge pressure with Mach number for a supercritical airfoil (Airfoil CAST 10-2)

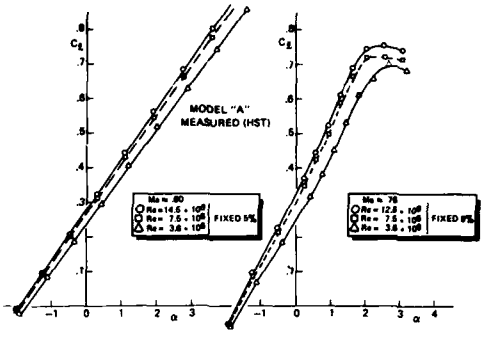

Fig. 3.3-13 Lift-curves of a supercritical airfoil for various Reynolds numbers (unpublished results of NLR/HST Model "A")

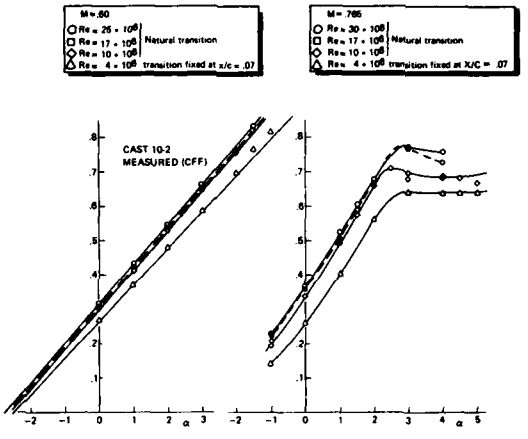

Fig. 3.3-14 Lift-curves of a supercritical airfoil for various Reynolds numbers (CAST 10-2 Airfoil)

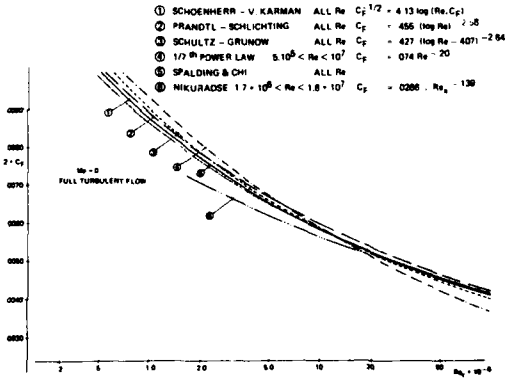

Fig. 3.3-15 Summary of flat-plate skin friction variation with Reynolds number

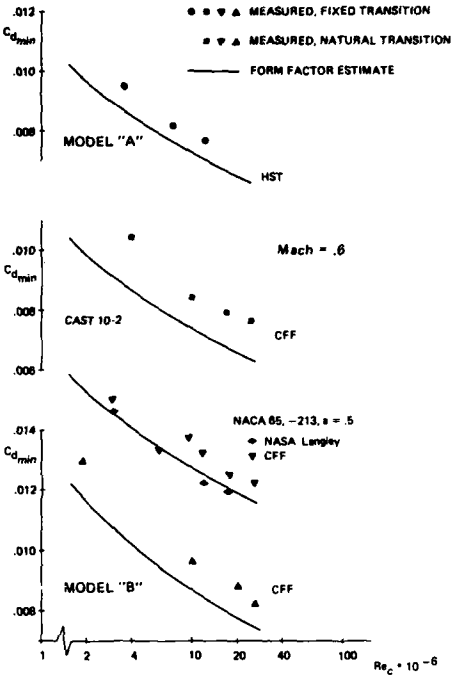

Fig. 3.3-16 Development of subsonic minimum airfoil drag with Reynolds number (various sources)

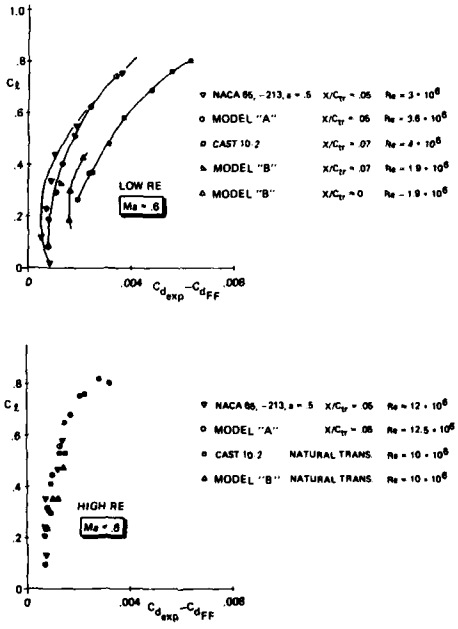

Fig. 3.3-17 Subsonic lift-dependent drag for low and high Reynolds numbers (various sources)

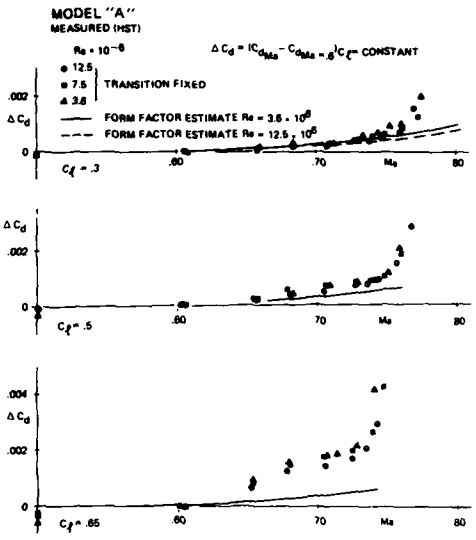

Fig. 3.3-18 Drag creep at constant lift for different Reynolds numbers (unpublished results of NLR/HST; Model "A")

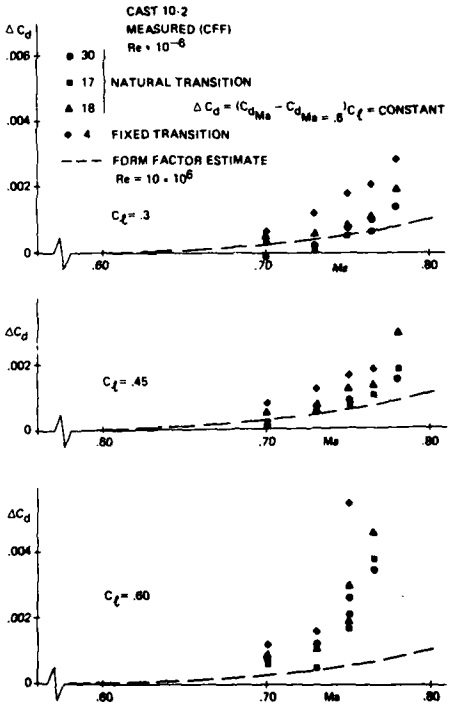

Fig. 3.3-19 Drag creep at constant lift for different Reynolds numbers (CAST 10-2 Airfoil)

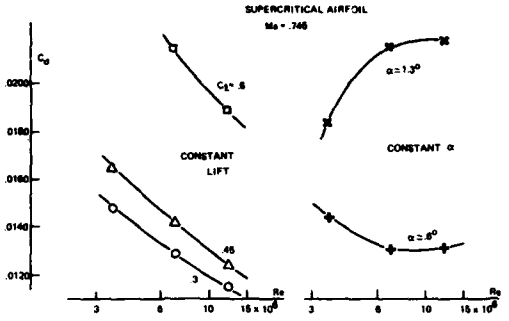

Fig. 3.3-20 Supercritical drag development with Reynolds number: evaluation at constant lift versus constant incidence

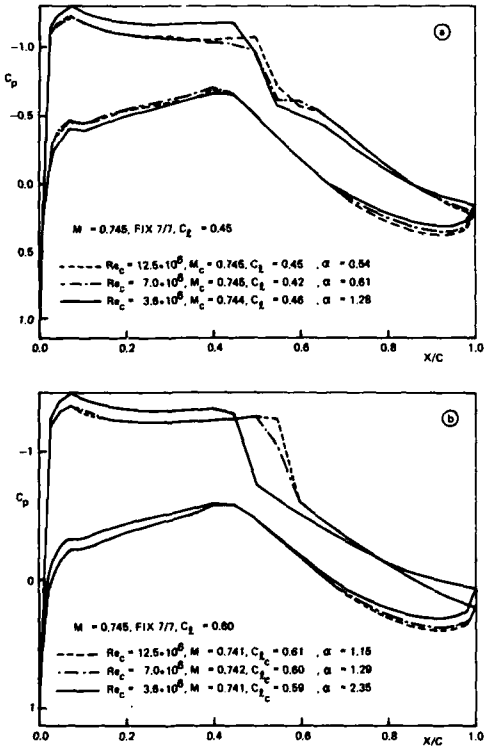

Fig. 3.3-21 Variation of a supercritical pressure distribution with Reynolds number at constant lift

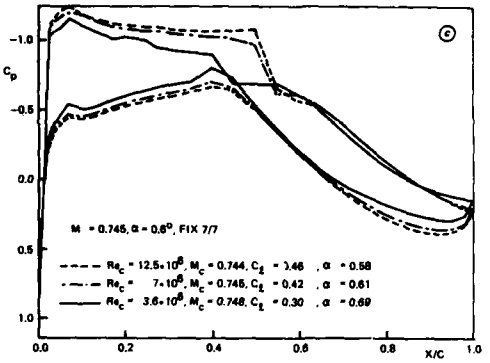

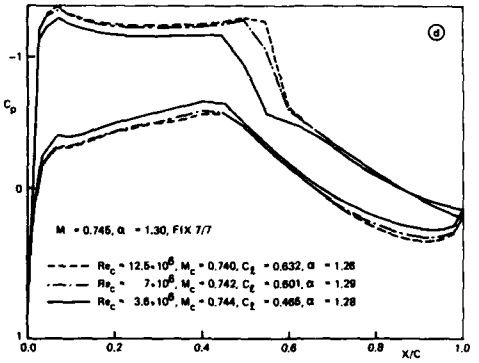

Fig. 3.3-22 Variation of a supercritical pressure distribution with Reynolds number at constant incidence

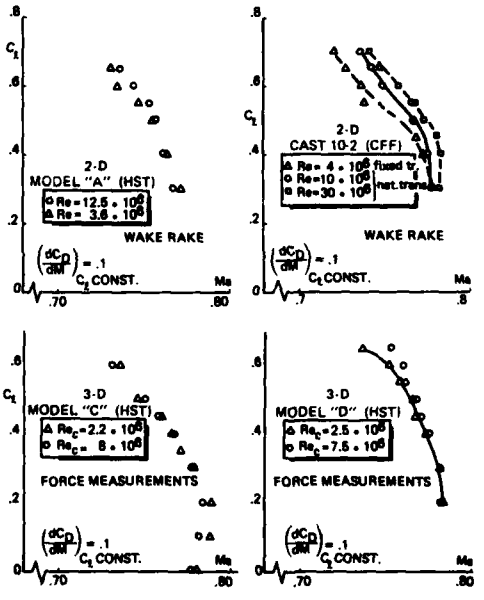

Fig. 3.3-23 Examples of Reynolds number influence on drag-divergence boundary

3.4 Flows with turbulent boundary layer separation

3.4.1 The classical distinction between type "A" and "B" separation

Most of the earlier work on Reynolds number effects was related to (the onset of) separated flow which directly influenced (fighter) aircraft performance through the Reynolds number dependence of phenomena like buffet and wing-rock (see section 1.1). The problem of adequately defining separated flow phenomena is of even more significance to-day in view of the demand of high manoeuvrability at conditions with partly separated flow. The situation is somewhat different for transport-type aircraft but nevertheless of great significance. The normal operating conditions of a transport aircraft are within the separation boundaries as defined in the lift/Mach number plane. They should be known for that reason. It then turns out that the buffet boundary is one of the critical parameters determining the wing area. For that reason it is important to predict the buffet boundary from wind tunnel tests.The flow regime beyond separation is also of interest for transport-type aircraft from the point of view of aircraft control and structural integrity. Drag is then of minor importance.

Figure 3.4-1 shows a comparison (in pairs) of pressure distributions for various cases. In each case the Reynolds number effect on the pressure distribution on the left side is small and the variations are similar to the ones discussed in section 3.3. On the right side of the figure the variations are much larger and reflect the theme of this and the following sections. In the latter cases the trailing edge pressures suggest that the flow has separated at the low Reynolds number which causes a significant shock movement. At the high Reynolds number the trailing edge flow is attached (possibly with the exception of a small local separation). Since the boundary between attached and separated flow can be reasonably well defined (e.g. by using the trailing edge pressure divergence as an indicator; see fig. 3.3-11 and -12), the systematic analysis will be mainly concerned with the variation of the separation boundary with Reynolds number. *Finally some remarks on Reynolds number effects for separated flows will be made.* Note that this approach is distinct from one in which the wing or airfoil is kept at constant incidence in order to follow the development of the flow from separated to attached flow conditions with increasing Reynolds number.

Just after the second world war it was realized that shock wave boundary layer interaction was one of the prime causes for separation at transonic flight. Many valuable studies of shock wave boundary layer interaction have been published since (see [Ref. 85/12]) but it was not untill 1968 that Pearcey, Osborne and Haines presented a kind of classification of the shock induced boundary layer separation on airfoils [Ref. 68/2]. Some illustrative figures, taken from their report, are reproduced in the figures 3.4-2 to 3.4-5. Since that time the type "A" and type "B" separation are often associated with Reynolds number effects on airfoils with shock waves present.

The figures 3.4-2 and 3.4-3 help to explain the basic differences between the two types of separation. In both types the final state is a boundary layer separation from shock to trailing edge. However, in the type "A" separation this final state is achieved by a growth of the separation bubble underneath the shock. In the type "B" separation a local trailing edge separation appears before the final state is reached. The trailing edge separation is amplified by the adverse effects on the boundary layer development due to the upstream shock wave boundary layer interaction. The final state is reached as soon as the two separated areas (at the shock and the trailing edge) merge. Therefore the two types differ with respect to the development up to the condition of a complete separation as can be observed from an analysis of the pressure distribution (see fig. 3.4-4 and 3.4-5; the latter is a so called "Pearcey-plot").

The important point for Reynolds number effects is that, as was argued in reference [68/2], the type "B" separation was considered to be much more Reynolds number sensitive than the type "A" separation. This clear distinction in Reynolds number sensitivity should be understood from previous work at NPL in England (e.g. Ref. [54/1] and [55/1]) showing that the local shock Mach number causing separation (indicated by divergence of trailing edge pressure) was a weak funtion of the free stream Mach number. In other words, a single shock Mach number defines the beginning of shock induced separation. (It was noted that shocks close to the leading edge behave differently). The effect of a Reynolds number variation (with fixed boundary layer transition!) was not studied in detail at that time. In the 1968 paper by Pearcey et al this shock-induced separation criterion is not mentioned anymore, but it is argued that the local flow at the foot of the shock (notably the development of a supersonic tongue, see ref. [60/2]) is the dominant factor in the subsequent development of the separation bubble. From these observations the circa 1955 conclusions were that the shock strength was the most important factor and the incoming boundary layer was less important.

In the type "B" flow the interaction with the trailing edge separation is essential and since the trailing edge separation is a pressure induced boundary layer separation, Reynolds number is bound to have an effect as well. Fully in line with this description it was also argued that for a sufficiently high Reynolds number the rear separation might disappear. In other words, the type "B" separation developes into a type "A" separation at higher Reynolds numbers. This opens the possibility that a type "B" separation as observed in the wind tunnel will not appear on the full scale aircraft. This situation is not very comfortable for the aircraft designer.

The distinction betwen a type "A" and "B" was based on a very detailed analysis of the available information at that time. The question should be posed in this AGARDograph if the (still) limited information that has become available since gives rise to a modification of this basic distinction.

3.4.2 The flow break-down boundary revised

The experimental information on flow break-down or separation boundaries is very limited and often confidential. This is even more so for the description of physical flow models that calculate or correlate the separation developme-t. Nevertheless, it will be attempted to discuss the major elements of the separation process on airfoils.

Separation occurs when the flow breaks away from the surface leading to regions of reversed flow. When these regions are confined to the inner part of the turbulent boundary layer, a situation that was discussed in some detail in section 3.3.2 in relation to trailing edge separation, the effects on the outer flow field will be gradual and of limited extent. However, when the reversed flow is no longer confined to the thin shear layer, the outer flow field will be modified drastically, leading to almost discontinuous changes in the pressure distribution, most often resulting in a sudden loss of lift and change in pitching moment. This situation will be called flow break-down. The flow break-down boundaries mark in the C_L-Mach number plane the regions of normal operating conditions of an airplane. They are closely con-

nected with, but not necessarily identical to the buffet and maximum lift boundaries. Various definitions are in use like a kink in the C_L-α curve, a break in pitching moment or tangential force development, or a rapid divergence of trailing edge pressure.
In the transonic regime the flow break-down boundary of particular interest involves shock induced separation from shock to trailing edge. In this kind of flow the distinction has been made in the past between type "A" and "B" separation as discussed before. Separation at the foot of the shock and/or trailing edge separation are the main elements in this process of flow break-down.

The length of the separation bubble L underneath the shock can be written as:

$$L_{sep,shock}/c = f\ \{M_{shock},\ M_\infty,\ Re_c,\ H_{sh},\ (\theta/c)_{sh},\ \text{press. distr....}\} \qquad \text{(Ia)}$$

whereas the trailing edge separation can be described as:

$$L_{sept,TE}/c = g\ \{Re_c,\ H_{TE},\ (\theta/c)_{TE},\ \text{press. distr....}\} \qquad \text{(Ib)}$$

Flow break-down is defined as the condition at which the separated boundary layer underneath the shock fails to re-attach to the airfoil surface (type "A"):

$$L_{sep,shock}/c \geq 1 - x_{sh}/c \qquad \text{(IIa)}$$

or when the shock bubble and trailing edge separation merge (type "B"):

$$(L_{sep,shock} + L_{sep,\ TE})/c \geq 1 - x_{sh}/c \qquad \text{(IIb)}$$

The expressions I and II constitute a general flow break-down criterion although much more simplified expression are actually used. Fundamental studies (e.g. see [Ref. 85/12]) indicate that the upstream shock Mach number for the start of separation (incipient separation) is a very weak function of the upstream boundary layer shape factor H and for that reason almost Reynolds number independent. In the 1950's a single correlation, based on shock strength (and hence Reynolds number independent) was used to define flow break-down (fig. 3.4-6 taken from Ref. [55/1]). Also more recently simple correlations can be found in the literature to define flow break-down that make use of a critical shock Mach number without addressing the Reynolds number dependence explicitly (fig. 3.4-7 taken from Ref. [82/3] and also [Ref. 81/3]). In the mean time other fundamental studies (e.g. Ref. [67/1], [78/3] and [81/1]) do indicate a Reynolds number dependence as also discussed in the report of the Research Committee of AGARD WG-09 [Ref. 00/1]. Unpublished (and independent) studies from NLR and ARA suggest a correlation for the separation boundary with M_{shock} and θ_{shock}/c as the dominant parameters. This correlation does reflect a Reynolds number dependence since $(\theta/c)_{shock}$ varies roughly as $Re^{-1/5}$. More recently Fulker and Ashill [85/4] have published very detailed studies on the separation length in connection with flow break-down. In their correlation the separation length $L_{sep,shock}/\theta_{shock}$ is expressed as a function of $Re_{\theta_{shock}}$ (though weakly) and the shock Mach number (fig. 3.4-8). When the separation length exceeds a critical value, dependent on the pressure distribution, the boundary layer will not re-attach and the separation boundary is reached. This most recent correlation for flow break-down by Fulker and Ashill can be represented schematically:

$$L_{sep,shock}/c + x_{shock}/c \geq (x/c)_{critical} \qquad \text{(IIc)}$$

where $(x/c)_{critical}$ depends on the pressure distribution and hence the airfoil type.

Many criteria can be found in the literature to described the more classical type of pressure induced trailing edge separation [Ref. 00/1]. Just one of these expressions is reproduced here (from Ref. [72/5]) to illustrate a fundamental Reynolds number dependency through the influence on θ:

$$(\theta/c)_{TE} \cdot d\ c_p/d\ x/c \geq .007 \qquad \text{(III)}$$

The situation is, unfortunately, more complex than this simple correlation seems to indicate. The separation onset and the separation length can, from a fundamental point of view, only be calculated from a simultaneous solution of the boundary layer and the outer flow equations since the development of the (thick) boundary layer close to separation provides a relief in the external flow pressure gradient that counteracts the separation development. Moreover, the boundary layer conditions at the trailing edge will depend on the upstream history with shock wave boundary layer interaction as a complicating factor.

How do the various types of separation interact with each other? It is to be expected that prior to incipient separation at the foot of the shock (for shock Mach numbers less than roughly 1.3) trailing edge separation is the dominant phenomenon. Such situations might occur at low lift values for Mach numbers close to and beyond the design Mach number. The Reynolds number dependence enters into a direct way, in a way similar to expression *III*.
When the shock Mach number is higher than 1.3 a local bubble at the foot of the shock will be formed. The extent of this separation will be Reynolds number dependent in a direct way as suggested with expression I.a. The most recent work of Fulker and Ashill has shown that the over-ruling factor for the condition of flow break-down appears to be the growth of the separation bubble underneath the shock, irrespective of a possible trailing-edge separation (expression II-c). This, however, does not mean that trailing edge separation is not important at all. Trailing edge separat'on will modify the pressure distribution in a Reynolds number dependent way. This indirect Reynolds number effect, as discussed extensively in section 3.3, will alter the shock strength and hence the conditions for the separation at the foot of the shock. This in turn will influence the conditions of the boundary layer at the trailing edge. This interaction can be very significant in view of the sensitivity of the length of the separation bubble underneath the shock for the shock Mach number (fig. 3.4-8). The final result of this interaction process from the point of view of Reynolds number sensitivity will depend very much on the pressure distribution and hence the type of airfoil. Fulker and Ashill noted already the importance of the type of pressure distribution for their evaluation. Most airfoils from before the 1960's show a rapid increase in shock

strength with increasing Mach number or angle of attack. Viscous effects were small, unless the Reynolds number was very low. For modern supercritical airfoils the variation in shock wave strength has been restricted through design. Rear loading has increased the pressure gradients over the rear of the airfoil. Viscous effects and hence the indirect Reynolds number effects, will be much more important for these airfoils. It is therefore to be expected that the flow break-down boundary will also be more sensitive to Reynolds number, as compared with the airfoils of the 1950's.

Since the trailing edge separation appears to be only of importance for the (gradual) indirect Reynolds number effects, the original distinction between type "A" and "B" flow might be less relevant for the flow break-down boundary. This is illustrated very schematically in figure 3.4-9. The distinction will still be very relevant prior to flow break-down for the evaluation of drag and pitching moment as discussed in section 3.3. For the flow break-down boundary the Reynolds number sensitivity might very well depend primarily on the airfoil type rather then the particular Reynolds number range.

This view appears to be supported by the experimental information as far as available to the author. The figures 3.4-10 till 3.4-14 show some examples of the variation of the flow break-down boundary with Reynolds number. All results are related to modern supercritical airfoils (some of them discussed above). In figure 3.4-10 Reynolds number trends for various models of the same airfoil measured in various wind tunnels are compared [Ref. 82/4, 83/10]. Note that although the absolute values are very much different, the variations with Reynolds number are very similar. In figure 3.4-11 the Reynolds number trend for one airfoil is presented for a range of Mach numbers. The figure depicts the importance of transition fixation in the analysis of the separation boundary as discussed in section 3.2. Also, some increase in Reynolds number dependence can be noted for higher Mach numbers. Figure 3.4-12 compares various airfoils for a typical transonic design Mach number. Apart from some variation in Reynolds number dependence, all models, including the three dimensional model "C" (a high aspect ratio transport-type wing) indicate a regular variation of C_L-max with Reynolds number.

None of the results show a tendency to level off at higher Reynolds numbers (with a possible exception of the Mach = .6 data in fig. 3.4-11; for that condition the shock is close to the leading edge). This is also supported for some of these airfoils by figure 3.4-13 in which the shock Mach number at flow break-down and for a constant shock position has been plotted versus Reynolds number. Again, a very regular trend is found. In a last example (figure 3.4-14 taken from Ref. [85/2]) the pressure distributions of a three-dimensional high aspect ratio wing (the one discussed in Ref. [76/1]) were analyzed in order to classify the separation as a function of Mach and Reynolds number. Also in that case no change from type "B" to type "A" separation was actually observed although such a change was tentatively indicated in the figure.

From the design point of view it might be reassuring to know that no discontinuous changes in the development of the flow break-down boundary with Reynolds number are to be expected. However, clearly more research is required to substantiate this view. Also there will be limits imposed by the "inviscid limit" of the outer flow field and surface roughness effects that render the boundary layer development Reynolds number independent.

3.4.3 Post stall behaviour

Only very limited information is available with respect to Reynolds number effects beyond separation. The problem is nevertheless of considerable importance for stability and control and for the determination of aerodynamic loads. One extreme appears to be very well defined: a flow that is separated along a salient edge is independent of Reynolds number. But for pressure gradient or shock induced separations on the smooth surface of an airfoil contour, the Reynolds number will have a strong influence on the separation position and hence the dimensions of the separated flow field. For a good understanding of the problem it is essential to allow for the interaction between the viscous flow and the non-viscid outer flow. Moreover, the complete flow field is often highly unsteady and essentially three-dimensional, even for two-dimensional airfoils. A sound theoretical treatment seems therefore beyond the present capabilities.

Nevertheless, for conditions not too far away from the flow break-down boundary, there appears to be a more or less systematic development of the separation. Cahill [Ref. 79/1] has presented a method to extrapolate pressure distributions with flow separation as measured in the wind tunnel to flight Reynolds numbers. The procedure is based on the observation that the relations between trailing edge pressure on the one hand and a viscous flow parameter ("B_2") and shock position on the other hand, preserve their shape, independent of Reynolds number. Moreover, the trends with Reynolds number appear to be rather general. The principle of the method is shown schematically in figure 3.4-15 and a typical example of a so corrected pressure distribution is presented in figure 3.4-16. In a later publication [Ref. 83/1] the purely empirical viscous shock parameter "B_2" has been replaced by a physically more meaningful parameter defined by:

$$K = \frac{(M^2_{sh} - 1)}{(\gamma+1).\varepsilon.M^2_{sh}} \text{ with } \varepsilon = \sqrt{C_f/2}$$

that follows from asymptotic theory for shock wave boundary layer interaction. With this parameter the correlation improved slightly. The method is reported to be primarily used for the prediction of aerodynamic loads.

For the same class of flows as described by Cahill's correlation it might very well be possible (under certain restrictions of tunnel Reynolds number, shock position and the three-dimensionality of the flow) to simulate in the wind tunnel the high Reynolds number flow with the help of the so called aft-fixation technique. This technique will be discussed very shortly in section 3.6.

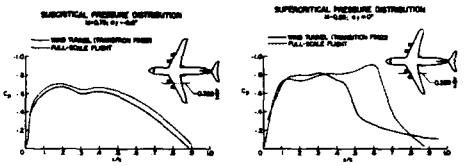

RE-EFFECT : ONE AIRCRAFT

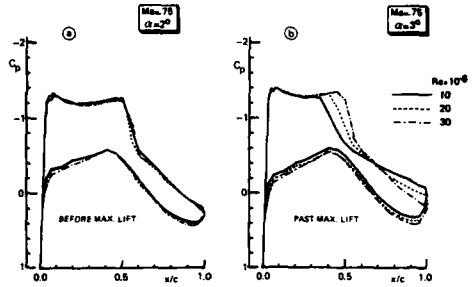

RE-EFFECT : ONE W/T MODEL

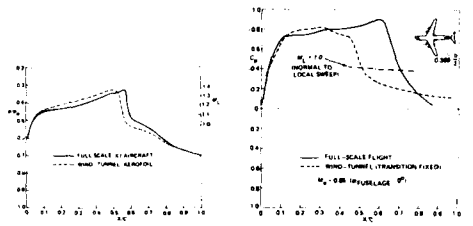

RE-EFFECT : TWO TYPES (?)

Fig. 3.4-1 *Observed Reynolds number effects:* before and after the separation boundary (from various sources)

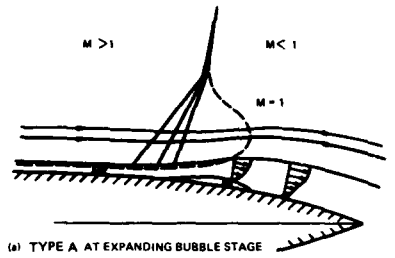

(a) TYPE A AT EXPANDING BUBBLE STAGE

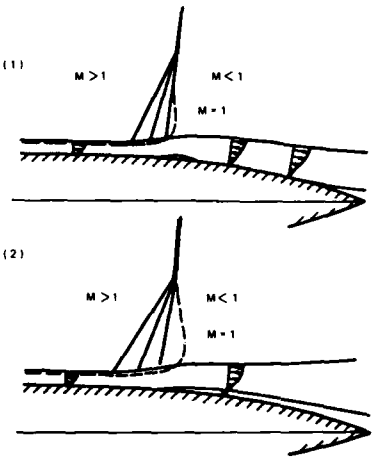

(b) TYPE B (1) AT EARLY STAGE WITH LOCALISED SHOCK BUBBLE AND REAR SEPARATION
(2) AT LATER STAGE WITH ONE SEPARATION EXTENDING FROM SHOCK TO TRAILING EDGE

Fig. 3.4-2 Some details (schematic) of the region of interaction between turbulent boundary layer and shock wave (from ref. 68/2)

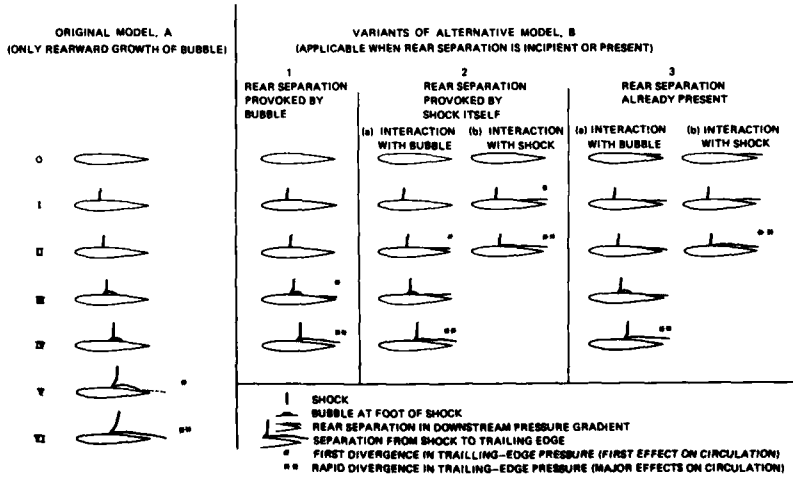

Fig. 3.4-3 Classification of separation development according to type "A" and "B" separation (from ref. 68/2)

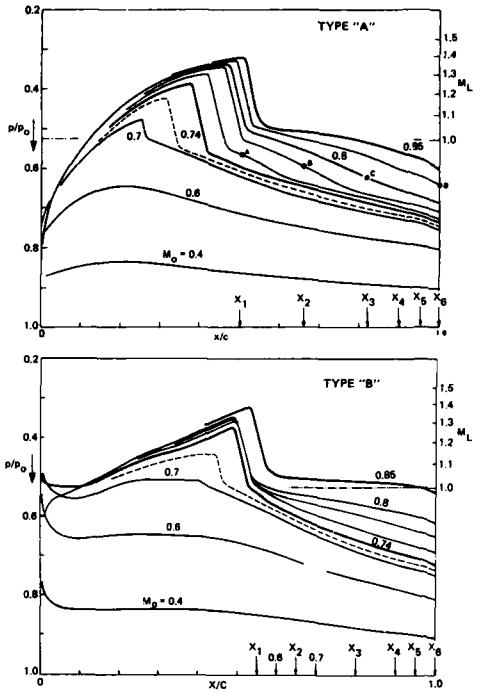

Fig. 3.4-4 Development of pressure distribution for type "A" and "B" separations (from ref. 68/2)

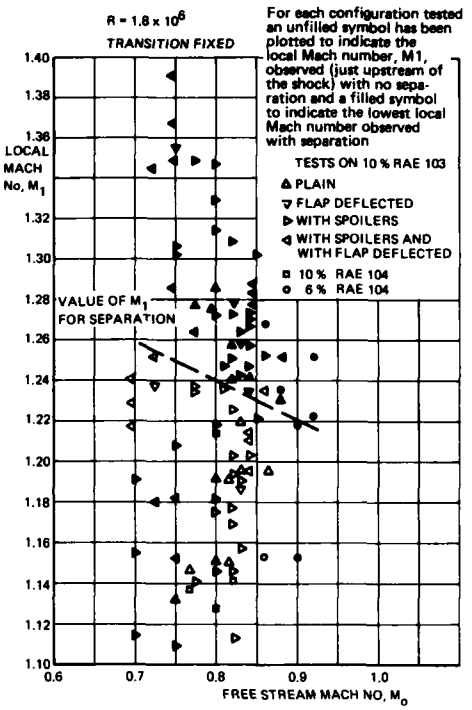

Fig. 3.4-6 Early correlation of the shock-upstream Mach number to cause separation (from ref. 55/1)

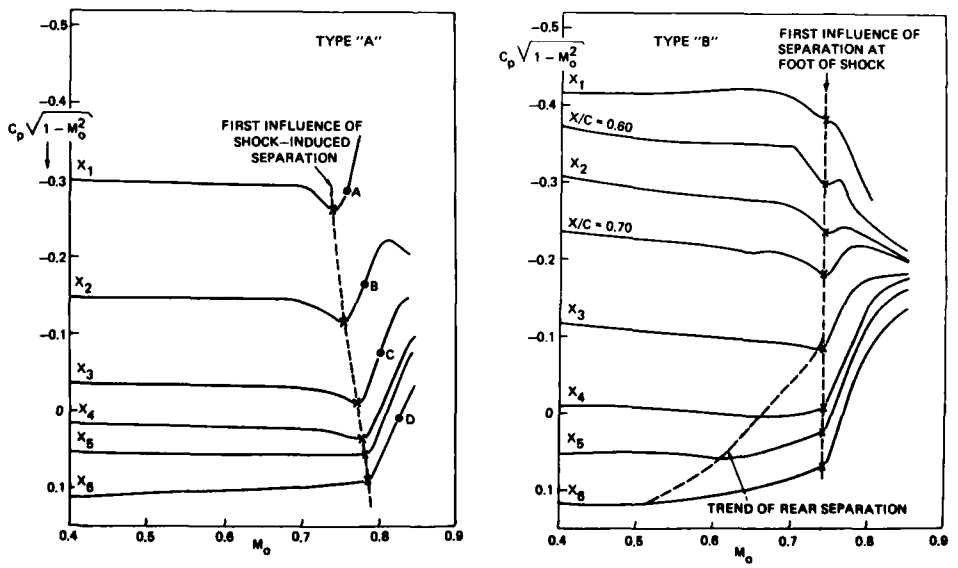

Fig. 3.4-5 So-called "Pearcey-plots" to distinguish between type "A" and "B" separation (from ref. 68/2)

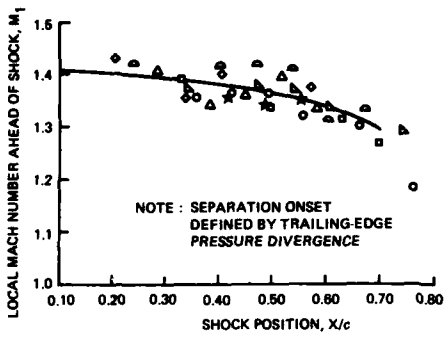

Fig. 3.4-7 A more recent correlation of the shock-upstream Mach number to cause separation (from ref. 82/3)

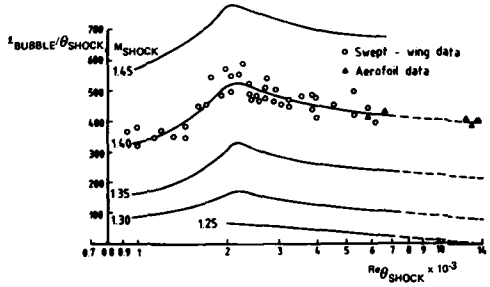

Fig. 3.4-8 Fulker and Ashill's shock-bubble correlation

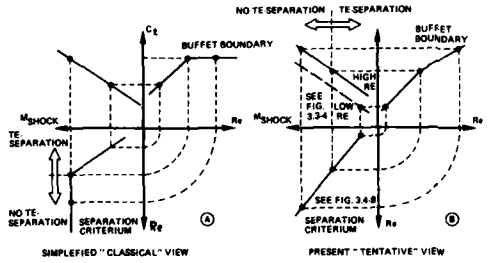

Fig. 3.4-9 Hypothetical models to describe the Reynolds number sensitivity of the separation boundary

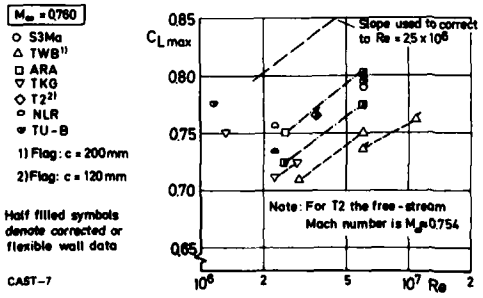

Fig. 3.4-10 Observed variation of maximum lift for one model in various wind tunnels (from ref. 83/10)

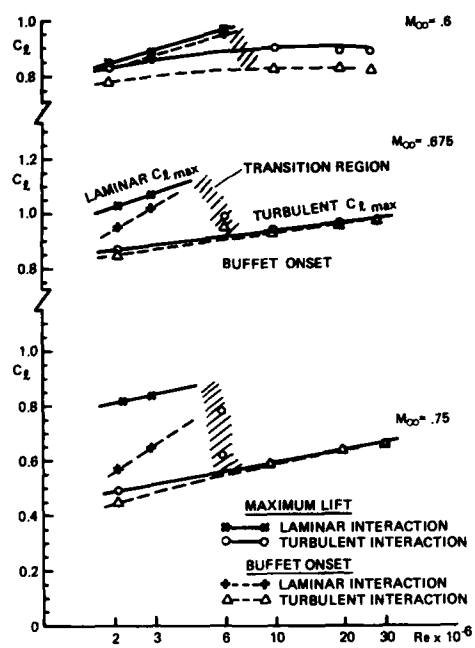

Fig. 3.4-11 Observed variation of maximum lift for one model at various Mach numbers (unpublished results of NLR)

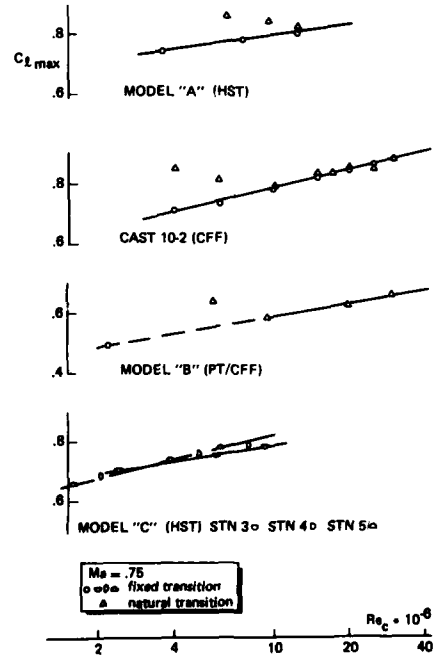

Fig. 3.4-12 Reynolds number effect on maximum lift for various models near design Mach number (unpublished results of NLR and DFVLR)

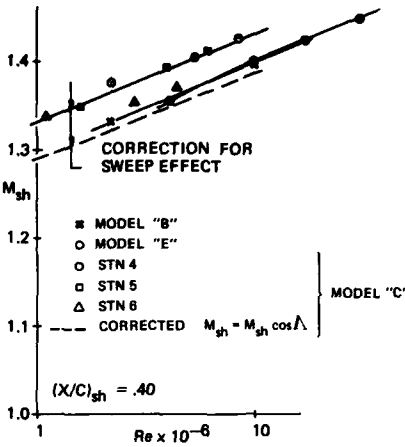

Fig. 3.4-13 Shock-upstream Mach number at maximum lift as a function of Reynolds number for a fixed shock location (unpublished results of NLR)

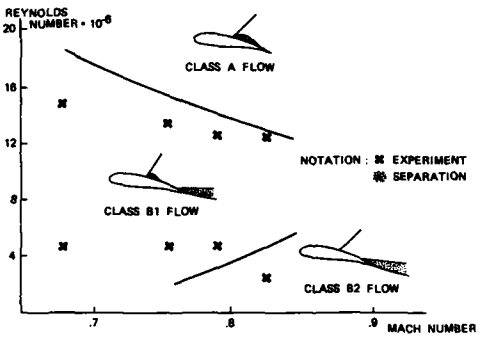

Fig. 3.4-14 Tentative and actually observed types of flow separation (from ref. 85/2)

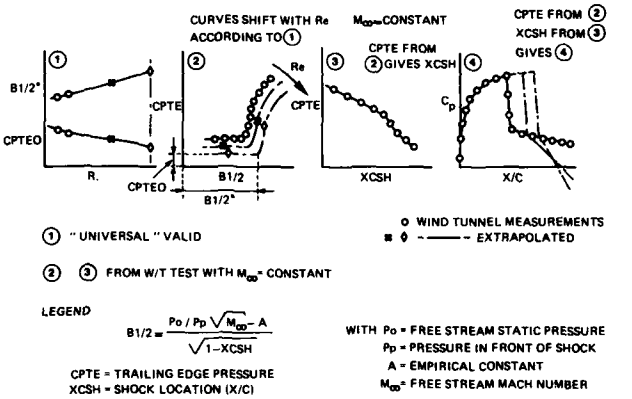

Fig. 3.4-16 Examples of extrapolated pressure distributions according to the method of ref. 79/1

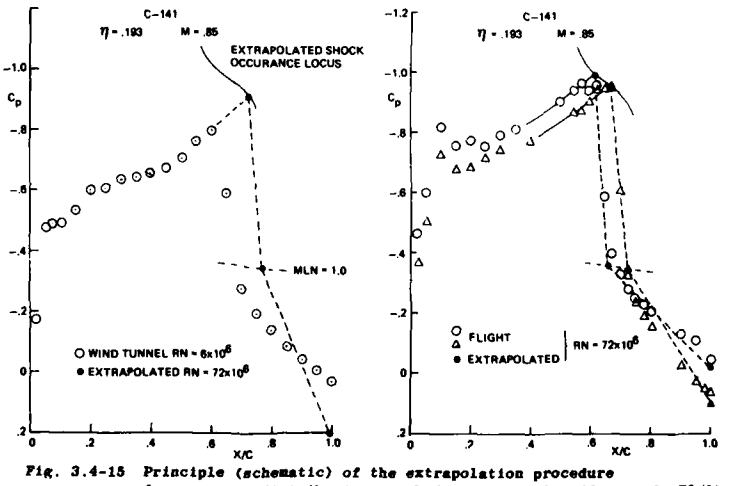

Fig. 3.4-15 Principle (schematic) of the extrapolation procedure for pressure distributions with flow separation (from ref. 79/1)

3.5 Three-dimensional effects

3.5.1 The correspondence between two- and three-dimensional flow

The discussion sofar was restricted to two-dimensional flows. But how relevant is the two-dimensional flow for the general case of a high aspect ratio wing? The design of such a wing is generally based on one or more so called basic airfoil sections. For the larger part of the wing the pressure distribution can be derived from these two-dimensional basic sections by assuming that:

$$C_{L,3\text{-}D} = C_{L,2\text{-}D} \cdot \cos^2 \Lambda$$

$$M_{\infty,3\text{-}D} = M_{\infty,2\text{-}D}/\cos \Lambda$$

where Λ is the sweep angle. Approximate corrections can be introduced to allow for wing-taper and the fuselage influence (see e.g. ref. [62/2]). The wing tip and the wing root are essentially three-dimensional. The tip is only a small part of the wing and most likely of minor influence (unless winglets are used). The wing root flow is of considerably more importance. There, very often, a double shock pattern can be observed with an intersection point close to the kink-section of the wing (fig. 3.5-1). This influence restricts the two dimensional flow to a region between the kink-section and the tip. But even then one has to be careful: it is the local direction of the isobars (more precisely the shock Mach number perpendicular to the shockfront) that is of importance from a two-dimensional point of view. This direction can be different from the wing generators depending on the particular wing design.

The correspondence between two- and three-dimensional flow is even less clear for the boundary layer development. In the ideal case of an infinite swept wing some basic differences with respect to the corresponding unswept airfoil should be noted. Only for laminar boundary layers the so called "independence principle" holds, stating that the velocity components in a direction perpendicular to the leading edge are identical for two- and (quasi) three-dimensional flows [Ref. 68/4]. Laminar boundary layer separation will therefore occur at the same relative chord position for the swept and the unswept wing. This no longer holds, in principle, for turbulent flows, due to a cross-coupling effect of the turbulent motion. It is to be expected, however, that for flows with a strong pressure gradient (when turbulent shear stresses are less important) the independence principle is still of some value. For a discussion of the independence principle in relation with shock wave boundary layer interaction see Ref. [85/5]. When the isobars on the wing are not parallel (due to taper or other three dimensional effects) the flow will endure an additional effect of streamline con- or divergence, relative to the infinite swept wing case. This causes an additional in- or decrease in boundary layer thickness (see Ref. [85/3] for a theoretical treatment). The most important differences between 2-D and 3-D flows, however, are related to transition and boundary layer separation.

In two-dimensional flows the Tollmien-Schlichting instability is the primary cause for transition. In three-dimensional flows two more transition agents can be found: leading edge contamination and cross flow instability as discussed in more detail by Michel in ref. 00/1. Thus there are two more mechanisms to produce discrepancies in transition location between wind tunnel and flight. Figure 3.5-2 summarizes the various transition causing factors for a typical swept wing.

The process of boundary layer separation is much more complex in three-dimensional flows as pointed out by Hall in Ref. [71/5]. Theoretically, two dimensional flows will exhibit two-dimensional separations that appear as closed bubbles (on or behind the airfoil) of re-circulating air. Such closed bubbles can still be observed in the three-dimensional case of an infinite swept wing (near the nose or at the shock foot), however with an additional spanwise component (see fig. 3.5-3a). In the more general case of a three-dimensional wing with finite aspect ratio the closed bubble can also appear as a cell-like structure (fig. 3.5-5), as is also often found in two-dimensional testing. Much more important and without parallel in the two-dimensional case is the open separation with the formation of one or more vortices (fig. 3.5-3b). Very often, these vortices start from a closed bubble and develop in the spanwise direction. Depending on the magnitude and growth of this spanwise flow, the inboard wing might have a large influence on the flow over the outboard wing as remarked also by Yoshihara (see fig. 3.5-7 taken from Ref. [75/4]). In the figures 3.5-4 to 3.5-6 some examples of various separation types as actually observed on high aspect ratio wings, are presented. From this it is quite clear that the open separation affects the outer flow field in an essentially three dimensional way. For this kind of flow all correspondence with two-dimensional flows is lost.

3.5.2 Some examples of three dimensional effects

One should not conclude from the foregoing discussion that the two-dimensional airfoil is without relevance for high aspect ratio wings. The larger part of the Reynolds number effects can be carried over to high aspect ratio wings, provided that:

- Only the quasi two-dimensional part of the wing is considered (say from kink-section to near the tip);
- The boundary layer is turbulent (either natural or by tripping);
- The flow has not separated.

The consequencies of the first restriction will depend on the particular wing design. When the aspect ratio is high enough (say 8 or more) the larger part of the wing is well outside the kink section. Also, the flow on the wing root is often less sensitive for Reynolds number changes due to a higher local chord Reynolds number and a favourable effect of the double shock on the boundary layer development.

Spanwise variations in boundary layer transition location are of considerable influence. Fig. 3.5-8a is an old example [Ref. 52/2] of very large spanwise variations in load distribution with Reynolds number. It is believed that in this case transition point variations, in combination with shock boundary layer interactions are to blame. In this particular case, a complete reversal in pitching moment variation with angle of attack was the dramatic result (fig. 3.5-8(b)). A more recent example (fig. 3.5-9 taken from Ref. [76/1]) is included to show that when the transition point variation is suppressed by artificial boundary layer fixation, a qualitatively much more systematic flow development in accordance with the higher Reynolds number situation, can be obtained. Figure 3.5-10 and 3.5-11 illustrate a similar observation, also for the flow break-down boundary. Again, the results with fixed transition appear to be much more syste-

matic as compared with free transition, as discussed in section 3.2. It is even more important that the fixed transition results are similar to the two-dimensional data in figure 3.4-12, -13 (the model "C" in these figures is the same one as used for the results shown in figure 3.5-10 and -11). Also the correlation between shock Mach number and Reynolds number at the flow break-down boundary is well in line with the available two-dimensional data. Fulker and Ashill [Ref. 85/4] did not find a systematic difference in their separation correlation between two- and three-dimensional results. The examples indicate that even at the onset of flow separation the correspondence between two- and three-dimensional flows can be maintained. However, in view of the essential three-dimensional nature of the separation itself, it is very unlikely that this correspondance will still be found beyond the flow break-down boundary. The uncertainty with respect to Reynolds number effects for two-dimensional separated flows is more severe for three-dimensional configurations.

A word of caution should finally be expressed with respect to drag evaluation for a three-dimensional configuration. The concern stems from the sensitivity of compressibility drag to small variations in shock wave strength and, for the three-dimensional case, the sweep angle of the shock. The shock wave pattern on a 3-D wing is basically determined by the 3-D inviscid flow development modified by local viscous effects. In reference [76/2] the risk of over- or under-fixation of the boundary layer for a high aspect ratio wing is discussed. It is argued that as a result of non-optimal fixation, the sweep-angle of the shock might be influenced (see figure 3.5-12) with serious effects on the overall flow field. The important point to note here is that similar effects may be introduced by a Reynolds number variation with fixed transition near the leading edge. The argument goes as follows. When the (corresponding 2-D) Reynolds number sensitivity of the inner and outer wing is significantly different (e.g. because one part of the wing is closer to separation) the sweep angle of the shock may change in this case due to a Reynolds number increase. When the sweep angle of the shock is increased (because the shock at the wing tip moves faster downstream than the shock near the kink section) the effect on the overall flow development will be favourable (because the Mach number component perpendicular to the shock decreases) and the Reynolds number sensitivity of the wing will increase, compared with the mean of the 2-D stations. When the kink-section is more critical, the reverse is true and the Reynolds number sensitivity will be reduced. Figure 3.5-13 (reported in Ref. [84/3]) further illustrates the importance of three-dimensional effects on the wave drag in relation to the total wing drag. In this figure an estimate of the wave drag contribution is depicted (note that the two shaded regions follow from different approximation to derive wave drag from the wake rake traverses). At the lowest Reynolds number and highest lift the mid-wing region is just beyond the local drag divergence boundary and experiences for that reason some increase in wave drag. For the other presented conditions (higher Reynolds number and lower lift) the wave drag contribution is much smaller with a modest variation over the span.

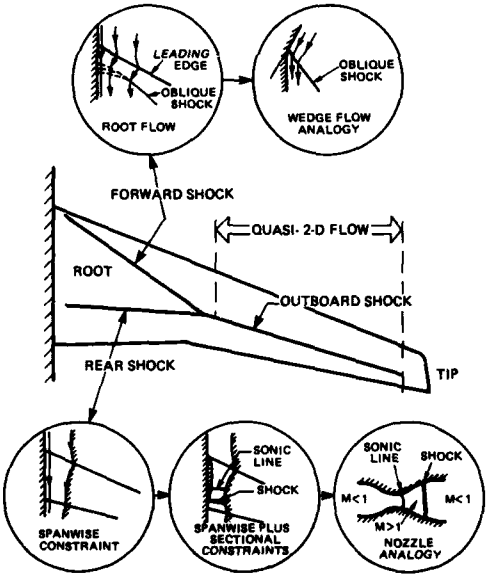

Fig. 3.5-1 Schematic representation of three-dimensional effects in the flow over a high aspect ratio wing (after Slooff)

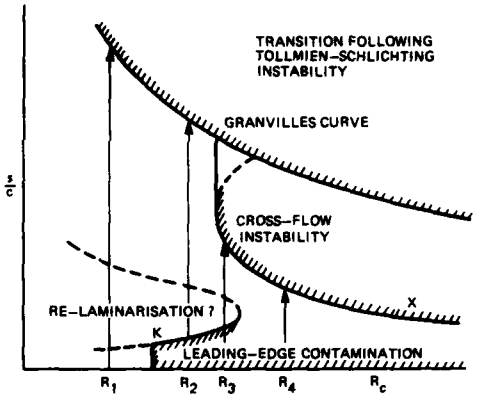

AT R_1 TRANSITION FOLLOWS FROM TOLLMIEN–SCHLICHTING INSTABILITY

AT R_2 LEADING–EDGE CONTAMINATION, FOLLOWED POSSIBLY BY RE–LAMINARISATION AND THEN TRANSITION THROUGH TOLLMIEN–SCHLICHTING INSTABILITY

AT R_3 LEADING–EDGE CONTAMINATION, FOLLOWED POSSIBLY BY RE–LAMINARISATION AND THEN TRANSITION THROUGH CROSS–FLOW INSTABILITY

AT R_4 TRANSITION FOLLOWS FROM CROSS–FLOW INSTABILITY IF LEADING–EDGE CONTAMINATION WERE ABSENT

Fig. 3.5-2 Example of different types of transition on a swept wing (from ref. 72/2)

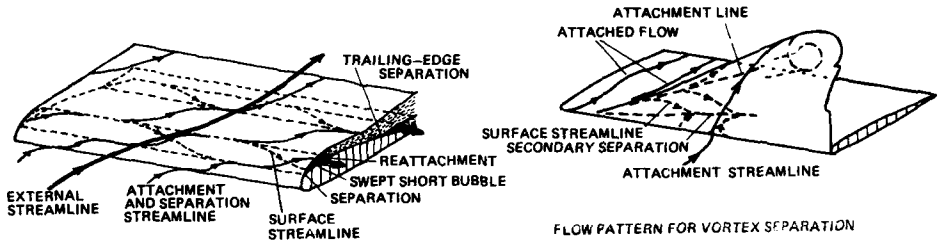

Fig. 3.5-3 Example of a closed and open three-dimensional separation (from ref. 71/5)

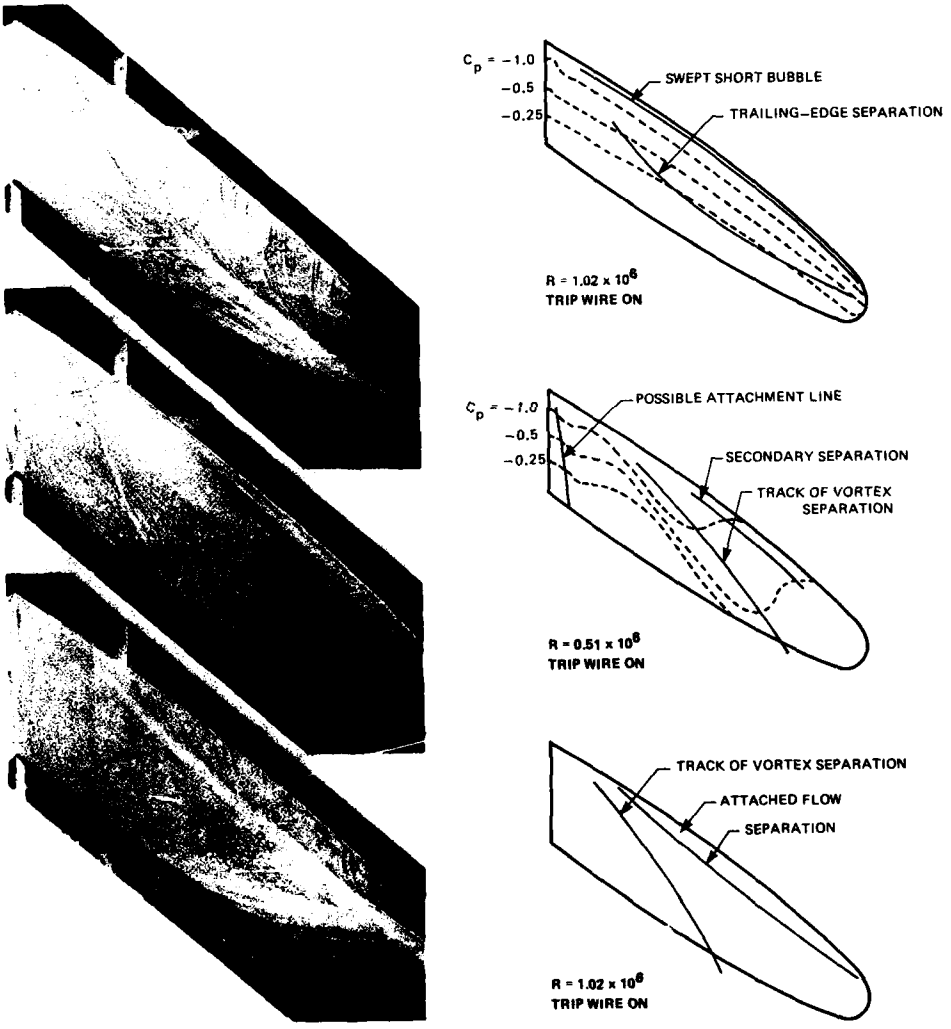

Fig. 3.5-4 Flow and isobar patterns on a threedimensional wing with separation (from ref. 71/5)

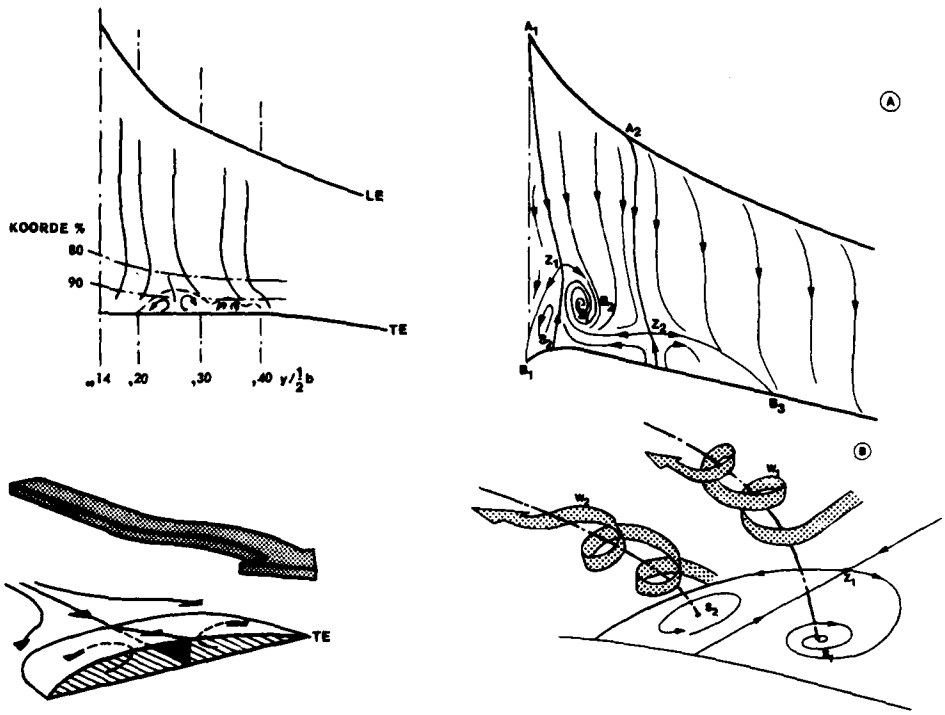

Fig. 3.5-5 Typical local three-dimensional separation at the wing-root section (from ref. 80/6)

Fig. 3.5-6 Typical non-local three-dimensional separation on a wing with shocks (from ref. 75/4)

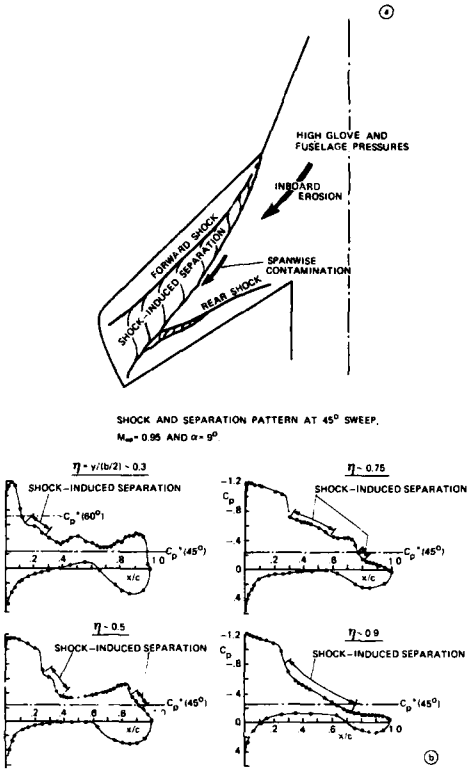

Fig. 3.5-7 Typical local three-dimensional separation with spiraling vortices at the wing root (from ref. 80/5)

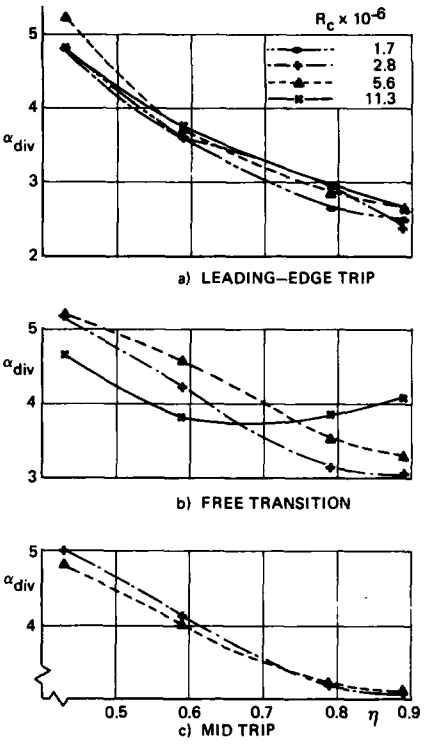

Fig. 3.5-9 Example of spanwise variation of trailing edge pressure divergence as a function of Reynolds number with and without boundary layer fixation (from ref. 76/1)

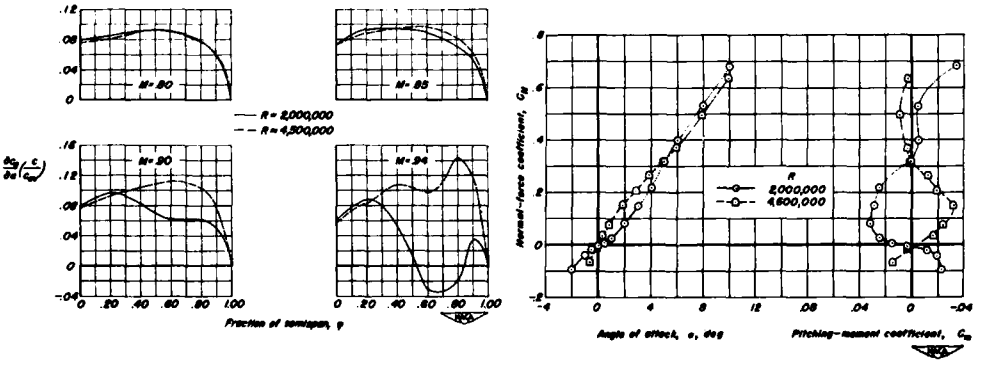

Fig. 3.5-8 Example of Reynolds number effect on the wing loading (from ref. 52/2)

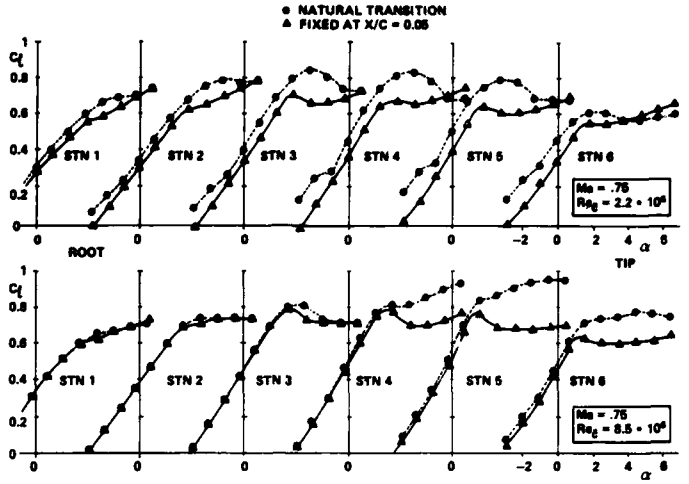

Fig. 3.5-10 Local lift development along wing span at two Reynolds numbers with and without boundary layer fixation (from ref. 84/2)

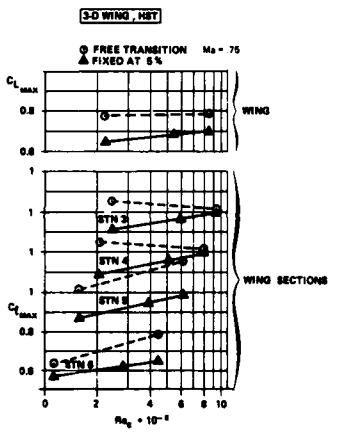

Fig. 3.5-11 Local maximum lift development with Reynolds number for a high aspect ratio wing (from ref. 84/2)

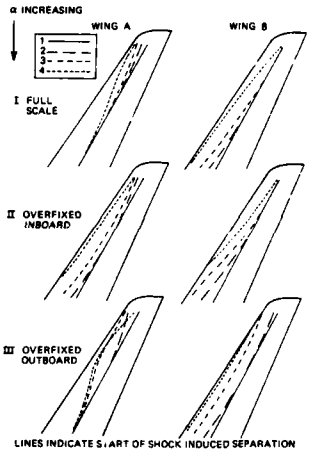

Fig. 3.5-12 Possible distortions of stall patterns by spanwise variation of overfixing (from ref. 76/2)

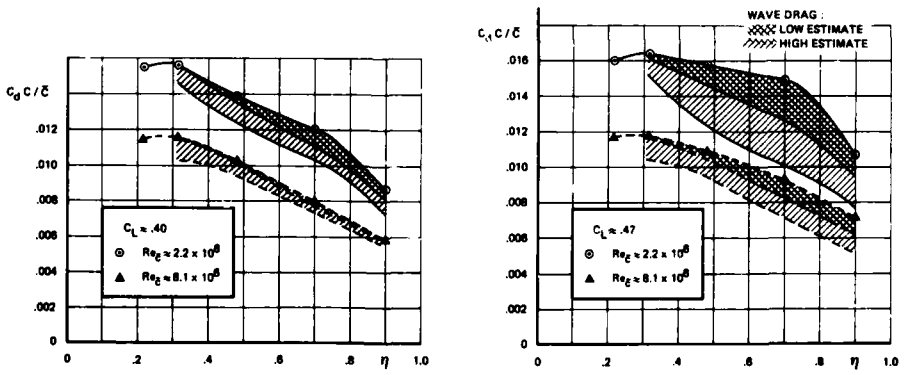

Fig. 3.5-13 Spanwise drag variation as a function of Reynolds number for a high aspect ratio wing (from ref. 84/3)

3.6 Concluding remarks: from wind tunnel to flight

Is the wind tunnel still an adequate tool for the design of aircraft in view of the Reynolds number deficiency of most existing wind tunnels? And if the answer is yes, what procedure should be followed in wind tunnel testing to cope with this deficiency? These questions, inevitable after the discussions of the previous sections, will not be discussed here in great depth. AGARD assigned to Working Group 09 "Wind Tunnel Boundary Layer Simulation and Control" the task to propose a methodology to estimate flight performance from wind tunnel tests. For more information the reader is referred to the final report of this working group [Ref. 00/1]. In this section only a few remarks will be made to conclude the discussion on Reynolds number effects for two-dimensional airfoils and high aspect ratio wings.

The available information suggests that two phenomena are of prime importance for the understanding of differences between wind tunnel and flight:

transition location variations also in connection with laminar versus turbulent shock wave boundary layer interaction

and

flow separation either locally (near the leading or trailing edge, at the shock) or of large scale (between shock and trailing edge).

The first phenomenon appears to be the easiest one to deal with for transport-type configurations at transonic speeds if one assumes that transition in flight is near the leading edge. There is no doubt that large transition location variations and laminar shock wave boundary layer interactions should be avoided in wind tunnel testing. Numerous examples (see section 3.2) show clearly misleading variations in aerodynamic characteristics if the transition point can move around freely. This requirement means that the boundary layer must be tripped artificially. This is a technique in itself that will not be discussed here (see e.g. Ref. [84/2].

When transition has been fixed artificially, the next most important problem is related to flow separation, either limited in extent or from shock to trailing edge as discussed in the sections 3.3 and 3.4. Only in the latter case are large variations in pressure distribution observed with Reynolds number. For conditions with attached or almost attached flow the effect on the pressure distribution (the so called "indirect Reynolds number effect"; see section 1.2.2) appears to be small, though certainly not insignificant. For example a limited region of trailing edge separation tends to increase this indirect Reynolds number effect. Some aerodynamic characteristics, notably drag and pitching moment, are very sensitive to these small variations. Very large changes in pressure distribution are observed when the flow changes from an attached to a separated flow condition when Reynolds number is decreased. The separation boundary (flow break-down, characterized by separation from shock to trailing edge) defines the boundary between the attached flow and conditions with large scale separations. If the indirect Reynolds number effects are small for attached flow conditions and if the Reynolds number enters a separation criteria in an unambigious way (as appears to be the case at least beyond a certain Reynolds number; see fig. 3.4-8), it then follows that the separation boundary itself varies in a systematic way with Reynolds number. This, in principle, provides a basis for an extrapolation procedure of the separation boundary in the lift-Mach number plane. A careful analysis of the results (in terms of pressure distributions, separation development and wake drag analysis) is still needed to prove the validity of such a procedure for a particular configuration. The preceeding chapters, in fact, are intended to provide information ("rules" and "exceptions to the rules" as a warning) that might be helpful with such an extrapolation procedure. A good understanding of the basic flow mechanism involved is equally important in this respect.

Since boundary layer development is the very origin of Reynolds number effects it might be possible to manipulate the boundary layer on the model such that the pressure distribution for flight conditions is simulated, or at least approximated in the wind tunnel. This can be done in various ways: by the so called aft-fixation technique, by energizing the boundary layer with suction, blowing or vortex generators or by modifying the airfoil contour (relief of pressure gradient through the use of a thick trailing edge).

Of these methods, the aft-fixation technique is the best known and most widely used. Most transonic airfoils show, at tunnel Reynolds numbers, an appreciable region of laminar flow in front of the shock. The boundary layer can then be tripped such that the boundary layer is turbulent at the shock and resembles the flight condition over the rear part of the airfoil. This is illustrated in fig. 3.6-1 taken from a study by Blackwell [Ref. 68/1]. This is one of the earliest publications on this technique, although the method was also suggested by D.L. Loving in his classical paper on shock induced separated flow [Ref. 66/1]. The sequence of figures clearly shows that the aft-fixation technique helps to suppress the separation over the rear of the airfoil. In this case transition location was selected such that the high Reynolds number trailing edge conditions were duplicated with aft-fixation at the lower tunnel Reynolds number. No large changes are noticeable for attached flow conditions, very much in line with the observations made before. A more recent illustration for a three-dimensional configuration is presented in the figures 3.6-2 and 3.6-3 taken from Ref. [85/4] by Fulker and Ashill. A more refined simulation criterion was applied in this case based on the duplication of the relative (to the chord) separation length of the bubble underneath the shock as discussed in section 3.4.2. Also in this case the aft-fixation technique was used primarily to suppress premature flow break-down in the wind tunnel. The technique can also be used to simulate a separated flow condition as figure 3.6-4b taken from Ref. [83/3] illustrates. In this case details of the flow in the vicinity of the shock were not well represented. Finally, aft-fixation can be used to assess the effects of local separation at the trailing edge or in the lower surface rear loading region by comparing aft- and forward fixation results. In this way relevant information can be obtained for an extrapolation procedure.

This powerful technique is often used to study Reynolds number effects in the wind tunnel. But there are some limitations as well. First of all, the range of simulated conditions is restricted by the length of the laminar flow region ahead of the shock wave. In figure 3.6-5 the useable region in the lift-Mach number plane has been indicated for a three-dimensional wing with a strip at 30% (mid wing) chord position. In this particular case the useable region appears to be very small and limited by the forward move-

ment of the shock, either due to decreasing lift and/or Mach number or due to flow break-down at the higher lift values at the upper surface or the development of the pressure distribution with lift on the lower surface. The usuable region can be extended by application of a more forward trip but at the expense of the Reynolds number simulation capability. Thus a particular strip location provides only adequate simulation in a limited (though very important!) region of the operating conditions as figure 3.6-6 taken from Ref. [76/1] illustrates once more. At the wing tip and root, the natural transition is very often close to the leading edge. In that case a cranked strip must be used (see fig. 3.6-7a) and only the mid section of the wing is adequately represented. And even this is questionable when the fixation causes a significant variation on the local sweep angle of the shock as diaccused in section 3.5. These restrictions may cast some doubts on the ability of the aft-fixation technique to simulate flight conditions that can only be removed after a careful analysis of the results.

Vortex generators are used extensively to control flow separation in flight (see Ref. [61/6] by Pearcey for an excellent review). The same technique can also be used in a wind tunnel to suppress flow breakdown at a lower-than-flight tunnel Reynolds number. Figure 3.6-7b taken from Ref. [74/3] shows that the effect on pitching moment is similar (though far from identical) to the effect of aft-fixation. This technique is more difficult to control than the aft-fixation technique and certainly less suitable for drag assessment. It was reported [Ref. 85/6] that contour modifications have been used and are still being studied as a way to simulate the shock wave development (and hence compressibility drag) in drag evaluation studies. The principle is that a thickening of the airfoil contour over the aft part of the airfoil might provide a pressure relief such that the boundary later thickness and (possibly) the overall circulation is comparable with flight conditions. These and other techniques, like boundary layer suction as suggested by Gree [Ref. 71/2] are difficult to apply and have not yet reached the state of application for industrial testing.

Is Computational Aerodynamics (CFD) capable of bridging the Reynolds number gap between wind tunnel and flight? Such a method must be able to describe direct and indirect Reynolds number effects. The direct Reynolds number effect (the change in boundary layer development due to a change in Reynolds number for a "frozen" pressure distribution) can be adequately represented by most boundary layer calculation methods. In that respect they can be used to extrapolate e.g. viscous drag to higher Reynolds numbers. With local separations present, the assumption of a "frozen" pressure distribution is no longer valid and the so called "strong coupling" between the outer flow and the boundary layer flow is essential (e.g. by using inverse boundary layer methods; see Ref. [80/7], [82/5] and [84/4] for reviews). For the representation of the indirect Reynolds number effect (change in pressure distribution due to the change in boundary layer development) the trailing edge region (Kutta condition) is extremely important. This requires for the calculations the inclusion of normal pressure gradients in the viscous shear layers and wake curvature effects (see e.g. Ref. [81/4]). Figure 3.6-8 shows, as an illustration, the indirect Reynolds number effects as calculated by (an old version of) the VGK-method of RAE. The calculations closely reflect the experimental results for this relatively simple case without trailing edge separation. However, when local separations are present, the situation becomes increasingly complex. This is even more so beyond flow break-down when large scale separations are present. In that case the usual thin shear layer assumptions are no longer valid and the solution of the full Navier Stokes Equations is required. Recent developments (see e.g. Ref. [00/1]) indicate that the mathematical tools are "in hand" to solve this problem. Numerical schemes can be constructed and computers are powerful enough to find a solution in a reasonable time. This does not mean that the task is a simple one, but the future looks bright. Dark clouds, however, are still present in the form of turbulence modelling. Due to the complexity of this problem, progress has been slow over the last decade. Research in this field moves away from "universal turbulence modelling" into the direction of specific models for special classes of flow (see e.g. Ref. [81/5] and [84/5]). Empirical information, to determine the "variable constants" is essential here. For that reason calculation methods should be validated over a range of flow conditions (from attached to separated flow) rather then by comparing a few pressure distributions with experiment. In fact, the ability of a calculation method to describe the Reynolds number effect of an airfoil close to separation would be an ideal test case. The actual situation is almost paradoxial in the sense that accurate and reliable (not influenced by "pseudo Reynolds number effects" as discussed in chapter 2) experimental information on Reynolds number effects is rather limited as this AGARDograph shows. And this in turn hampers the development of more advanced calculation methods.

This does not mean that CFD is of no use for Reynolds number assessment. Computational methods that can adequately describe attached or almost attached flow conditions are of great help in the interpretation of the wind tunnel test results. They can be used and are actually used to estimate differences in transition location between wind tunnel and flight, to determine the simulation parameters for the aft fixation technique, to estimate at what Reynolds number trailing edge separation will disappear, to extrapolate drag results to higher Reynolds numbers etc. etc. In this way computational methods are essential for the enrichment of the information provided by the wind tunnel. The very detailed information from CFD-methods allows the test engingeer to make a much more reliable estimate of flight characteristics starting from wind tunnel test results.

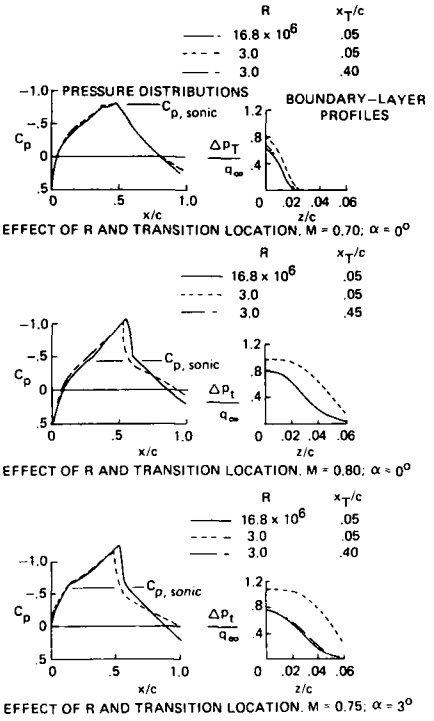

Fig. 3.6-1 Illustration of the aft-fixation technique (from ref. 68/1)

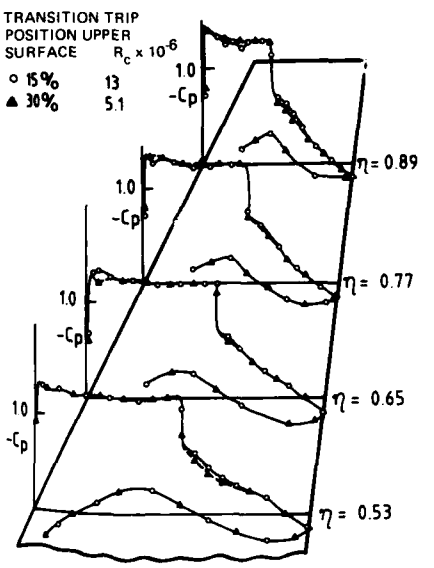

Fig. 3.6-3 Two independent simulations of "full scale" pressure distributions, outer wing, Mach = .78, C_L = .7 (ref. 85/4)

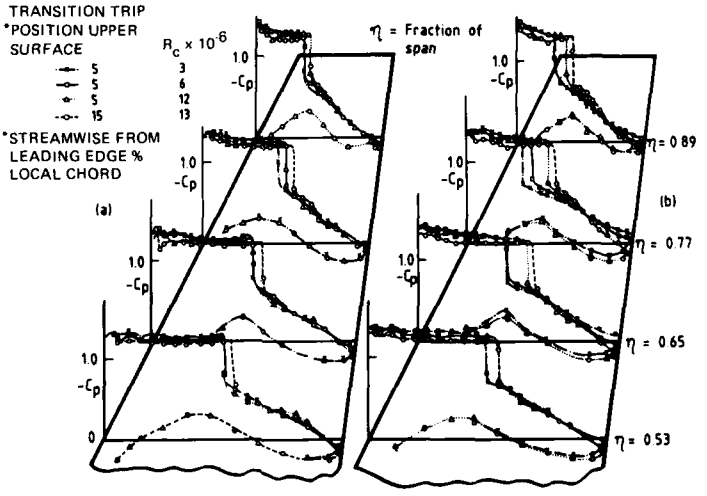

Fig. 3.6-2 Scale effects on outer wing pressure distributions. (a) C_L = .66; (b) C_L = .70 (from ref. 85/4)

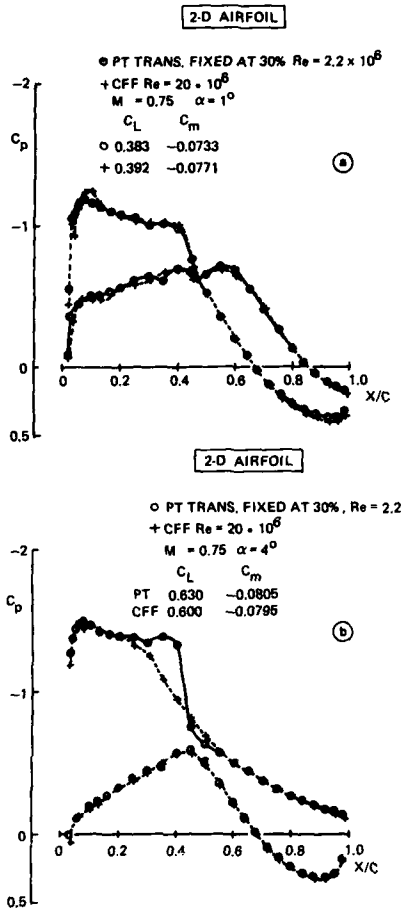

Fig. 3.6-4 Examples of high Reynolds number simulation with aft-fixation on a two-dimensional airfoil (from ref. 83/3)

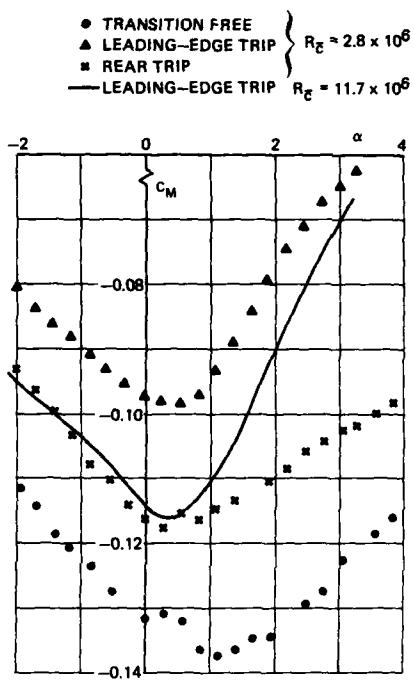

Fig. 3.6-6 Effect of strip position on pitching moment development with incidence (Mach = .85) (from ref. 76/1)

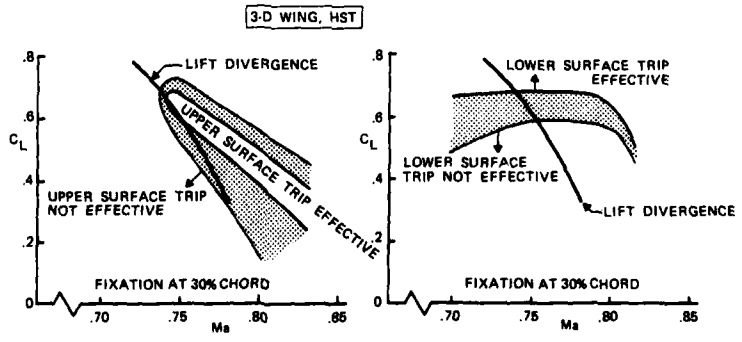

Fig. 3.6-5 Regions of applicability of the aftfixation technique in the lift-Mach-number plane (from ref. 83/3)

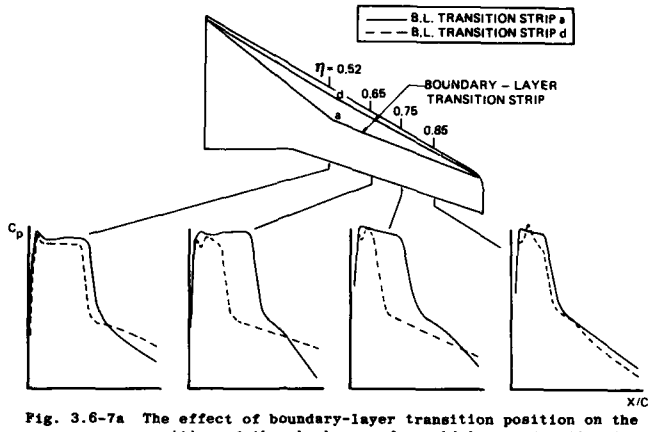

Fig. 3.6-7a The effect of boundary-layer transition position on the position of the shock wave for a high aspect ratio wing (from ref. 74/3)

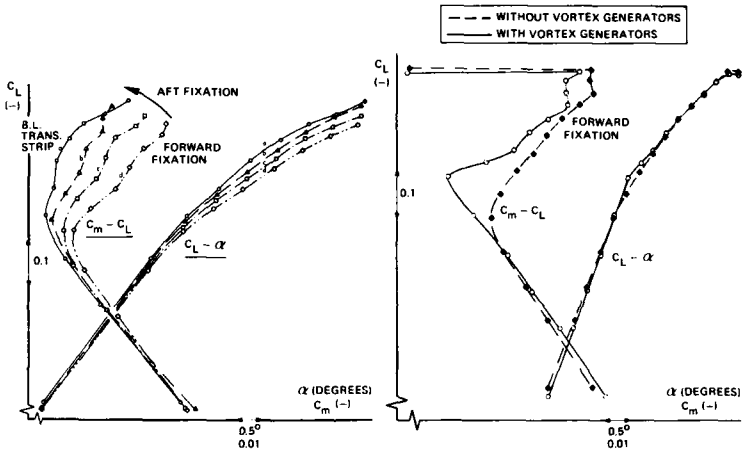

Fig. 3.6-7b The effect of aft-fixation and vortex generators on the lift and pitching moment development (from ref. 74/3)

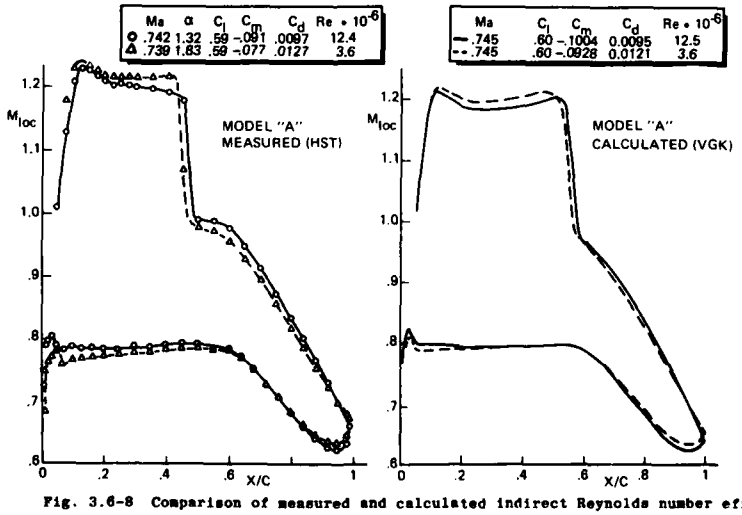

Fig. 3.6-8 Comparison of measured and calculated indirect Reynolds number effect on a two-dimensional airfoil (unpublished results of NLR)

4.0 OBSERVED REYNOLDS NUMBER EFFECTS: LOW ASPECT RATIO WINGS AND BODIES

by
T. W. Binion, Jr.
Calspan Corporation/AEDC Operations
Arnold Air Force Base, TN 37389
and
E. Stanewsky
Institut für Experimentelle Strömungsmechanik
Deutsche Forschungs- und Versuchsanstalt für Luft- und Raumfahrt e.V.
Göttingen, F.R.G.

4.1 Low Aspect Ratio Wings

Reynolds number effects on low aspect ratio configurations are potentially manifested in four factors: transition location, displacement thickness, shock position, and separation loci. While in two-dimensional flows, natural transition occurs primarily because of Tollmien-Schlichting instabilities, transition in highly 3D flows inherent with low aspect ratio configurations can be the result of leading edge contamination, cross flow instability, and in some situations Goertler instabilities as well. The modification of the spatial distribution of displacement thickness due to Reynolds number is, of course, coupled with the local flow vector distribution. The effects of Reynolds number on shock position and separation loci are closely coupled with those acting on displacement thickness. Because of the complex nature of the flows and because low aspect ratio configurations are used primarily for military applications, definitive information is not frequently published. Aside from some generic delta wing studies, there have been no systematic investigations of the basic aerodynamic characteristics of low aspect ratio configurations reported. The richest source of Reynolds number effects data seems to be wind tunnel to flight comparisons. Such comparisons are fraught with many difficulties because of pseudo-Reynolds effects which creep into wind tunnel data and inherent inaccuracies and measurement difficulties in flight testing. Thus, we feel that the data which follow should be viewed with some caution; the conclusions depicted may, with refined techniques and insight, be shown to be incorrect.

4.1.1 Zero-Lift Drag

Saltzman and Bellman [71/9] presented data correlations for the X-15 and the YF-102 aircraft. Wind tunnel zero-lift drag data were extrapolated using the Karnam-Schoenherr flat plate skin friction relationship [63/2] which obtains the best correlations in terms of Re_θ rather than Rex. Extrapolation of the data, Fig. 4.1.1, is excellent. Note however, that the X-15 data had to be correlated with the base drag removed because of the influence of sting interference on the blunt base configuration. It is further noted that the X-15 airplane and model were both very rigid; there were no leading edge slats, spoilers, or hinged rudders; no inlet flows, propulsion jets or bypass airflows to simulate on the model; and, the problem of measuring thrust in flight was avoided by considering only gliding flight. Thus, all of the pitfalls associated with the flexible, airbreathing aircraft were avoided. Even at that, it was necessary to subtract the base drag from both data sets because of sting interference in the wind tunnel. No explanation was given for the good agreement with the YF-102. However, the only "Reynolds number effect" for both configurations apparently was that due to skin friction.

4.1.2 Delta Wings

The formation of stable vortices over swept wings at angle of attack is a useful lift-generating phenomenon utilized as either the primary lift production mechanism or to augment the lift produced by a conventional airfoil, see [83/9] for example. From a phenomenological viewpoint, wings which produce lift can be classified according to their leading edges. In order to make a statement about Reynolds number effects for delta wings, it is necessary to specify the type of flow that exists over the wing. It has become traditional to categorize delta wing flow in terms of the Mach number and the flow incidence angle in a plane normal to the leading edge. Stanbrook and Squire [64/1] in evaluating data for sharp leading edge delta wings established demarcation regions for separated and attached flows at the leading edge in the Mn/αn plane. Szodruch [77/1] extended their idea by defining boundaries of other types of separation, Fig. 4.1.2. Not only do the specific effects of Reynolds number depend on the region of interest in the Mn/αn plane, but the boundaries themselves seem to be a function of Re, although truly definitive studies are lacking. Systematic studies for rounded leading edges are also sparse. Szodruch has summarized the present knowledge with respect to Reynolds number for

each class of wings [88/1]. It is felt unnecessary to repeat that summary here. The main points therefrom are:

(1) With sharp leading edge wings for which the primary flow separation is fixed at the leading edge, the main vortex position and strength is essentially constant with Reynolds number. However, the location of the secondary separation lines and hence the secondary vortex strength appears to be a moderately weak function of Re.

(2) A systematic study of Reynolds number effects for rounded leading edges has not appeared. Nevertheless, one may deduce from the existing data that the larger the leading edge radius, the greater the Reynolds number dependency. However, Poll [83/13], based on the comparison of his work with other results, states "Reynolds number, sweep, and incidence are insufficient in themselves to determine the type of (vortex) flow which will occur on a given airfoil section." He suggests the wind tunnel disturbance environment also may be a significant factor affecting the data.

(3) There is conflicting evidence on the effect of Reynolds number on vortex breakdown. Again, no systematic investigations have been published. However, Erickson [80/9] has compiled a group of data from several swept wings tested in both wind and water tunnels, Fig 4.1.3, which show no correlation between the angle of attack at which vortex breakdown begins and Reynolds number in the range between 9800 and 40 million.

4.1.3 Aerodynamic Derivatives

Teige, et al. [75/5], have reported a comparison of flight and wind tunnel obtained aerodynamic derivatives for the SAAB 37 fighter, Fig. 4.1.4. After applicable corrections, the flight data were reduced through a least-square regression process involving 75 equations. The results were cross checked using a 6-deg of freedom digital simulator with the flight control surface pulses as inputs to reproduce the flight motion. Wind tunnel tests were conducted with 1/30- and 1/50-scale models at Reynolds numbers of 6- and 12-million. Scatter in the $C_{n\beta}$ wind tunnel data in the transonic regime was attributed to nonlinear Cn-ß curves. Experience in other tunnels has shown that nonlinear Cn-ß data can be caused by flow non-uniformities in the test section flow if the pitch-roll technique is used to obtain yaw. However, as the sample data in Fig. 4.1.5 show, while aeroelastic corrections are necessary, no Reynolds number effects were found. The flight and wind tunnel predictions are in good agreement.

4.1.4 Buffet

Figure 4.1.6 [81/6] depicts a typical flow pattern on a transonic swept wing at buffet onset and with moderate buffet. At buffet onset, there is a bifurcated shock in the planform plane, mild shock induced separation, and the beginning of trailing edge separation in the wing root region. As incidence is increased, the flow pattern becomes much more complex with thickened shear layers, leading edge as well as shock induced separated regions, and regions of complete flow breakdown. The flow structure in the vicinity of the surface has much lower energy and is therefore more unstable. One would expect that since buffet is associated with such complex phenomena, Reynolds number would be a strong influencing parameter in buffet characterization. Such, however, does not appear to be the situation.

Because of the nature of buffet determination in conventional wind tunnels, aeroelastic effects can mask Reynolds number effects when Re is varied by changing total pressure. Such a difficulty can be avoided by using a cryogenic facility wherein Re can be varied by changing temperature keeping the dynamic pressure constant. Boyden [81/7] has conducted such a test using a 65-deg swept wing. The data, Fig. 4.1.7, are presented in terms of a steady, $\bar{C}_B$, and an unsteady, C_B, bending moment coefficient. The steady component is completely independent of Reynolds number as is the dynamic component prior to vortex breakdown. The reason for the rise in C_B beyond flow breakdown at the higher Re is believed to be associated with the increased frequency parameter rather than Re, see Mabey [81/6].

Butler and Spavins [77/2] tested a large half model of a 43-deg swept wing at Reynolds numbers up to the flight value which showed no Re effects and an excellent agreement with flight data, Fig. 4.1.8.

Buffet tests on the YF-4 showed that, of 8 methods tried to discern buffet, wing-tip accelerometers were the most sensitive and reliable indicator [70/2]. Wind tunnel data were obtained with a 5% model at unit Reynolds numbers between 3.4- and 7.8-million depending upon Mach number. Correlation of flight and wind tunnel data both using wing-tip accelerometers to detect buffet onset, Fig. 4.1.9, shows that at a given Mach number,

the wind tunnel predicted the onset of flow separation from 0.5- to 1-deg higher angle of attack than was experienced in flight. Whether that discrepancy is caused by a Reynolds number mismatch or some other factor was not investigated.

4.1.5 Transonic Technology Wing Program

A transonic technology wing program specifically designed to compare wind tunnel and flight data was conducted by Dornier in cooperation with several other agencies [82/11] [82/12]. The experimental aircraft, Fig. 4.1.10, and a 1/10-scale wind tunnel model were equipped with pressure orifices at identical locations. Comparison of pressure distributions from flight and Tunnel 16T showed generally very good agreement even though the Reynolds number differed by a factor of 6 to 10. Typical examples are shown in Fig. 4.1.11. Boundary-layer transition was free in each instance. Drag polars for one TST configuration are shown in Fig. 4.1.12. The wind tunnel data were obtained in the ONERA S2Ma at 2.5-million Reynolds number. The agreement is quite good except at Mach number 0.85. The wind tunnel data at Mach number 0.85 probably contains a large increment due to wall interference since the blockage was 1.2%.

4.1.6 Summary

Available data for low aspect ratio configurations depicting Reynolds number effects are sparse. No systematic investigations, other than a few for sharp edge delta wings, have been conducted. The data which are available, however, suggest that for most of the flight regime of interest, Reynolds number effects are small to nonexistent.

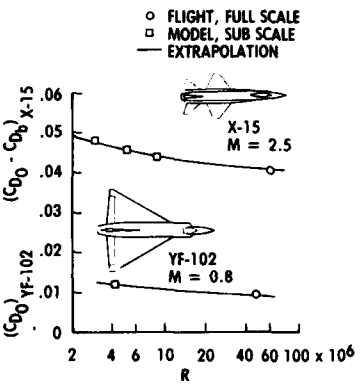

Fig. 4.1-1. Comparison of extrapolated wind tunnel model drag coefficients with full-scale flight results, [71/9].

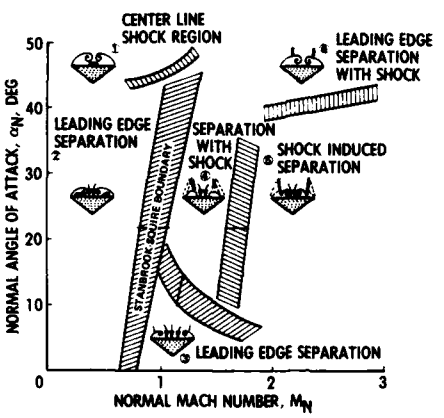

Fig. 4.1-2. Leeside flow regimes over thick Delta wings at supersonic speeds - α_N versus M_N diagram, [77/1].

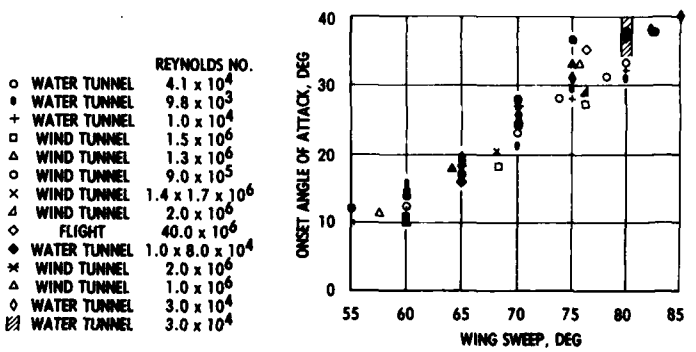

Fig. 4.1-3. Effects of wing sweep and Reynolds number on Delta wing vortex breakdown at the trailing edge, [80/19].

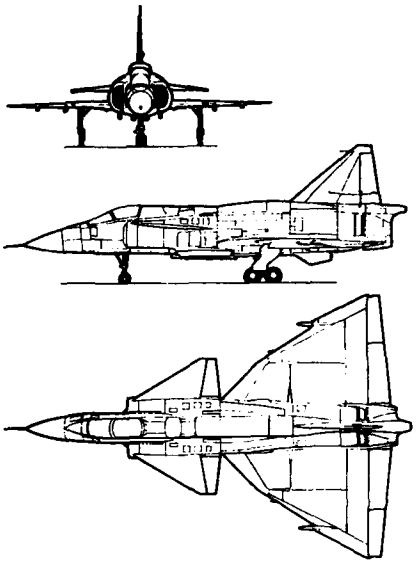

Fig. 4.1-4. SAAB 37 Viggen, [75/5].

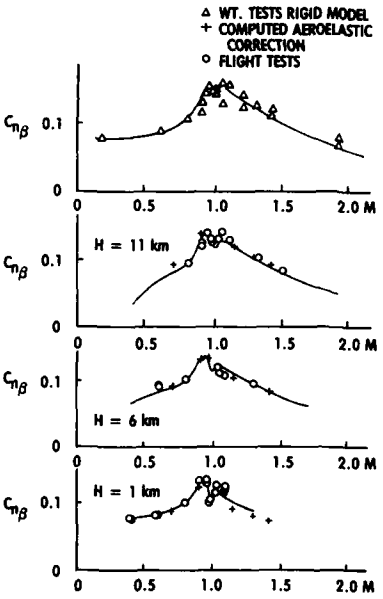

Fig. 4.1-5. Comparison of wind tunnel and flight derived C_{n_β}, SAAB-37 fighter, [75/5].

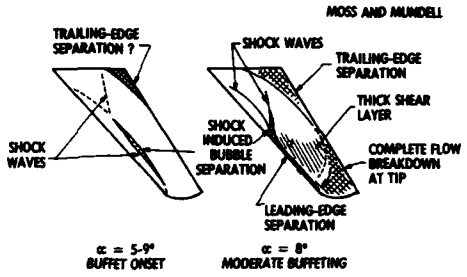

Fig. 4.1-6. Transonic flow on swept wing, M = 0.80, [81/6].

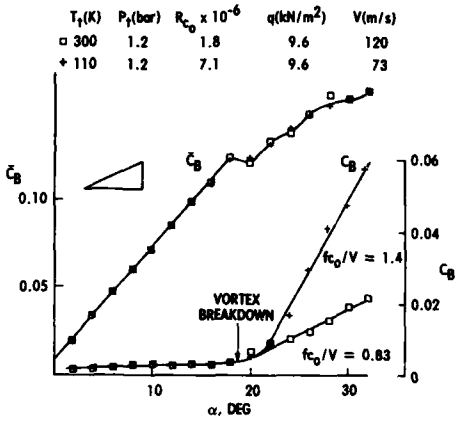

Fig. 4.1-7. Effect of Reynolds number on buffet, M = 0.35, 65-deg swept wing, [81/7].

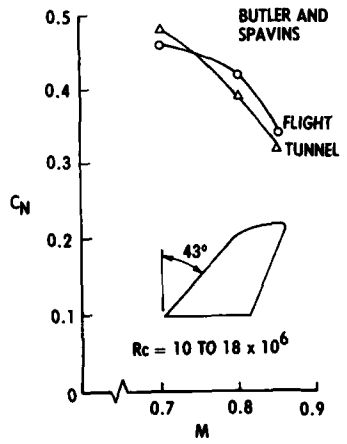

Fig. 4.1-8. Flight/tunnel comparison for buffet onset on a small fighter aircraft, [77/2].

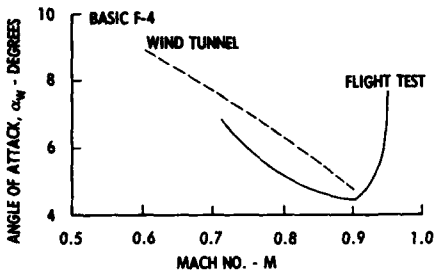

Fig. 4.1-9. Wingtip accelerometer, rms indication of airflow separation, comparison of wind tunnel and flight test results, [70/2].

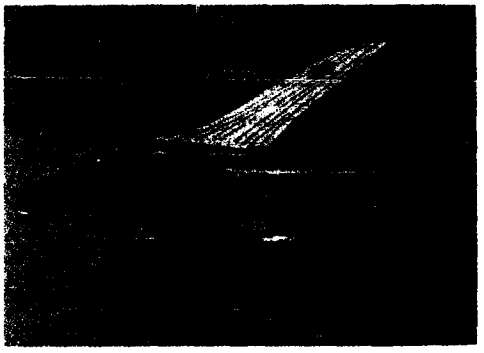

Fig. 4.1-10. Transonic technology wing on the Alpha jet, [82/12].

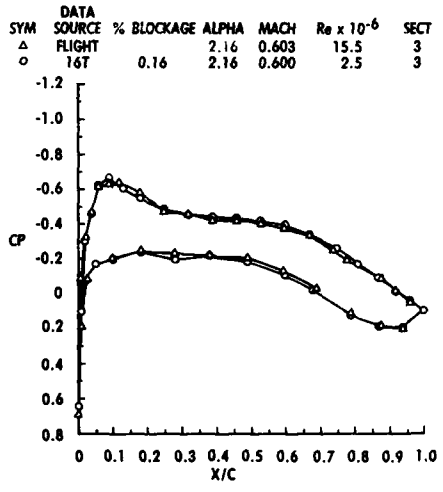

a. M = 0.6

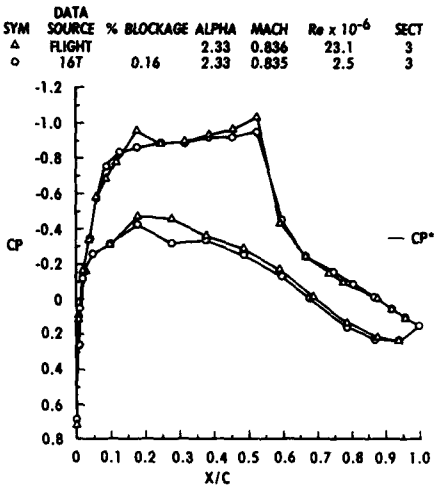

b. M = 0.835

Fig. 4.1-11. Comparison of wing surface pressure distribution from flight and wind tunnel, TST wing, [82/12]. Concluded.

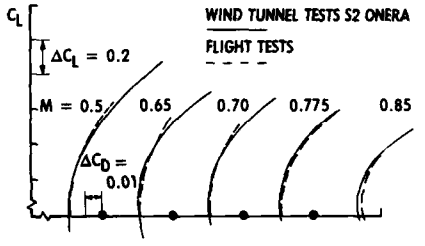

Fig 4-1.12. Comparison of forces from wind tunnel and flight test, TST configuration, [82/11].

4.2 BODIES

4.2.1 Introduction

Considering the flow about bodies typical of missile configurations and/or fighter fuselages, there exists an area particularly sensitive to Reynolds number effects, viz., the high angle of attack domain of freestream conditions. The strong interest in achieving high maneuverability for both missiles and fighter aircraft has increased the importance of that domain and hence the need for an accurate prediction of the vehicle performance at such conditions. We will, therefore, discuss here mainly the Reynolds number dependence of the aerodynamic characteristics of bodies at high angles of attack but also briefly treat the less sensitive lower incidence range as well as afterbody and base flow and their contributions to the overall Reynolds number dependence.

Before proceeding it should be noted that an extensive and thorough review of viscous effects related to bodies at high angles of attack (with an abundance of references) was carried out by Polhamus in 1984 [84/7]. We will essentially follow his discussion - where relevant - but restrict the present discussion to some characteristic examples of Reynolds number effects supplemented by results on afterbody and base flow.

4.2.2 Cylinders in normal flow

Many of the Reynolds number dependent viscous flow phenomena encountered by missiles and fuselages at high angles of attack can be related, at least qualitatively, to the flow about circular cylinders. Here, the various phenomena and regimes covered as the Reynolds number is increased, say, from the low Reynolds number wind tunnel tests to full-scale conditions can best be explained. These regimes are defined in Figure 4.2.1 where the drag coefficient for a circular cylinder is plotted versus the Reynolds number based on the diameter of the cylinder [84/7].

In the subcritical range, below a Reynolds number of $R_D=2x10^5$, the flow is laminar and a laminar separation occurs at a separation angle of $\theta_S=80°$. Since the flow does not reattach, a wide wake and a correspondingly high drag coefficient results. In this range a dominant vortex shedding frequency is present. When increasing the Reynolds number, the laminar separation is followed by a turbulent reattachment with transition having occurred in the separated shear layer. In this "critical" range a renewed but turbulent separation takes place further downstream - for $R_D=4x10^5$, for instance, at $\theta_S=130°$ - resulting in a narrowing of the wake with an associated strong decline in drag coefficient. Other than stated by Polhamus [84/7], evidence is given, for instance, by Horvath et al. [86/3] and Schewe [83/11] that a narrowband coherent vortex shedding still exists in the critical Reynolds number range. Note, that flows with laminar separation and transition taking place in the separated shear layer are known to give a similarly favorable effect on drag for airfoils and wings in transonic flow [68/2] [81/1].

In the supercritical range, $R_D\approx4x10^5$ to about $R_D=6x10^6$, transition to turbulent flow moves upstream to a position ahead of separation and eventually to the vicinity of the foreward stagnation point. In that range the separation point shifts, due to the change in boundary layer conditions, also upstream from the extreme downstream position $\theta_S=130°$ to about $\theta_S=115°$; there is, due to the widening of the wake, a corresponding increase in the drag coefficient. Spectra signatures from this regime are wideband with no predominant frequency except for a small region at the high Reynolds number end where a narrowband vortex shedding prevails. The flow development in the supercritical range is very sensitive to freestream turbulence and surface roughness [86/3].

At the high Reynolds number end of the supercritical range, the drag levels off since the upstream movement of the transition point eventually comes to a halt. At still higher Reynolds numbers in a range termed "hypercritical" by Polhamus [84/7], the boundary layer is fully turbulent and the drag coefficient is likely to decrease with increasing Reynolds number, predominantly due to a slight downward shift in the separation location. The vortex wake flow becomes here at least quasi-periodic.

Many correlations have been made of the effect of the Reynolds number on the flow about circular cylinders. These correlations have often shown a wide band of data uncertainty which was explained as being caused, for instance, by differences in surface roughness, compressibility and end conditions, i. e., the tunnel width to cylinder diameter ratio. Polhamus [84/7] has carried out a careful selection of results from various sources, restricting the data to incompressible flow

($M \leq 0.15$)[1]) , which are essentially free from "secondary" effects; they are depicted in Figure 4.2.2. The data basically exhibit the Reynolds number dependence described above. The reader is also referred to the investigation of Schewe [83/11] who covered a Reynolds number range between $Re_D=2.3x10^4$ and $Re_D=7x10^6$ with one experimental setup by varying the total pressure between one and 51 bar. The investigation revealed interesting details of the flow behavior in the critical Reynolds number range where distinct discontinuities in the Reynolds number dependence were observed, Figure 4.2.3. Here, the discontinuity at A is attributed to the formation of a laminar separation with turbulent reattachment and subsequent far aft separation on one side of the cylinder and a laminar separation without reattachment on the other side. This asymmetric flow development is accompanied by a steady lift force, Figure 4.2.4, which disappears as soon as the flow re-establishes its symmetric condition with increasing Reynolds number; the latter results in the discontinuity at B. Note, that the lift force observed in the critical range is associated with one mechanism generating side forces (out-off-plane forces) on, say, a three-dimensional ogive-cylinder body at angle of attack.

It was mentioned earlier that two effects, namely the effects of roughness and compressibility, frequently obscured a comparison of results on flows about cylinders obtained from different sources. Their individual influence is, therefore, shown in Figures 4.2.5 and 4.2.6: Roughness of sufficient height essentially promotes an early transition so that the transition point may always be located upstream of the separation point as is the situation of the upper two curves of Figure 4.2.5 ($r/Dx10^5=900$ and 450, respectively). Here, an increase in Reynolds number, starting, say, at $R_D=10^5$, initially moves the transition point further upstream to the vicinity of the stagnation point resulting in an increase in drag. At a further increase in Reynolds number the drag gradually decreases with the behavior of the flow being as in the hypercritical range, although at much lower Reynolds numbers. As the roughness height is decreased , various stages in the Reynolds number dependence of the flow development can be observed: At $r/D=110x10^5$, for instance, a very noticeable critical as well as a supercritical domain still exist; however, both extend over a much smaller Reynolds number range than is obtained with a smooth surface. Concerning compressibility, Figure 4.2.6, one observes that the classical Reynolds number dependence persists at least up to the vicinity of the critical Mach number with the drag increasing as the Mach number is raised. As soon as shock waves occur, strong enough to separate the turbulent boundary layer, the characteristic drop in drag in the critical Reynolds number range is likely to disappear (also see Figure 4.2.12.). Note, that the drag coefficient decreases in the hypercritical range as was conjectured when discussing Figure 4.2.1.

Besides the circular cylinder, other cross-sectional shapes are of interest such as, for instance, a rectangular cross section with rounded corners which might be selected for a missile body to improve the packing density for submunition [83/12]. Furthermore, such shapes can be found on fuselages of modern combat aircraft which are required to maneuver at high angles of attack. Figure 4.2.7, again taken from Ref [84/7], summarizes some typical results concerning the Reynolds number dependence of the drag coefficient for cylinders with square cross sections having various values of the normalized corner radius. One observes a strong effect of the corner radius on both the value of the drag and on the Reynolds number for the transition from subcritical to supercritical flow. For the smallest radius, $r/w=0.021$, separation occurs on the windward corners, essentially fixed by geometry, at least at the low Reynolds numbers considered here, and the strong Reynolds number effects observed for the circular cylinder cannot be expected. The drag is similar to that for a flat plate perpendicular to the flow. As the corner radius is increased, the adverse pressure gradients at the corners are reduced and, as a consequence, separation is now affected by Reynolds number in a way similar to the circular cylinder, although the drag of the latter is not reached here.

Ref. 84/7 also considers the influence of the flow angle on drag and side forces for cylinders with non-circular cross sections and cross sections with other than rectangular shapes. The results show basically similar Reynolds number dependences as the ones depicted in Figure 4.2.7. Finally, it should be noted that data for non-circular cross sections are mainly available for incompressible flow and Reynolds numbers of $Re_D \leq 2x10^6$; there is a considerable need to extend investigations to compressible flow and to higher Reynolds numbers.

4.2.3 Cylinders in oblique flow

An interim stage between the cylinder in normal flow and, say, a cone-cylinder body at angle of attack is the cylinder of infinite length in oblique flow (swept

---

[1]) Applicable to three-dimensional bodies in transonic flow at low angles of attack

cylinder). Results for such a configuration are depicted in Figure 4.2.8 in the form normal force, $C_N/\sin^2\alpha$, versus effective Reynolds number, Re_{eff} , for various sweep angles α [84/7]. Here, the effective Reynolds number corresponds to the one defined by Esch [75/6], viz.,

$$Re_{eff} = Re_D \cdot K_\alpha$$

where

$$K_\alpha = [0.983 / \sin\alpha + 0.311 + 0.287 \cdot \sin\alpha] / 1.581$$

In this formulation, K_α is equal to the ratio of the circumferential length of the body in the plane parallel to the freestream (ellipse) to that in the cross flow plane (circle), thus accounting for the actual change in streamline length, say, to the separation line, as the sweep angle is changed. One observes that this effective Reynolds number correlates the data of Figure 4.2.8 with regard to the onset of the critical Reynolds number regime quite well - as a matter of fact, better than any other correlation. This indicates that the flow component normal to the cylinder is not instrumental in determining separation and transition conditions, at least not at sweep angles of $\alpha \leq 60°$, a fact also supported by the dependence of the normal force coefficient $C_N/\sin^2\alpha$ on the sweep angle in the supercritical Reynolds number range. Such a limit in the applicability of the independence principle, i.e., the independence of the flow components normal and parallel to the body considered, which holds strictly only for laminar flow, was also found for shock-induced separation on wings in transonic flow [88/1]. For further discussions on the Reynolds number dependence of the flow about infinitely swept cylinders, the reader is referred to Ref. 84/7.

4.2.4 Three-dimensional bodies

As a slender body is pitched through the angle of attack range $0° \leq \alpha \leq 90°$, it experiences four distinct flow patterns that reflect the diminishing influence of the axial flow component eventually leading to conditions discussed in the previous sections, Figure 4.2.9 [87/4] [79/3] [81/8]. At low angles of attack the axial component dominates ; the flow is attached and essentially vortex free. As the angle of attack is increased, cross flow developes and the boundary layer separates on the leeward side of the body forming a symmetric vortex pair. This condition is depicted in Figure 4.2.9 (a) for $\alpha=30°$. Note, that the vortex lifts off the body at the extreme downstream end. In the next higher α-regime, the cross flow effects start to dominate and the vortices become asymmetric thereby producing a side force at zero side slip or yaw, Figure 4.2.9 (a), $\alpha=50°$. Finally, at very high angles of attack, the cross flow dominates completely and the vortices are shed either in a periodic form or in a wideband random fashion dependent on the Reynolds number as discussed in Section 4.2.2 for the cylinder in normal flow.

It can be expected that the flow development in the various regimes is more or less strongly influenced by the Reynolds number. To show this the normal force coefficient, based on freestream conditions and base area, for a typical ogive-cylinder body is first depicted as function of the angle of attack with the Reynolds number as parameter, Figure 4.2.10 [78/5]. Also indicated in this figure is the angle of attack dependence of the normal force according to cross flow theory assuming a purely laminar and a fully turbulent separation with separation angles corresponding to the maximum drag in the subcritical and the minimum drag in the supercritical Reynolds number regime, respectively, for the cylinder in normal flow [51/3]. One observes that the flow development is highly dependent on Reynolds number, starting already at relatively low angles of incidence, and that a particularly strong change in normal force occurs as separation shifts from a laminar to a fully turbulent state.

A still better illustration of the flow development is obtained when cross-plotting the results of Figure 4.2.10 as function of the Reynolds number with the angle of attack as parameter. This was carried out by Polhamus [84/7] supplementing these results by data of Foley [71/10] at an incidence of $\alpha=30°$, Figure 4.2.11. The different Reynolds number regimes, discussed in Section 4.2.2 for the cylinder in normal flow, become clearly distinguishable: the subcritical range where a laminar separation prevails, the critical Reynolds number domain where a transitional separation with subsequent turublent reattachment and a renewed separation takes place - and where the drag coefficient for the cylinder in normal flow has a minimum - and the super- and hypercritical domains where the separation eventually becomes fully turbulent. Figure 4.2.11 also illustrates the large reduction in the critical Reynolds number, based on cylinder diameter and freestream conditions, with decreasing angle of attack which is associated with the corresponding increase in streamline length similar to the conditions for the infinitely swept cylinder discussed earlier. (For the establishment of the characteristic boundaries, marked

by the dashed lines in Figure 4.2.11, from results for the cylinder in normal flow, the reader is referred to Ref. 84/7.) Note, that the influence of compressibility on the critical Reynolds number is still minor at the freestream Mach number considered (M_∞=0.5), even at the extreme angles of attack.

In order to explore the influence of compressibility on the Reynolds number dependence, the data of Hartmann [78/5] are cross-plotted in Figure 4.2.12 for constant Mach numbers at angles of attack of α=30° and α=60° . It can be observed that the critical Reynolds number increases slightly with Mach number and that, at the same time, the Reynolds number sensitivity in the critical Reynolds number range gradually disappears. The latter is due to the fact, already pointed out in Section 4.2.2, that the cross flow Mach number becomes large enough to establish supersonic regions on the body with terminating shock waves strong enough to separate the boundary layer essentially independent of the condition of the boundary layer upstream of the shock. This is in agreement with evidence presented in Ref. 88/1 which indicates that the onset of shock-induced separation (incipient separation) is, for a turbulent boundary layer, only weakly dependent on viscous effects so that only a marginal decrease in normal force with Reynolds number can be expected here. Note, that the second set of Reynolds number boundaries given in Figure 4.2.12, termed "laminar, transitional and fully turbulent", will be discussed below.

It is well known that side (or out-off-plane) forces on slender bodies at zero side-slip or yaw angle pose a serious problem to the maneuverability of such configurations so that a closer look at the Reynolds number dependence of side forces in the various angle of attack domains seems warranted. There are essentially two mechanisms that may generate side forces: One occurs only in the critical Reynolds number regime and is related to the steady lift forces on the cylinder in normal flow caused by different developments of transition and separation on the upper and lower side of the cylinder (see Figure 4.2.4 and Section 4.2.2). The other mechanism, referred to at the beginning of this section, also operates in the subcritical (laminar) and the super- and hypercritical (fully turbulent) separation regimes; this mechanism is directly related to hydrodynamic instability and is qualitatively described by the impulsive flow analogy [82/13]. For a more detailed study of vortex-induced asymmetric loads, the reader is referred to the review of Ericsson and Reding [81/8] and the papers by Lamont [82/13], Hartmann [87/4] and Champigny [86/4].

The true effect of Reynolds number and angle of attack on side forces can only be determined when first considering the variation of the side force with roll angle which occurs even if the flow is steady and extreme care has been taken to manufacture a model without apparent geometric asymmetry [82/13]. The phenomenon is illustrated in Figure 4.2.13 for two angles of attack and Reynolds numbers of Re_D=2.5x10^5 and Re_D=7.3x10^5, corresponding - see Figur 4.2.11 - to the subcritical and supercritical Reynolds number range, respectively. One observes that in the test cases considered two side force cycles occur during a complete roll and that, furthermore, pronounced maxima are present which seem to decrease as the Reynolds number is raised. Considering henceforth only the absolute maximum during a complete roll as representative of the overall side force, it is indicated in Figure 4.2.14, taken from Ref. 82/13, that there is a strong variation of that force with angle of attack as well as with Reynolds number. Side forces start to develop, nearly independent of the Reynolds number, at an angle of attack of about α=30° and persist almost up to α=90°, especially at Re_D=0.4x10^6, a Reynolds number which lies within the critical Reynolds number range where for the cylinder in normal flow spurious lift forces existed.

The effect of the Reynolds number on the maximum side force is illustrated in Figure 4.2.15 for two test cases [82/13] [85/13]. The maximum side force falls from a high value at a Reynolds number of approximately Re_D=2x10^5 (laminar separation) to almost zero at the end of the critical Reynolds number range before climbing again to a higher value at Reynolds numbers of Re_D=2x10^6 to Re_D=4x10^6 at which a fully turbulent separation exists. The Reynolds number range where the side forces become almost zero is the same as the one where the cylinder in normal flow exhibits a minimum in the Reynolds number dependence of the drag coefficient and where the steady lift force, Figure 4.2.4, falls again to zero. At these conditions separation occurs furthest downstream, as indicated by the corresponding circumferential pressure distribution in Figure 4.2.16, and the symmetric vortex pattern becomes stable. The results of Figure 4.2.15 are somewhat contrary to a statement of Ericsson and Reding [81/8] who claim that the largest side forces develop in the critical Reynolds number regime due to differences in the transition pattern on opposite sides of the cylinder. Note, that the vortex-induced side loads decrease with increasing subsonic cross flow Mach number ($M_\infty \geq 0.4$) and become insignificant at supersonic cross flow Mach numbers [81/8] [84/7].

At various instances we have referred to boundaries identifying characteristic Reynolds number domains for three-dimensional bodies: One set of boundaries, i.e., subcritical, critical and super- and hypercritical, was derived from the conditions on the cylinder in normal flow utilizing the relation for the effective Reynolds number $K_\alpha = Re_{eff} / Re_D$ (see Section 4.2.2 and Figures 4.2.8 and 4.2.11). Another classification is based simply on the type of separation occurring on the body, i.e., laminar, transitional - with transition taking place within the separated region - or fully turbulent separation. Lamont derived such boundaries from pressure distributions similar to the ones depicted in Figure 4.2.16 for an ogive-cylinder body [82/13]. These boundaries are shown in Figure 4.2.17 in the Reynolds number / angle of attack plane. One observes that the Reynolds number boundary between transitional and fully turbulent separation is a strong function of angle of attack, whereas the laminar-transitional separation boundary is much less dependent on incidence. Note, that these boundaries may strictly only be applied to smooth cylinders in low turbulence streams for which they were derived. It seems likely that freestream turbulence and surface roughness will have an effect on inclined cylinder flows similar to the one experienced for the cylinder in normal flow (see Figure 4.2.5).

Also of interest, for reasons outlined in Section 4.2.2, is the Reynolds number dependence of three-dimensional bodies with non-circular cross sections. Unfortunately, there is only a very limited number of results available and of the few, just one example is shown here, depicting the effect of the Reynolds number on the normal force coefficient for the fuselage of an orbiter-type vehicle with various corner radii, Figure 4.2.18 [84/7] [71/11]. The dependence on Reynolds number and corner radius is essentially the same as for the corresponding cylinder in normal flow and, at a given corner radius, say r/w=0.086, the effect of viscosity is very similar to the one for an ogive-cylinder configuration: a nearly constant normal force in the subcritical Reynolds number range and a strong decrease in normal force as the critical Reynolds number is exceeded. Note, that also for the present configuration, the Reynolds number sensitivity in the critical Reynolds number range disappears as the normal Mach number component exceeds critical freestream conditions.

4.2.5 Afterbody and base flow

The investigation of afterbodies, either by detailed studies of the local flow development or by determination of the overall forces acting on the afterbody, is an integral part of the flight vehicle design and development process [85/14]. The importance of such investigations derives, in part, from the fact that afterbodies, either as a component of the fuselage or as part of the propulsion/exhaust system of jet-propelled aircraft, may contribute considerably to the overall drag of the flight vehicle. Accurate prediction of the full-scale flow development requires the understanding of possible Reynolds number effects on afterbody flow. Note, that a critical review of computational and experimental techniques concerned with afterbody/nozzle aerodynamics, jet airframe interference effects, and nozzle integration is presented in the report of the AGARD Working Group "Aerodynamics of Aircraft Afterbody" [86/5] (also see 85/14), unfortunately without addressing the issue of Reynolds number effects to any extent.

A review of the effect of Reynolds number on afterbody drag was given by Pozniak in Ref. 81/9. Concerning the Reynolds number influence, he comes to the following conclusions:

- At subsonic Mach numbers and in the absence of major flow separation, significant but compensating pressure changes are found such that there is little effect on the afterbody pressure drag of complete afterbodies as Reynolds number in varied.

- In the presence of flow separation, the effects of Reynolds number tend to be small when the location of flow separation is fixed as a result of a sudden change in the boattail contour, but on afterbodies with more continuous contours the point of separation can be affected. Conflicting factors are then involved and the afterbody drag can increase or decrease by modest amounts or remain unaffected by Reynolds number changes.

- Significant increases in drag with increasing Reynolds number have been consistantly reported for high subsonic Mach numbers above the transonic drag rise and at supersonic speeds.

- Misleading Reynolds number effects on afterbody drag may occur due to the influence of the Reynolds number on wall interference and the wind tunnel environment.

In this section some representative results relating to these conclusions shall be presented, utilizing data that are considered essentially free of "secondary" effects caused by changing models, test setups and wind tunnels to cover a wide Reynolds number range or by the effect of the Reynolds number on the wind tunnel environment.

Figure 4.2.19 shows the dependence of the pressure drag for a circular-arc-cone afterbody on the Reynolds number, the latter based on the forebody length, L. The data were obtained in the NASA-Langley 0.3-m cryogenic tunnel at Mach numbers of M_∞=0.60 and 0.9 over a wide Reynolds number range [76/6]. Note, that in addition to the temperature and pressure of the tunnel, the forebody length was varied to cover the Reynolds number range up to $Re_L = 130 \times 10^6$, as indicated by the open and half-filled symbols in Figure 4.2.19.

One observes at both Mach numbers considered and for both body lengths utilized a moderate increase in afterbody pressure drag, based on maximum body cross section area, with Reynolds number. There is also a noticeable difference in drag for the different body lengths. The latter is judged to be due to the differences in the condition of the boundary layer approaching the afterbody, mainly the displacement thickness, which is for the same Reynolds number Re_L larger in the case of the longer body. At the lower Mach number, the drag thus seems to increase with displacement thickness, while at M_∞=0.90 the pressure drag decreases slightly, at least in the lower Reynolds number range, which is in accordance with the trend observed with increasing Reynolds number. This behavior shall be further analyzed by considering the corresponding pressure distribution.

One of the reasons for the low Reynolds number sensitivity of the afterbody drag observed here is the compensation that occurs in the Reynolds number dependence of the pressure distribution. This is illustrated in Figure 4.2.20 where the minima and maxima in the pressure distribution, identified in the inset to this figure, are depicted as function of the Reynolds number for the conditions outlined above. One notices that the minimum pressure decreases with Reynolds number, which can essentially be attributed to the reduction in the displacement thickness at the shoulder of the afterbody; this is confirmed by comparing the pressures for the two different body lengths. The reduction in displacement thickness results in an increased curvature of the effective body contour and thus in a stronger expansion. The pressure recovery improves with Reynolds number and - for the same reason - with decreasing displacement thickness, similar to the effects observed on transonic airfoils and wings [81/1], thus compensating, at least in part, the higher suction peaks. Figure 4.2.20 also provides an explanation why at M_∞=0.60 the pressure drag increases at a given Re_L with increasing displacement thickness: the lower pressures over the rear of the afterbody in case of the thicker boundary layer are not able to compensate the suction peak, which results in a net increase in drag. This may be due to a rear separation occurring at these conditions. Generally, the test cases considered correspond to conditions prior to the transonic drag rise, and (shock- induced) separation does not play a major role in the flow development. Overall changes in the pressure drag are correspondingly small.

It was stated in the conclusions cited above (Pozniak 81/9) that the Reynolds number sensitivity of afterbody drag becomes larger in the vicinity of and especially above the drag rise boundary. This is illustrated in Figure 4.2.20 for the boattail "6524", investigated in a comprehensive test program, involving several body geometries, conducted by Blaha et al. [76/7]. The displacement thickness - rather than the Reynolds number - was here the parameter representing viscous conditions; it was varied by changing body length and roughness. At M_∞=0.60, for a flow that is mainly attached, the flow development is similar to the one described above: increases in the suction peaks and improved pressure recoveries compensate to give near-zero drag changes with decreasing displacement thickness, Figure 4.2.21 (c). At the higher Mach numbers, say, $M_\infty \geq 0.9$, significant areas of separation were present, which tended to be reduced in extent as the initial displacement thickness was raised, Figure 4.2.21 (b). (Note, that the areas denoted "highly turbulent" in that figure mark regions of intermittent backflow.) As shown by the pressure distributions at $M_\infty = 0.90$, the thinner boundary layer resulted here in a remarkably strong increase in the suction, indicating the presence of a supersonic pocket with a terminating shock wave, the latter causing the boundary layer to separate early. For the larger displacement thickness, the suction pressure barely exceeds the one for M_∞=0.60. The high suction values and the reduced pressure recoveries due to separation are, of course, the reason for the large increase in pressure drag observed for the thinner boundary layers, Figure 4.2.21 (a).

Figure 4.2.22 summarizes the influence of increasing displacement thickness on boattail pressure drag for the body "6524" just discussed. Also shown is the Reynolds number dependence for body "2524", characterized by larger pressure gradients, at M_∞=0.90. Due to the larger pressure gradients, the response to viscous changes is much more severe.

The results described in the preceding paragraphs were obtained on simple forebody/afterbody configurations, and, in general, the afterbody drag increased with increasing Reynolds number or decreasing displacement thickness. In the following, results for a more complex configuration shall briefly be considered: Measurements of the installed boattail drag over a wide range of Reynolds numbers have been made by NASA on boattails mounted behind underwing nacelles on an F-106 type delta aircraft during tunnel and flight tests [75/7]. Examples of the measured pressure drag at M_∞=0.60 and 0.90 are depicted in Figure 4.2.23, replotted from Ref. 81/9, for the flight tests only, being consistent with the initial statement to restrict the illustration of Reynolds number effects to results obtained with one configuration and one test setup to avoid "secondary" effects of obscuring the results.

The flight test data for the various boattail geometries consistently indicate a reduction in boattail drag with increasing Reynolds number, although the exact rate is uncertain due to the scatter of data. There are several comments to be made concerning this Reynolds number dependence: One reason for the drag reduction with Reynolds number might be due to the dominant effect of the Reynolds number on separation, hence on pressure recovery, rather than on the suction peak, contrary to the development observed for the bodies in Figures 4.2.21 and 4.2.22; a favorable effect of an increase in Reynolds number on separation, determined by wool tufts, was indicated during the flight tests. Another possible contribution to the observed variation in drag may arise from the presence of a significant and favorable interference effect from the closeness of the contoured part of the afterbody to the wing coupled with a positive influence of increasing Reynolds number on the wing flow. There is, however, further - indirect - evidence from other flight tests [74/4] that boattail separation in relation to the suction peak development may essentially determine this drag behavior: Little effect of Reynolds number on drag was shown in cases where little movement of the separation point occurred.

There are many parameters - besides the ones associated with viscous changes - that may have an influence on afterbody flow, especially for complex geometries. For a more detailed study of these, the reader is referred to Refs. 85/11 and 81/9 and the many literature sources given there.

Base pressure is likely to be affected by the boundary layer condition upstream of the base in a way similar to the afterbody pressure distribution, at least as far as the expansion around the shoulder is concerned. There seems, therefore, no need to address here viscous effects on base flow to any great extent. In addition, a detailed study of the aerodynamics of base flow, including the influence of combustion, also containing major correlations of base pressure with viscous and geometric parameters, is given in Ref. 76/8, to which the reader is referred.

A characteristic example of the influence of the state of the boundary layer on base pressure is depicted in Figure 4.2.24 for a cone-cylinder model with L/D=5[76/8]: In the laminar region, the base pressure coefficient decreases with increasing Reynolds number, mainly due to the corresponding reduction in displacement thickness at the corner of the base. In the transitional region and the initial turbulent domain, the base pressure increases with Reynolds number, probably due to boundary layer transition progressing upstream towards the apex of the body with a corresponding increase in the boundary layer thickness. For fully turbulent flow approaching the corner, the base pressure decreases again as the Reynolds number is raised; this is illustrated in Figure 4.2.25 by a large body of experimental data presented in a correlation according to Chapman [58/1].

As a further example of the Reynolds number effect on base flow, some results of measurements on a space shuttle orbiter-type configuration at transonic speeds - however, only over a very limited Reynolds number range - are depicted in Figure 4.2.26 [72/7]. The data, obtained for free and forced transition and at various angles of incidence, all show the same trend: an increase in base-drag coefficient - due to a drop in base pressure - with increasing Reynolds number similar to the behavior observed on the simpler geometry discussed above.

4.2.6 Conclusion

The Reynolds number dependence of the flow about bodies, including afterbody and base flow, has briefly been reviewed. This review showed examples characteristic of Reynolds number effects for cylinders with circular and non-circular cross sections in normal flow, sheared cylinders of quasi-infinite span, three-dimensional fuselage- and missile-type bodies, and afterbodies as they exist on fighters and nacelles as part of the exhaust/propulsion system.

Two-dimensional bodies at subcritical speeds and three-dimensional bodies with subcritical cross flow velocities exhibit essentially the same behavior with increasing Reynolds number: At low Reynolds numbers the flow is laminar and laminar separation occurs, drag and normal force, respectively, are relatively high. As the Reynolds number is increased, the critical Reynolds number range is entered, and drag and normal force drop rapidly due to transition occurring in the separated shear layer with a subsequent turbulent reattachment and renewed separation at a large circumferential angle. At transitional separation conditions, a steady lift force may act on the cylinder in cross flow which manifests itself on the three-dimensional body as a side force. These forces are caused by differences in the boundary layer, and hence separation development, on opposite sides of the body. The side force is nearly zero at the transition between the critical and the supercritical Reynolds number ranges where the drag and the normal force for the two-dimensional cylinder and the three-dimensional body, respectively, also have a minimum. Note, that these side forces may occur at any angle of attack and that they are, at a given incidence and wind tunnel environment, only dependent on Reynolds number. A further increase in Reynolds number results in an increase in drag and normal force up to conditions at which the movement of the transition point on the body ceases; hereafter, a reversal in Reynolds number dependence should develop; however, very little data is available in the hypercritical Reynolds number range to confirm this.

A second mechanism generating side forces on a three-dimensional body is related to hydrodynamic instability. These out-off-plane forces occur at angles of attack roughly between 30° and 60°, dependent on body length, in all Reynolds number regimes; they have, however, as indicated above, a minimum in the critical/supercritical Reynolds number range.

With increasing Mach number, the classical Reynolds number dependence disappears due to the development of supersonic regions with terminating shock waves strong enough to separate even the turbulent boundary layer. At such conditions, the flow development seems not very susceptible to viscous changes The freestream conditions at which this occurs may, however, dependent on angle of attack, already be supersonic since the freestream Mach number component normal to the body is the dominant parameter.

Note, that single or distributed roughness in a form that fixes transition well upstream of separation also strongly reduces the Reynolds number dependence, as do bodies with corner radii that essentially fix separation itself.

Concerning afterbody flow, it was found that at subsonic Mach numbers in the absence of major flow separation significant but compensating pressure changes occur such that there is little effect of Reynolds number on afterbody pressure drag. However, strong increases in drag with increasing Reynolds number were consistantly observed at subsonic Mach numbers above the transonic drag rise and at supersonic speeds. At the lower Mach numbers, the stronger expansion in the shoulder region of the afterbody caused by reduced displacement thickness as Reynolds number increases is compensated by the improved pressure recovery; at the higher Mach numbers, reducing displacement thickness by increasing Reynolds number causes such a strong expansion that shock waves develop separating the boundary layer in a way that the pressure recovery can no longer compensate the expansion and a net increase in drag results.

There is also evidence obtained on more complex configurations, e.g., boattails mounted behind underwing nacelles, that the boattail pressure drag may well decrease with increasing Reynolds number. One reason for this behavior seems to be the positive effect of the Reynolds number on separation, hence on pressure recovery, rather than on the suction peak development, as was the case in the examples cited above.

The opposing trends in the Reynolds number dependence of afterbody drag suggests that further research is needed, especially for more complex configurations, to determine conditions at which either the effect of the Reynolds number on the suction peak or on separation is dominant, and, furthermore, to determine the influence of the closeness of the afterbody to adjacent aircraft components. Concerning the Reynolds number effect on the flow about two- and three-dimensional bodies, more information is needed at Reynolds numbers in the supercritical and hypercritical domains, especially at Mach numbers above critical freestream conditions and for bodies with non-circular cross sections. Also of interest are investigations related to the influence of the Reynolds number on the interference between bodies and control surfaces which was not explicitly discussed here.

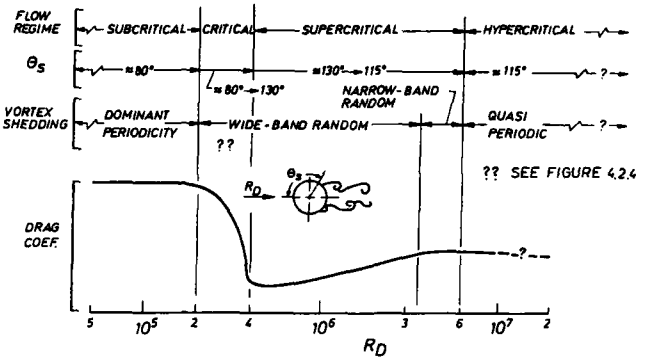

FIGURE 4.2.1: Identification of flow regimes on a circular cylinder [84/7]

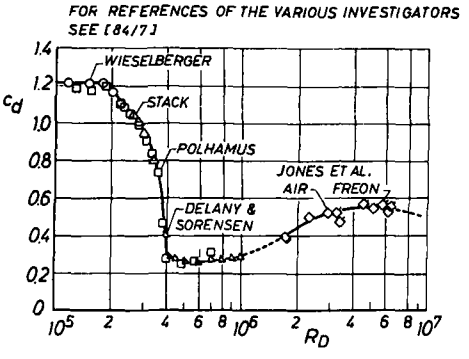

FIGURE 4.2.2: Drag coefficient for smooth circular cylinders (replotted from 84/7)

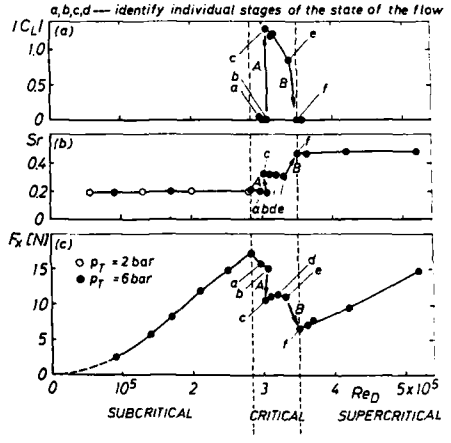

FIGURE 4.2.4: Characteristics of the flow about a circular cylinder: fine structure in the critical Reynolds number range [83/11]

a. Absolute value of the steady lift force coefficient
b. Strouhal number
c. Drag force

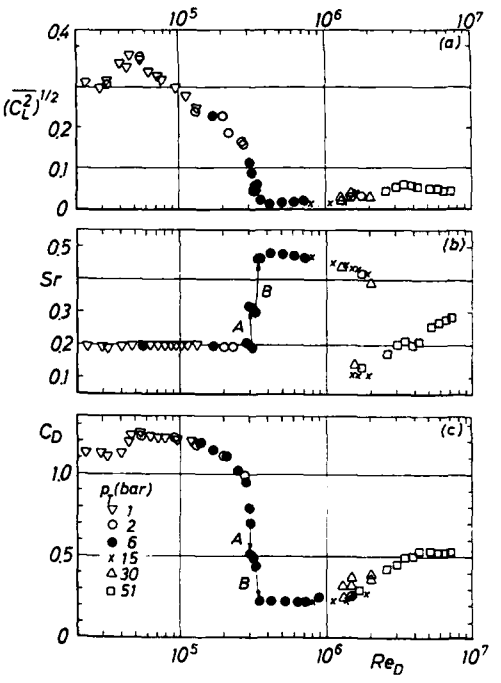

FIGURE 4.2.3: Characteristics of the flow about a circular cylinder [83/11]

a. Lift fluctuations (r.m.s.)
b. Strouhal number of the lift fluctuations
c. Drag coefficient

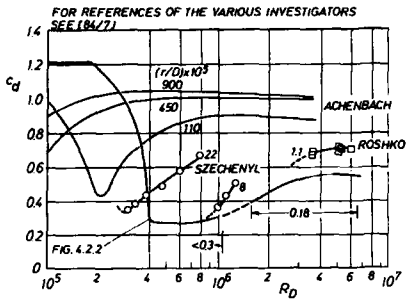

FIGURE 4.2.5: Effect of distributed roughness on the drag coefficient of circular cylinders (replotted from 84/7)

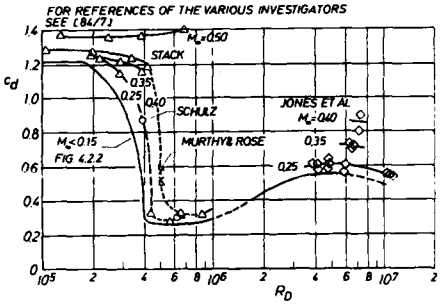

FIGURE 4.2.6: Effect of Mach number on drag coefficients of smooth circular cylinders (replotted from 84/7)

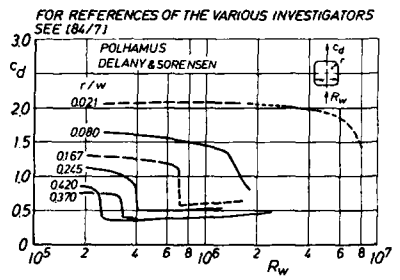

FIGURE 4.2.7: Influence of corner radius on drag coefficient of modified square cylinder (replotted from 84/7)

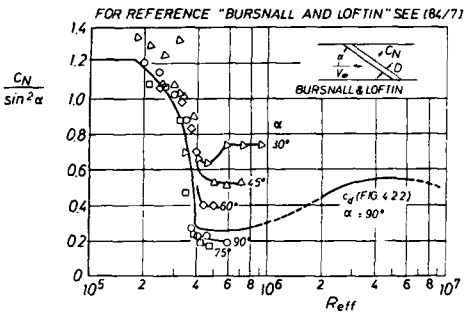

FIGURE 4.2.8: Effect of angle of attack (yaw) on normal force coefficient for a circular cylinder (replotted from 84/7)

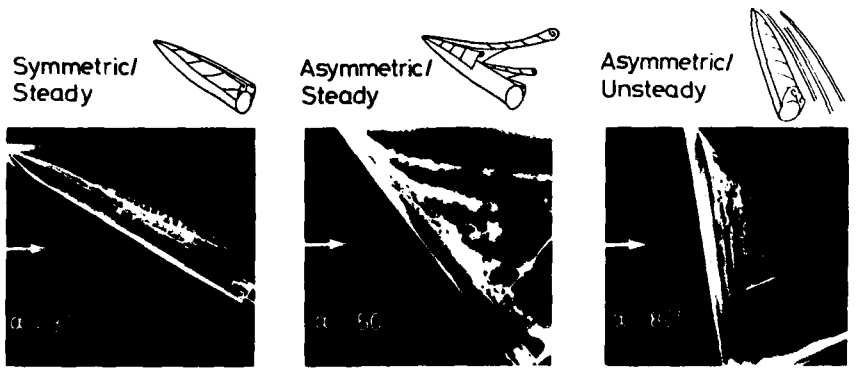

a. Typical conditions visualized by the hydrogen-bubble technique [87/4]

FIGURE 4.2.9: Flow domains of slender bodies

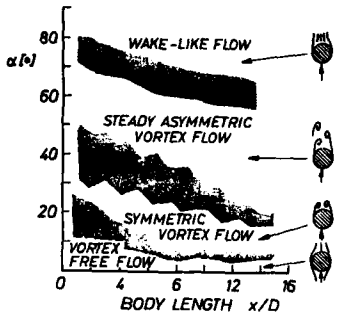

ⓑ Boundaries for an ogive-cylinder body [79/3]

FIGURE 4.2.9: Concluded

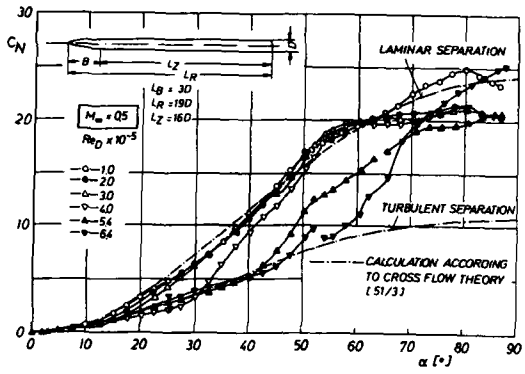

FIGURE 4.2.10: Normal force coefficient dependent on angle of attack and Reynolds number [78/5]

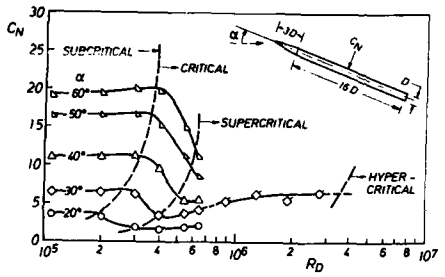

FIGURE 4.2.11: Effect of angle of attack on normal force coefficient for a slender body. M_∞ =0.50
Data of Hartmann [78/5] and Foley (α=30° only [71/10])

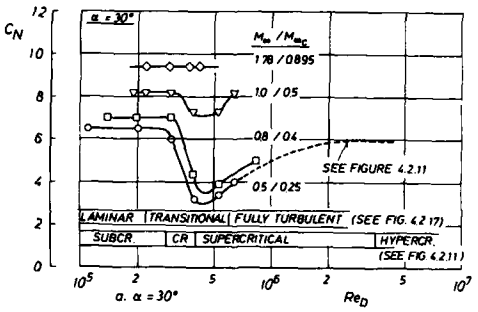

FIGURE 4.2.12: Effect of Mach number on normal force coefficient for an ogive-cylinder body [78/5]

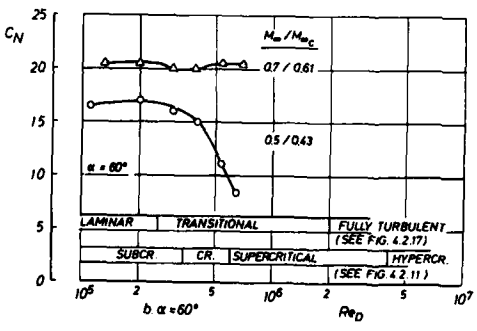

FIGURE 4.2.12: Concluded

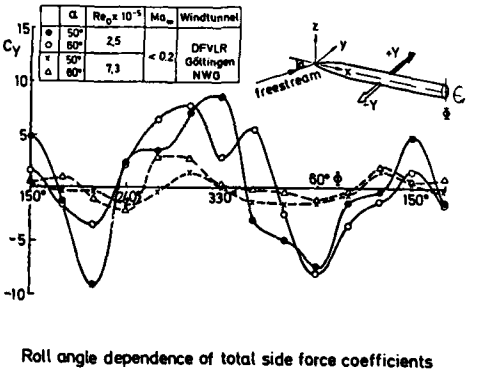

FIGURE 4.2.13: Roll angle dependence of total side force coefficients [87/4]

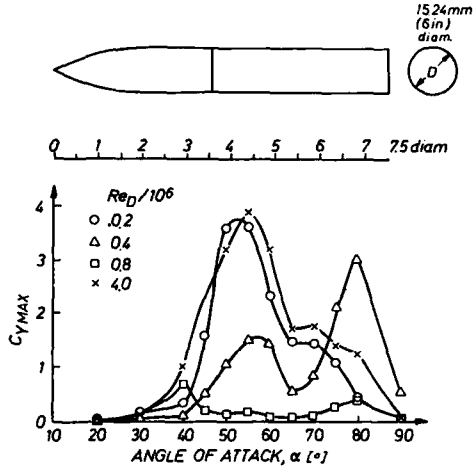

FIGURE 4.2.14: Variation of maximum overall side force with angle of attack [82/13]

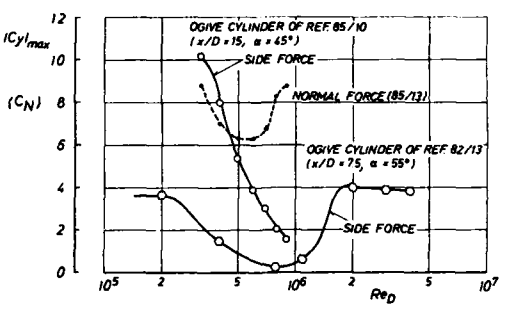

FIGURE 4.2.15: Variation of overall maximum side force with Reynolds number, $M_\infty \leq 0.24$

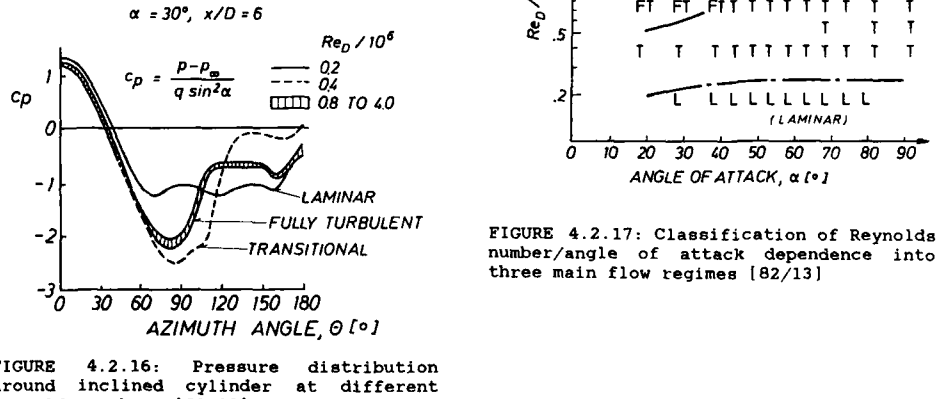

FIGURE 4.2.16: Pressure distribution around inclined cylinder at different Reynolds numbers [82/13]

FIGURE 4.2.17: Classification of Reynolds number/angle of attack dependence into three main flow regimes [82/13]

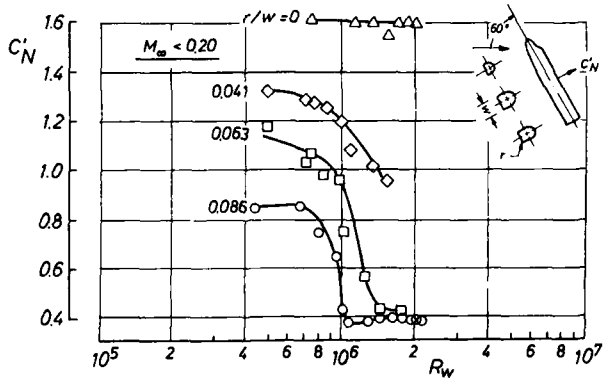

FIGURE 4.2.18: Effect of corner radius on normal force coefficient for a shuttle orbiter-type fuselage [84/7] [71/11]

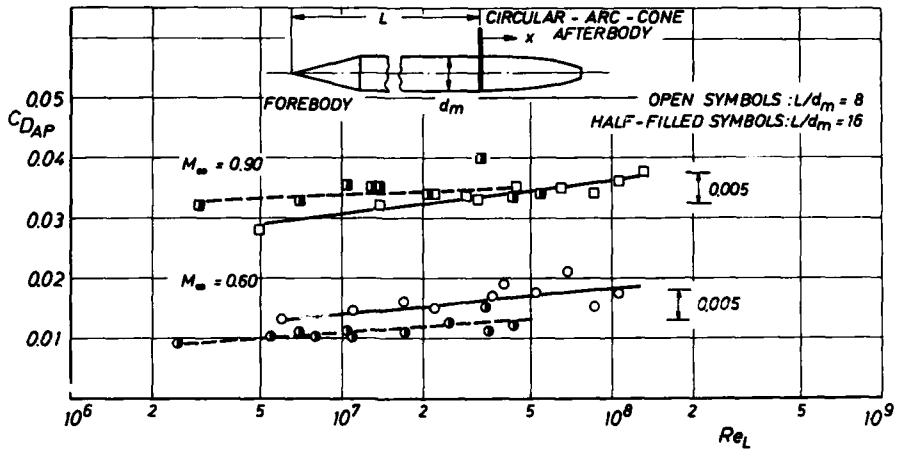

FIGURE 4.2.19: Reynolds number effect on afterbody pressure drag for two forebody lengths [76/6]

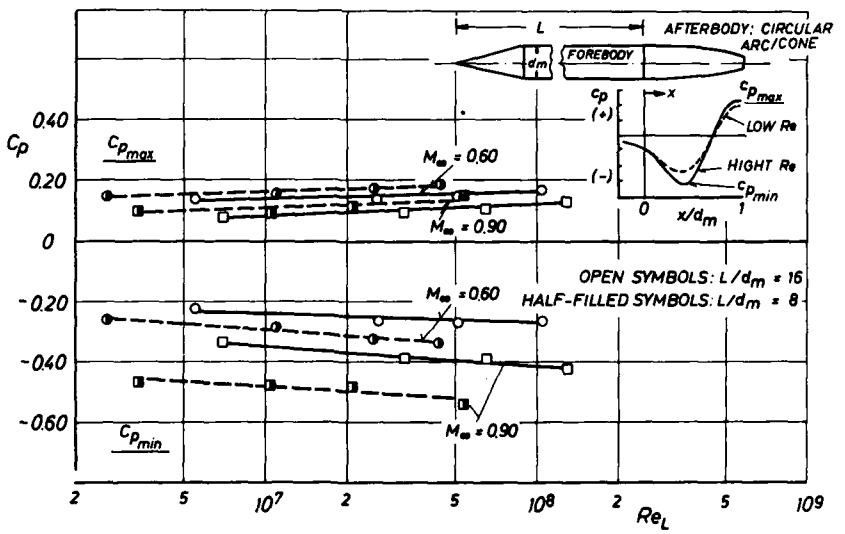

FIGURE 4.2.20: Reynolds number influence on minimum and maximum afterbody pressures [76/6]

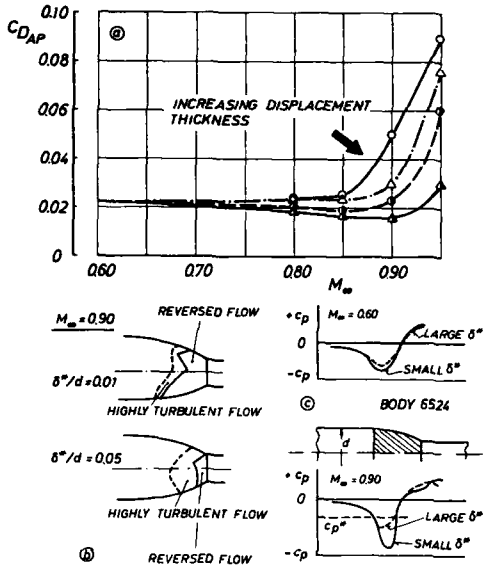

FIGURE 4.2.21: Influence of Mach number and displacement thickness on boattail drag [76/7]

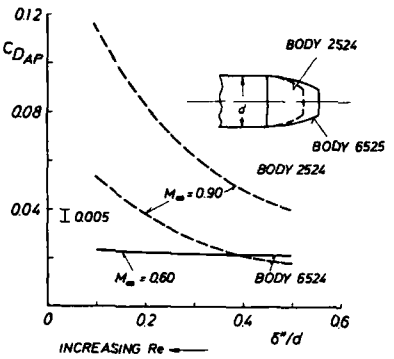

FIGURE 4.2.22: Effect of displacement thickness and body geometry on boattail drag [76/7]

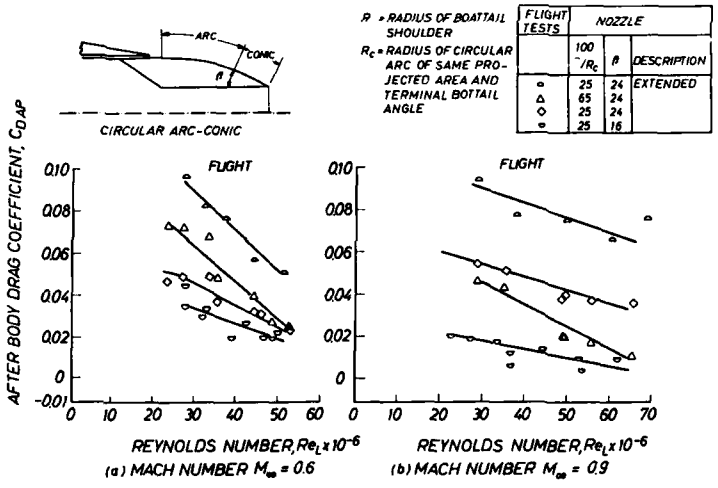

FIGURE 4.2.23: Reynolds number effect on pressure drag of circular arc boattails [75/7] (replotted from 81/9)

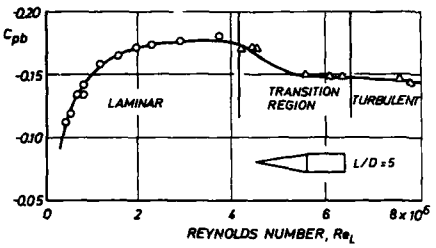

FIGURE 4.2.24: Reynolds number dependence of base pressure coefficient for cone-cylinder body [76/8]

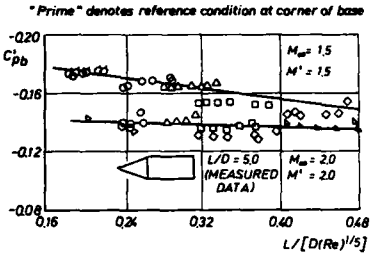

FIGURE 4.2.25: Chapman correlation of base pressure coefficient [58/1](replotted from 76/8)

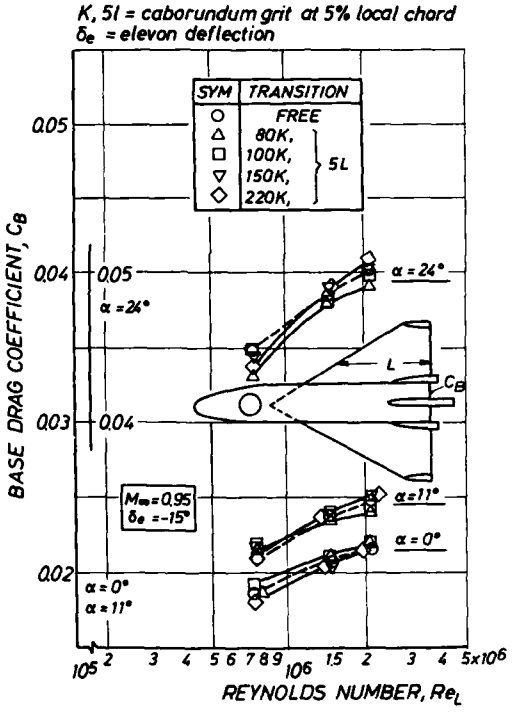

FIGURE 4.2.26: Dependence of base drag on Reynolds number for a space shuttle orbiter-type configuration [72/7]

5. CONCLUDING REMARKS

Reynolds number effects in transonic flow were critically reviewed. In this review, the following geometries were considered: Airfoils and high aspect ratio wings typical of transport aircraft configurations, fighter-type low aspect ratio delta wings, two- and three-dimensional bodies characteristic of missiles and combat aircraft fuselages, and afterbodies. Furthermore included in this review were pseudo-Reynolds number effects which may arise, for instance, due to the influence of the Reynolds number on the wind tunnel environment, and, as an introduction to the present topic, a brief review of the "history" of Reynolds number effects associated with transonic flow.

It was originally envisaged to also present a section on fundamental Reynolds number effects covering the influence of the Reynolds number on the boundary layer development, including transition, and on basic viscous / inviscid interactions such as shock boundary layer interaction and trailing edge separation; however, since this subject is comprehensively discussed in the report of the AGARD Working Group 09 "Boundary Layer Simulation and Control in Wind Tunnels", which will be published concurrent with the present AGARDograph, it was decided to omit that discussion here.

Systematic study of Reynolds number (scale) effects, which commenced some time after second world war when transonic flight itself became a matter of thorough scientific study and which obtained new impetus after Loving of NASA published his report on the large differences between C-141 wind tunnel and flight results in 1966, frequently reveal "anomalies" which can be traced to the wind tunnel environment and measuring techniques and their response to Reynolds number changes. Such "anomalies", sometimes labeled as "unit"-Reynolds number effects, are better described as "pseudo"-Reynolds number effects with the Reynolds number influencing the wind tunnel environment which, in turn, affects the flow about the model. Factors which have the potential of introducing pseudo-Reynolds number effects include wall interference, tunnel Mach number calibration, noise, turbulence, humidity, non-uniform flow (flow angle, temperature, pressure gradients), flow contamination, side wall effects in two-dimensional tests, model deformation and transition fixing. Here are examples of the manifestation of pseudo-Reynolds number effects: Changing Reynolds number was found to change the characteristics of partially open wind tunnel walls, hence the magnitude of wall interference for a given model, and therewith, for instance, the effective freestream conditions. Noise and turbulence may affect the transition location; noise and turbulence tend to increase due to an increase in wind tunnel power, the latter required to raise Reynolds number. Transition location may be influenced directly by an increase in Reynolds number and, superimposed, via the change in turbulence and noise level. In the same way - although the influence seems to be small - the effect of noise and turbulence intensity on the turbulent boundary layer development may induce a pseudo-Reynolds number effect. Humidity alters the pressure distribution including shock location; humidity effects change with total pressure, the latter utilized to alter Reynolds number. Wind tunnel contamination by particles small enough to be airborne and simultaneously hard enough to cause roughening of model surfaces in the stagnation region may contribute to pseudo-Reynolds number effects in a different way: Roughness in the stagnation region can cause premature transition thus obscuring the "true" influence of Reynolds number on transition point movement.

Tunnel calibration must be performed at all total pressure and temperature conditions that are expected during the actual model tests since the relation between the average test section Mach number and the reference Mach number may be Reynolds number dependent. Also considered in that regard should be flow non-uniformities, i.e., spatial gradients of pressure, temperature and angle of attack, for instance, and their Reynolds number dependence. Especially in two-dimensional flow, the influence of the Reynolds number on the side wall boundary layer development may cause spurious effects on the flow about the model which may falsely be interpreted as real Reynolds number effects; proper treatment of the side wall boundary layer or a sufficiently large aspect ratio (≥ 2.5) is required to avoid these influences. Undesireable thermal non-equilibrium, i.e., undesireable deviations of the model wall temperature from adiabatic wall conditions, may occur in short duration wind tunnels, for instance, due to the throttling process in the control valve, or in continuous (cryogenic) wind tunnels when Reynolds number is varied by temperature changes and time is not allotted for the model to acquire adiabatic wall temperature. Thermal non-equilibrium has a considerable influence on the boundary layer development and hence on aerodynamic parameters sensitive to viscous changes. Model deflections may easily introduce pseudo-Reynolds number effects if the deflections

are a result of changes in the model load associated with increasing total pressure; model deflections must be accounted for. Finally, transition fixing may be accompanied by pseudo-Reynolds number effects if the height of the roughness element, utilized to force transition , is not adjusted to the freestream conditions, including Reynolds number itself, and over- or underfixing occurs resulting in either too thick a boundary layer or transition taking place downstream of the tripping device.

Considering "true" Reynolds number effects on transport-type airfoils and wings, the available information suggests that two phenomena are of primary importance, especially when regarding the Reynolds number difference between wind tunnel and flight: transition point movement, itself and in conjunction with laminar versus turbulent shock boundary layer interaction, and flow separation, either locally near the trailing edge or of large scale between shock and trailing edge on the upper airfoil or wing surface. When transition is fixed artificially, Reynolds number effects are mainly related to flow separation; large variations in the pressure distribution and correspondingly in the force and moment coefficients were observed with Reynolds number when separation extended from the foot of the shock to the trailing edge, and especially, when the flow changed from an attached to a separated condition as Reynolds number is decreased (or vice versa). For conditions with attached or almost attached flow, Reynolds number effects appear to be smaller, though certainly not insignificant: A limited region of trailing edge separation, which frequently exists on rear loaded wing sections, tends to increase the Reynolds number effect and some aerodynamic characteristics, notably drag and pitching moment, are very sensitive to these small variations in the separated region with Reynolds number. Note, that the boundary between attached and separated flow as a function of Mach number and angle of attack varies itself with Reynolds number in a systematic way. If conditions are such that the separation location does no longer change with Reynolds number, its effect on the overall flow development is also small.

The second phenomenon to be considered in conjunction with observed Reynolds number effects is the transition point movement occurring due to a change in Reynolds number if transition is left free. Transition point movement has an effect on the flow development (e.g., separation) similar to a "pure" Reynolds number change. However, the effect of transition movement is much more pronounced since the change in the initial boundary layer parameters, which determine the overall flow development, is much greater than for the associated Reynolds number change with transition fixed. Concerning low Reynolds number wind tunnel tests and the scaling of results to full-scale conditions, uncontrolled transition point movements should be avoided, e.g., by adequately fixing transition (see the report of the AGARD WG 09), since misleading variations in the aerodynamic characteristics may occur if the transition point can move around freely.

Available data for low aspect ratio fighter-type configurations depicting Reynolds number effects are sparse. No systematic investigations, other than few for sharp-edge delta wings, have been conducted in a sufficiently wide Reynolds number range to allow firm conclusions to be made. The data which are available, however, suggest for most of the flight regime of interest that Reynolds number effects are small to nonexistent, the boundary layer state being controlled by leading edge contamination or cross flow instability.

The Reynolds number sensitivity of bodies, typical of missiles and fighter aircraft fuselages, is also strongly related to separation, and one can distinguish essentially four (classical) Reynolds number domains: Subcritical, in which the flow is laminar and laminar separation occurs without reattachment, critical, in which separation is transitional with turbulent reattachment and a subsequent far-aft turbulent separation, supercritical, in which separation is turbulent and the transition point moves upstream to the vicinity of the stagnation point with increasing Reynolds number, and hypercritical, in which the flow, including separation, is fully turbulent. The flow is not very sensitive to viscous changes in the subcritical (laminar) and the hypercritical (fully turbulent) Reynolds number domains since the separation location is essentially fixed. Especially in the critical Reynolds number range, large changes in the aerodynamic forces - large decreases in drag and normal force for the cylinder in cross flow and the three-dimensional body at angle of attack, respectively - occur due to the sensitivity of transitional separation to Reynolds number. Note, that for a three-dimensional body the boundary between the various Reynolds number regimes is angle of attack dependent.

The Reynolds number sensitivity in the critical and supercritical Reynolds number domains disappears with increasing Mach number due to the development of supersonic regions with terminating shock waves strong enough to separate even the turbulent boundary layer. The freestream velocity at which this happens is, for a three-di-

mensional body, again dependent on incidence. Distributed or single roughness in a form that fixes transition well upstream of separation also strongly reduces the Reynolds number sensitivity, as do bodies with corner radii that essentially fix separation.

At subsonic freestream Mach numbers and in the absence of major flow separation, significant but compensating pressure changes occur on afterbodies such that there is little effect on afterbody pressure drag as Reynolds number is varied. Significant increases in drag with increasing Reynolds number were consistently observed for subsonic Mach numbers above the transonic drag rise and at supersonic Mach numbers. However, also observed were flow developments, e.g., on boattails mounted behind underwing nacelles, where the boattail drag decreased with increasing Reynolds number. One reason for this behavior may be the positive effect of Reynolds number on separation, hence on pressure recovery, rather than on the value of the suction peak, as was the case for the configurations for which an increase in pressure drag with Reynolds number was observed.

The sensitivity of the flow development about transonic flight vehicles to Reynolds number changes illustrated in the present AGARDograph and the lack of sufficient high Reynolds number facilities, indicate the necessity to provide generally accepted means and ways to scale lower-than-flight Reynolds number results to full-scale conditions. This topic was not addressed to any extent since it was the task of the AGARD Working Group 09, "Boundary Layer Simulation and Control in Wind Tunnels", to provide a methodology for transonic wind tunnel testing and the extrapolation of low Reynolds number wind tunnel results to flight conditions. The results of the deliberations of that Working Group are published as an AGARD-report which contains, besides the said methodology, also a review of the present state-of-the-art in transonic wind tunnel testing, especially with regard to boundary layer simulation as well as a critical assessment of the physical background of viscous simulation. The present AGARDograph should be considered as complementary to the WG 09-report.

REFERENCES

43/1	A. Fage R. F. Sargent	"Effect on Aerofoil Drag of Boundary-Layer Suction Behind a Shock Wave." Aeronautical Research Council R & M 1913, October 1943.
45/1	B. Goethert W. A. Mair	"German High-Speed Wind Tunnel Results Collected by Rae." Tech. Note No. Aero 1684 ARC 9064, August 1945.
46/1	J. Ackeret F. Peldmann N. Rott	"Investigation of Compression Shocks and Boundary Layers in Fast Moving Gases." Institut fuer Aerodynamik E.T.M. Zuerich Report No. 10, 1946.
48/1	J. A. Beavan	"Measurements of Maximum Lift on 26 Aerofoil Sections at High Mach Number." Aeronautical Research Council R & M 2678, January 1948.
48/2	V. Outman A. A. Lambert	"Transonic Separation." *Journal of the Aeronautical Sciences*, Vol. 15, 1948, p. 671.
51/1	H. E. Gamble	"Some Effects of Reynolds Number on a Cambered Wing at High Subsonic Mach Number." RAE Report No. Aero 2423 ARC 14, 448, May 1951.
51/2	G. E. Cooper R. S. Bray	"Schlieren Investigation of the Wing Shock Wave Boundary-Layer Interaction in Flight." NACA RMA 51909 (NACA/TIB/2760) ARC 14, 485 - F.M. 1642, 1951.
51/3	H. J. Allen E. W. Perkins	"A Study of Effects of Viscosity on Flow over Slender Inclined Bodies of Revolution." NACA Rep. 1048, 1951.
52/1	G. E. Gadd	"Interaction between Wholly Laminar or Wholly Turbulent Boundary Layers and Shock Waves Strong Enough to Cause Separation." *Journal of the Aeronautical Sciences*, Vol. 20, No. 11, Nov. 1952, pp. 729-739.
52/2	B. E. Tinling A. E. Lopez	"The Effects of Reynolds Number at Mach Numbers up to 0.94 on the Loading on a 35-Deg, Swept-Back Wing Having NACA 65 1A012 Streamwise Sections." NACA RM A52 B20, June 1952.
53/1	D. Kuchemann	"Types of Flows on Swept Wings." *Journal of the Royal Aeronautical Society*, Vol. 57, November 1953, pp. 683-699.
54/1	H. H. Pearcey D. W. Holder	"Examples of the Effect of Shock-Induced Boundary-Layer Separation in Transonic Flight." Aeronautical Research Council Technical Report, R & M No. 3510, 1954 (re-issued 1967).
54/2	A. B. Haines D. W. Holder H. H. Pearcey	"Scale Effects at High Subsonic and Transonic Speeds, and Methods for Fixing Boundary-Layer Transition in Model Experiments." Aeronautical Research Council Technical Report R & M No. 3012, September 1954.
55/1	D. W. Holder H. H. Pearcey G. E. Gadd	"The Interaction between Shock Waves and Boundary Layers." Aeronautical Research Council Technical Report C.P. No. 180, 1955.
55/2	H. H. Pearcey	"Some Effects of Shock-Induced Separation of Turbulent Boundary Layers in Transonic Flow past Airfoils." Aeronautical Research Council Technical Report, R & M No. 3108, June 1955 (re-issued 1959).
58/1	D. R. Chapman D. M. Kuetin H. K. Larson	"Investigation of Separated Flows in Supersonic and Subsonic Streams with Emphasis on the Effect of Transition." NACA Report R-1356, 1958.
60/1	E. W. E. Rogers I. M. Hall	"An Introduction to the Flow about Plane, Swept-Back Wings at Transonic Speeds." *Journal of the Royal Aeronautical Society*, Vol. 64, p. 449 (1960).
60/2	J. Seddon	"The Flow Produced by Interaction of a Turbulent Boundary Layer with a Normal Shock Wave of Strength Sufficient to Cause Separation." Aeronautical Research Council R & M 3502, 1960.
61/1	H. H. Pearcey	"Shock-Induced Separation and Its Prevention by Design and Boundary-Layer Control." From: *Boundary Layer and Flow Control*, Vol. 2, G. V. Lachmann, ed., Pergamon Press, 1961.

62/1	H. H. Pearcey	"The Aerodynamic Design of Section Shapes for Swept Wings." *Advances in Aeronautical Sciences*, Vol. 3, London, 1962.
62/2	R. C. Lock	"An Equivalence Law Relating Three- and Two-Dimensional Pressure Distributions." NPL Aero Report 1028, 1962.
63/1	A. A. Pouring	"An Experimental and Analytical Investigation of Homogeneous Condensation of Water Vapor in Air during Rapid Expansion." Ph. D. Dissertation, Yale University, 1963.
63/2	J. B. Peterson, Jr.	"A Comparison of Experimental and Theoretical Results for the Compressible Turbulent Boundary-Layer Skin Friction with Zero Pressure Gradient." NASA TN D-1795, 1963.
64/1	A. Stanbrook L. C. Squire	"Possible Types of Flow at Swept Leading Edges." *Aeronautical Quarterly*, Vol. XV, 1964, pp. 72-82.
66/1	D. L. Loving	"Wind Tunnel Flight Correlation of Shock-Induced Separated Flow." NASA TN D-3580, 1966.
66/2	F. Thomas	"The Determination of Buffet Boundaries for Wings in the Transonic Speed Regime." Wissenschaftliche Gesellschaft fur Luft- und Raumfahrt, 1966, pp. 126-144.
67/1	B. H. Little	"*Effects of Initial Turbulent Boundary Layer on Shock-Induced Separation in Transonic Flow.*" VKI Technical Note No. 39 (1967).
68/1	J. A. Blackwell	"Effect of Reynolds Number and Boundary Layer Transition Location on Shock-Induced Separation." AGARD CP 35, September 1968, Paper 20.
68/2	H. H. Pearcey J. Osborne A. B. Haines	"The Interaction between Local Effects at the Shock and Rear Separation -- A Source of Significant Scale Effects in Wind Tunnel Tests on Aerofoils and Wings." AGARD CP 35, September 1968, Paper 11.
68/3	M. C. P. Firman T. A. Cook	"Detailed Exploration of the Compressible Viscous Flow over Two-Dimensional Airfoils at High Reynolds Numbers." ICAS Paper No. 09/68, Munich, September 1968.
68/4	H. Schlichting	"*Boundary-Layer Theory*." McGraw Hill, New York, 1968 (Sixth Edition).
69/1	M. Pindzola C. F. Lo	"Boundary Interference at Subsonic Speeds in Wind Tunnels with Ventilated Walls." AEDC-TR-69-47 (AD-687440), May 1969.
69/2	S. R. Pate C. J. Schueler	"Effects of Radiated Aerodynamic Noise on Model Boundary-Layer Transition in Supersonic and Hypersonic Wind Tunnels." AEDC-TR-67-236 (AD-666644), March 1969. (Also AIAA Journal, Vol. 7, March 1969, pp. 450-457.)
70/1	J. E. Green	"Interaction between Shock Waves and Turbulent Boundary Layers." *Progress in Aerospace Sciences*, Vol. II, Pergamon Press, 1970 (Ed. D. Kuechmann).
70/2	E. G. Hollingsworth M. Cohen	"Comparison of Wind Tunnel and Flight Test Techniques for Determining Transonic Buffet Characteristics on the McDonnell Douglas F-4 Airplane." AIAA Paper 70-584, May 18-20, 1970.
71/1	E. Stanewsky B. H. Little	"Studies of Separation and Reattachment in Transonic Flow." *Journal of Aircraft*, Vol. 8, No. 12, December 1971, pp. 952-958.
71/2	J. E. Green	"Some Aspects of Viscous-Inviscid Interactions at Transonic Speeds and Their Dependence on Reynolds Number." AGARD CP 83, April 1971, Paper 2.
71/3	A. B. Haines	Possibilities for Scale Effects on Swept Wings at High Subsonic Speeds: Recent Evidence from Pressure Plotting Tests. AGARD CP 83, April 1971, Paper 14. (Also ARA Report 18, 1971.)
71/4	J. F. Cahill	"Simulation of Full-Scale Flight Aerodynamic Characteristics by Tests in Existing Transonic Wind Tunnels." AGARD CP 83, April 1971, Paper 20.
71/5	M. G. Hall	"Scale Effects in Flows over Swept Wings." AGARD CP 83-71, 1971.

71/6	J. E. Green	"Some Aspects of Viscous-Inviscid Interactions at Transonic Speeds and Their Dependence on Reynolds Number." AGARD CP 83-71, 1971.
71/7	E. Thomas G. Redeker	"A Method for Calculating the Transonic Buffet Boundary Including the Influence of Reynolds Number." AGARD CP 83-71, 1971.
71/8	J. Osborne H. H. Pearcey	"A Type of Stall with Leading-Edge Transonic Flow and Rear Separation." AGARD CP 83-71, 1971.
71/9	E. J. Salzman D. R. Bellman	"A Comparison of Some Aerodynamic Drag Factors as Determined in Full-Scale Flight with Wind Tunnel and Theoretical Results." AGARD CP 83-71, 1971.
71/10	J. E. Foley	"Results of a Study of Mach Number and Reynolds Number on the Cross Flow Drag Characteristics of Ogive-Cylinder and Ogive-Cylinder-Frustrum-Cylinders at Angles of Attack to 30 Degrees." NASA CR-61356, October 1971.
71/11	J. J. Brownson R. E. Graham D. Banducci	"Static Stability Characteristics of Manned Spacecraft Center Straight-Wing Space Shuttle Orbiter: Effect of Reynolds Number and Body Corner Radius at M < 0.5." NASA TM X-62, 054, 1971.
72/1	LaWs Group	"The Need for Large Wind Tunnels in Europe." AGARD AR No. 60, 1972.
72/2	M. G. Hall D. A. Treadgold	"Difficulties in Predicting Boundary-Layer Transition on Swept Wings." RAE Technical Memorandum Aero 1465, ARC 35160, 1972.
72/3	Ms. G. C. Browne T. E. B. Bateman M. Pavitt A. B. Haines	"A Comparison of Wing Pressure Distributions Measured in Flight and on a Wind Tunnel Model of the Super VC-10." Aeronautical Research Council R & M 3707, 1972.
72/4		"The High Reynolds Number Tunnel -- A National Need -- Description and Justification." AEDC, February 1972.
72/5	J. P. Hartzuiker	"Scale Effects at Transonic Speeds; Basic Considerations." Notes for AGARD/VKI Short Course, "Transonic Aerodynamic Testing," 1972.
72/6	J. W. Green D. J. Weeks P. G. Pugh	"Heat Transfer as a Source of Spurious Scale Effects in Subsonic and Transonic Wind Tunnels." AGARD Laws Paper No. 135, 1972.
72/7	E. Stanewsky	"Effect of Reynolds Number and Transition on the Aerodynamic Coefficients of the MSC 040 A Orbiter at Transonic Speeds." DFVLR/AVA-Report 062. 72 A 18, 1972.
73/1	J. H. Paterson D. G. McWilkenson W. T. Blackerby	"A Survey of Drag Prediction Techniques Applicable to Subsonic and Transonic Aircraft Design." AGARD CP-124, April 1973.
73/2	J. E. Green	"On the Influence of Free-Stream Turbulence on a Turbulent Boundary Layer as it Relates to Wind Tunnel Testing at Subsonic Speeds." AGARD-AR-602, April 1973.
74/1	LaWs Group	"The Need for a Large Transonic Tunnel in Europe." AGARD AR No. 70, 1974.
74/2	F. Aulehla G. Besigk	"Fore- and Afterbody Flow-Field Interaction with Considerations of Reynolds Number Effects." AGARD CP 150, Paper 12, September 1974.
74/3	S.O.T.H. Han J. P. Hartzuiker	"On the Effect of Variation of Transition Position and of Vortex Generators on the High-Speed Stall Characteristics of a Swept-Wing Transport Aircraft Model." NLR TR 74008 U, 1974.
74/4	R. Chamberlin	"Flight Reynolds Number Effects on a Contoured Boattail Nozzle at Subsonic Speeds." NASA TM-X-3053.
75/1	L. L. Galigher F. M. Jackson C. E. Robinson	"Description of the AGARD Nozzle Afterbody Experiments Conducted by the Arnold Engineering Development Center." AGARD-AG-208, October 1975.
75/2	W. T. Blackerby J. F. Cahill	"High Reynolds Number Tests of a C141A Aircraft Semi-Span Model to Investigate Shock-Induced Separation." NASA CR 2604 (1975).

75/3	K. P. Burdges J. A. Blackwell, Jr. G. A. Pounds	"High Reynolds Number Test of a NACA 65_1-213, a = 0.5 Airfoil at Transonic Speeds." NASA CR-2499 (1975).
75/4	H. Yoshihara D. Zonars	"The Many Facets of 3D Transonic Shock-Induced Separation." AGARD CP 168 Paper 42 (1975).
75/5	S. Teige G. Strang K. E. Stake	"Swedish Experience on Correlations of Flight Results with Ground Test Predictions." Paper 21, AGARD-CP-187, June 1975.
75/6	H. Esch	"The Influence of Reynolds Number on the Normal Force Characteristics of Slender Cylindrical Bodies." ESA TT-170, 1975.
75/7	F. A. Wilcox R. Chamberlin	"Reynolds Number Effects on Boattail Drag of Exhaust Nozzles from Wind Tunnel and Flight Tests." AGARD-CP-150, Paper 21, 1975.
76/1	D. J. Weeks	"An Investigation of Scale Effects on the Transonic Flow over Swept Wings." Part I, Aeronautical Research Council R & M 3842, 1976; Part 2, Aeronautical Research Council R & M 3842, 1977.
76/2	A. B. Haines	"Further Evidence and Thoughts on Scale Effects at High Subsonic Speeds." AGARD CP NO. 174, March 1976, Paper 43.
76/3		"Workshop on High Reynolds Number Research." NASA CP-2009 (1976).
76/4	J. A. Blackwell, Jr.	"Scale Effects on Advanced Aircraft Wing Designs." *Proceedings of the Lockheed-Georgia Company Viscous Flow Symposium*, "Reviews in Viscous Flow." LG77 ER 0044, June 1976.
76/5	J. L. Jacocks	"An Investigation of the Aerodynamic Characteristics of Ventilated Test Section Walls for Transonic Wind Tunnels." Ph.D. Dissertation, University of Tennessee, December 1976.
76/6	D. E. Reubush L. E. Putnam	"An Experimental and Analytical Investigation of the Effect on Isolated Boattail Drag of Varying Reynolds Number up to 130 x 106." NASA TN D-8210, May 1976.
76/7	B. J. Blaha R. Chamberlin L. J. Bober	"Boundary Layer Thickness Effect on Boattail Drag." NASA TM-X-73443, 1976.
76/8	S. N. B. Murthy J. R. Osborn	"Base Flow Phenomena with and without Injection: Experimental Results, Theories and Bibliography." *Progress in Astronautics and Aeronautics*, Vol. 40, Aerodynamics of Base Combustion, 1976.
77/1	J. Szodruch	"Leeseiten-Stromung bei Schlanken Delta flugeln endlichier Dicke ILR Breicht 23." Technical Universtat Berlin, 1977.
77/2	G. F. Butler D. C. Conner	"Preliminary Investigation of a Technique for Prediction Loads in Flight from Wind Tunnel Measurements on Models of Conventional." Construction AGARD CP 204, February 1977.
77/3	J. F. W. Crane	"The Effect of Base Cavities on the Drag of an Axisymmetric Afterbody with a Sonic Nozzle between M_∞ = 0.8 and 1.3." RAE TR 77 144, 1977.
78/1	J. A. Blackwell, Jr.	"Scale Effects on Supercritical Airfoils." *Proceedings of the XI Congress of ICAS*, Lisbon, Portugal, 10-16 September 1978, Vol, 1, Paper No. B3, pp. 370-383.
78/2	J. A. van Egmond D. Rozendal	"The Design and Aerodynamic Characteristics of an 18% Thick Shock-Free Airfoil (NLR 7501)." NLR MP 78016 U, 1978.
78/3	J. W. Kooi	"Influence of Free-Stream Mach Number on Transonic Shock-Wave Boundary-Layer Interaction." NLR MP 78013 U, 1978.
78/4	F. M. Jackson	"Calibration of the AEDC-PWT 16-FT Transonic Tunnel with the Propulsion Test Section at Various Reynolds Numbers." AEDC-TR-77-121 (AD-A057877), August 1978.

78/5	K. Hartmann	"Uber den Einfluss der Reynolds Zahl auf die Nonmalkrafte Schlanker Flugkörpernimpfe." Z. Fluqwiss, Weltraum-forscg. 2, 1978, Heft 1, p. 23.
79/1	J. F. Cahill D. C. Conner	"Correlation of Data Related to Shock Induced Trailing Edge Separation and Extrapolation to Flight Reynolds Number." NASA CR 3178, 1979.
79/2	A. B. Haines	"Review of Post-1974 Evidence on Scale Effects at High Subsonic Speeds." ARA Memo No. 218, 1979.
79/3	G. T. Chapman E. R. Keener	"The Aerodynamics of Bodies of Revolution of Angles of Attack to 90 deg." AIAA Paper 79-23, 1979.
80/1	L. W. McKinney D. D. Baals	"High Reynolds Number Research - 1980." NASA Conference Publication 2183.
80/2	O. M. Pozniak	"A Review of the Effect of Reynolds Number on Afterbody Drag." ARA Report 56, May 1980.
80/3	Y. Brocard F. Manie	"Etude des caracteristiques de l'ecoulement tourbillonnaire sur une aile en fleche." L'Aeronautique et L'Astronautique No. 82, 1980-3.
80/4	N. S. Dougherty D. F. Fisher	"Boundary-Layer Transition on a 10-deg Cone: Wind Tunnel/Flight Data Correlation." AIAA Paper No. 80-0154, AIAA 18th Aerospace Sciences Meeting, January 14-16, 1980.
80/5	J.P.F. Lindhout B. van den Berg A. Elsenaar	"Comparison of Boundary-Layer Calculations of the Root Section of a Wing." The September 1975 Amsterdam Test Case - NLR MP 80028 U.
80/6	D. J. Peake M. Tobak	"Three-Dimensional Interactions and Vortical Flows with Emphasis on High Speeds." NASA TM 81169 (1980).
80/7		"Computation of Viscous-Inviscid Interactions." AGARD CP-291, 1980.
80/8	T. L. Kennedy	"An Evaluation of Wind Tunnel Test Techniques for Aircraft Nozzle Afterbody Testing at Transonic Mach Numbers." AEDC-TR-80-8 (AD-A091775), November 1980.
80/9	G. E. Erickson	"Flow Studies of Slender Wing Vortices." AIAA Paper No. 80-1423, AIAA 13th Fluid and Plasma Dynamics Conference, July 14-16, 1980.
81/1	E. Stanewsky	"Wechselwirkung Zwischen Aussenstromung und Grenzschicht an Transsonischen Profilen." Dissertation, Techniche Universität Berlin, May 1981.
81/2	L. C. Squire	"Experimental Work on the Aerodynamics of Integrated Slender Wings for Supersonic Flight." Progress in Aerospace Science, Vol. 20, pp. 1-96. Pergamon Press Lt. 1981.
81/3	T. S. Beddoes	"A Note on Shock Reversal at High Lift." Westland Helicopter Limited, Research Paper 633, 1981.
81/4	R. C. Lock M. C. P. Firmin	"Survey of Techniques for Estimating Viscous Effects in External Aerodynamics." RAE Tech Memo Aero 1900, 1981.
81/5	S. J. Kline (Editor)	"The 1980-1981 AFOSR-HTTM-Stanford Conference on Complex Turbulent Flows." Stanford University, 1981.
81/6	D. G. Mabey	"Some Remarks on Buffeting in Unsteady Airloads and Aeroelastic Problems in Separated and Transonic Flow." VKI Lecture Series 1981-4.
81/7	R. P. Boyden	"Preliminary Results of Buffet Tests in a Cryogenic Tunnel." NASA TM 81923, July 1981.
81/8	L. E. Ericsson J. P. Reding	"Review of Vortex-Induced Asymmetric Loads - Part I." Z. Fluqwiss, Weltraumforsch. 5, 1981, Heft 3, p. 162.
81/9	O. M. Pozniak	"A Review of the Effect of Reynolds Number on Afterbody Drag." AGARD-CP-301, Aerodynamics of Power Plant Installation, September 1981, pp. 16-1 to 16-21.
82/1	E. J. Ray	"A Review of Reynolds Number Studies Conducted in the Langley 0.3-m Transonic Cryogenic Tunnel." AIAA-82-0941.

82/2	A. B. Haines	"Notes on Transition Fixing and the Interpretation of Drag Data with Different Transition Fixes." ARA Memo 243, November 1982.
82/3	David Nixon (Editor)	"Transonic Aerodynamic Progress in Astronautics and Aeronautics." Vol. 81, 1982.
82/4	A. Elsenaar E. Stanewsky	"A Report of a GARTEur Action Group "Two-Dimensional Transonic Testing Methods." AGARD CP No. 335, Paper 5, 1982.
82/5	J. C. le Balleur	"Viscid-Inviscid Coupling Calculations for Two- and Three-Dimensional Flows." VKF Lecture Series 1982-4, 1982.
82-6	Y. Y. Chan	"*Wall Boundary-Layer Effects in Transonic Wind Tunnels.*" AGARD CP-335, September 1982.
82/7	N. S. Dougherty, Jr. D. P. Fisher	"Boundary-Layer Transition on a Slender Cone in Wind Tunnels and Flight for Indications of Flow Quality." AEDC-TR-81-26 (AD-A111328), February 1982.
82/8	S. Raghunathan R. J. W. McAdams	"Free-Stream Turbulence and Attached Subsonic Turbulent Boundary Layer." AIAA Paper 82-0029, January 1982.
82/9	F. Aulehla A. Eberle	"Reynolds Number Effect on Transonic Shock Location, *In* Wall Interference in Wind Tunnels." AGARD CP-335, September 1982.
82/10	R. W. Barnwell W. G. Sewall	"Similarity Rules for Effects of Sidewell Boundary Layer in Two-Dimensional Wind Tunnels." in "Wall Interference in Wind Tunnels," AGARD CP-335, September 1982.
82/11	D. Jacob D. Welte H. Wunnenberg	"A Comparison between Wind Tunnel and Flight Results for Aerodynamic Performance." AGARD CP-339, October 1982.
82/12	C. J. Spurlin H. Lueck	"Comparison of Flight and Wind Tunnel Data on the Dornier TST Configuration." AIAA Paper No. 84-0612-CP, March 1984.
82/13	P. J. Lamont	"Pressures Around an Inclined Ogive Cylinder with Laminar, Transitional, or Turbulent Separation." AIAA Journal, Vol. 20, No. 11, November 1982, p. 1492.
83/1	M. M. S. Khan J. F. Cahill	"New Considerations on Scale Extrapolation of Wing Pressure Distributions Affected by Transonic Shock Induced Separation. NASA Contractor Report 166426, March 1983.
83/2	A. E. P. Veldman	"A Numerical View on Strong Viscous-Inviscid Interaction." NLR MP 83049 U, 1983.
83/3	A. Elsenaar	"Experience with Transition Fixation in the High-Speed Regime at NLR." NLR Memorandum AC-83-039 U, 1983.
83/4	S. J. Boersen A. Elsenaar	"Half-Model Testing in the NLR High-Sped Wind Tunnel HST: Its Technique and Application." AGARD CPP 348, August 1983.
83/5	S. Raghunathan R. J. W. McAdams	"Free-Stream Turbulence and Transonic Flow overa 'Bump' Model" *AIAA Journal*, Vol. 21, No. 3, March 1983, pp. 467-469.
83/6	S. Raghunathan R. J. W. McAdams	"Boundary-Layer and Turbulence Intensity Measurements in a Shock Wave/Boundary-Layer Interaction." *AIAA Journal*, Vol. 21, No. 9, September 1983, pp. 1349-1350.
83/7	E. Stanewsky	"Interaction between the Outer Inviscid Flow and the Boundary-Layer on Transonic Air Foils." Z. Flugwiss., Weltraumforsch 7 (1983), Heft 4, pp. 242-252.
83/8	M. Mokry Y. Y. Chan D. J. Jones	"Two-Dimensional Wind Tunnel Wall Interference." AGARD AG-281, November 1983.
83/9	A. D. Young (Editor)	"Aerodynamics of Vortical Type Flows in Three Dimensions." AGARD CP 342, July 1983.
83/10	GARTEur ACTION GROUP AD(AG-02)	"Two-Dimensional Transonic Testing Methods." GARTEur/TP-011, also NLR TR 83086U, 1983.
83/11	G. Schewe	"On the Force Fluctuations Acting on a Circular Cylinder in Crossflow from Subcritical up to Transcritical Reynolds Numbers." *Journal of Fluid Mechanics*, Vol. 133, p. 265, 1983.

83/12	W. Schneider	"Experimental Investigation of Bodies with Non-Circular Cross Section in Compressible Flow." AGARD-CP-336, February 1983, pp. 1-19 to 19-19.
83/13	D. I. A. Poll	"On the Generation and Subsequent Development of Spiral Vortex Flow Over a Swept-back Wing." AGARD-CP-342, July 1983, pp. 6-1 to 6-14.
84/1	R. C. Luh M. D. Mack	"A Numerical Procedure to Predict the Effects of Reynolds Number and Trip Strip Variation on Three-Dimensional Wing Lift and Pitching Moment." AIAA-84-0255, 1984.
84/2		"Grenzschtsteuerung durch transitionfixierung." DFVLR-Mitt 84-17.
84/3	S. J. Boersen A. Elsenaar	"Half-Model Testing in the NLR High-Speed Wind Tunnel HST: Its Technique and Application." AGARD CP 348, Paper 23, 1984.
84/4	G. Meauze	"Viscous-Inviscid Flow Interaction Methods/Shock Boundary-Layer Interaction." ONERA TP 1984-114, 1984.
84/5	D. A. Johnson L. S. King	"A New Turbulence Closure Model for Boundary-Layer Flows with Strong Adverse Pressure Gradients and Separation." AIAA-84-9175, 1984.
84/6	W. Burgsmueller	"Transitionfixierung im Hochgeschwindigkeits-bereich bei der Fleugelentwicklung für zivile Flugzeuge, im Grenzschichtsteuerung durch Transitionsfixierung." DFVLR Mitteilung 84-17, October 1984.
84/7	E. C. Polhamus	"A Review of Some Reynolds Number Effects Related to Bodies at High Angles of Attack." NASA Contract Report 3809, 1984.
85/1	J. B. Doc	"The T2 Cryogenic Induction Tunnel in Toulouse." AGARD/FDP Special Course "Cryogenic Technology for Wind Tunnel Testing," V.K.I., 22-26 April 1985.
85/2	A. G. T. Cross	Report of the Review Committee of AGARD Working Group 09, Section 2.2.4, "Complex Configurations" (1985) to be published as part of the final working group report.
85/3	P. R. Ashill P. D. Smith	"An Integral Methods for Calculating the Effects on Turbulent Boundary Layer Development of Sweep and Taper." Aeronautical Journal 882, February 1985.
85/4	J. L. Fulker P. R. Ashill	"A Model of the Flow over Swept Wings with Shock-Induced Separation." Paper presented at the IUTAM Symposium, "Turbulent Shear-Layer/Shock-Wave Interactions," September 1985, Palaiseau, France.
85/5	G. R. Inger	"Supersonic Viscous-Inviscid Interaction of a Swept Compression Ramp with a Turbulent Boundary Layer." IUTAM Symposium.
85/6	A. B. Haines	Private Communication.
85/7	A. Mignosi	"Fundamental Reflections on Cryogenic Testing." AGARD/FDP Special Source - Cryogenic Technology for Wind Tunnel Testing, V.K.I., 22-26 April 1985.
85/8	C. E. Robinson R. C. Bauer R. H. Nichols	"Estimating Water Vapor Condensation Effects for Transonic and Supersonic Flow Fields." AIAA Paper 85-5020, October 14-16, 1985.
85/9	S. Raghunathan R. J. W. McAdams	"Relative Effects of Reynolds Number and Free-Stream Turbulence in Transonic Flow." *AIAA Journal*, Vol. 23, No. 4, April 1985.
85/10	R. Clock	"Prediction of Viscous and Wave Drag at High Subsonic Speeds by Viscous-Inviscid Interaction Techniques." AGARD VKI Special Course, "Aircraft Drag Prediction and Reduction," May 1985.
85/11	R. E. Melnik R. R. Chow H. R. Mead A. Jameson	"An Improved Inviscid/Inviscid Interaction Procedure for Transonic Flows over Airfoils." NASA CR-3805, 1985.
85/12	J. Velery J. G. Marvin	"Turbulent Shock Wave Boundary Layer Interaction." AGARD-ograph No. 280, 1985.

85/13	V. Kanagarajan K. Hartmann	"Force Measurements on a Body-Tail-Combination at Different Reynolds Numbers and Roll Angles up to Incidences of 45 Degrees." DFVLR-Report IB 222-85 A 38, 1985.
85/14	E. E. Covert (Editor)	"Thrust and Drag: Its Prediction and Verification." *AIAA Progress in Astronautics and Aeronautics*, Vol. 98, 1985.
86/1	B. Ewald G. Krenz	"The Accuracy Problem of Airplane Development Force Testing in Cryogenic Wind Tunnels." AIAA Paper 86-0776, AIAA Paper 86-0776, AIAA 14th Aerodynamic Testing Conference, March 1986.
86/2	S. V. Merthy F. W. Steinle, Jr.	"Effects of Compressibility and Free-Stream Turbulence on Boundary-Layer Transition in High Subsonic and Transonic Flows." AIAA Paper 86-0764, AIAA 14th Aerodynamic Testing Conference, March 1986.
86/3	Th. J. Horvath G. S. Jones P. C. Stainback	"Coherent Shedding from a Circular Cylinder at Critical, Supercritical, and Transcritical Reynolds Numbers." SAE Technical Paper Series, Paper 861768, 1986.
86/4	P. Champigny	"Stability of Side Forces on Bodies at High Angles of Attack." AIAA 4th Applied Aerodynamics Conference, Paper AIAA 86-1776-CP, 1986.
86/5		"Report of the Working Group on Aerodynamics of Aircraft Afterbody (Chairman P. Sacher)." AGARD-AR-226, June 1986.
87/1	F. Auleha	"Pseudo Reynolds Number Trends, AIAA Paper 87-2612-CP." Presented at the AIAA 5th Applied Aerodynamics Conference, Monterey, CA, Aug. 17-19, 1987.
87/2	F. T. Lynch C. B. Johnson	"Wind Tunnel Side Wall Boundary-Layer Effects in Transonic Airfoil Testing -- Some Correctable, But Some Not." AGARD FDP Conference on Aerodynamic Data Accuracy and Quality: Requirements and Capabilities in Wind Tunnel Testing, Naples, Italy, September 28-October 1, 1987.
87/3	H. U. Meier U. Michel H. P. Kreplin	"The Influence of Wind Tunnel Turbulence on the Boundary-Layer Transition. Perspectives in Turbulence Studies," dedicated to the 75th birthday of Dr. J. C. Rotta. International Symposium, DFVLR Research Center, Gottingen, May 11-12, 1987.
87/4	K. Hartmann	"Experimental Investigation on an Ogive-Nosed Body at High Incidence and Different Reynolds Numbers." International Conference on Fluid Mechanics, Beijing, China, July 1-4, 1987.
88/1	AGARD WG09	"Boundary Layer Simulation and Control in Wind Tunnels." AGARD-AR-224, April 1988.

83

REPORT DOCUMENTATION PAGE			
1. Recipient's Reference	**2. Originator's Reference**	**3. Further Reference**	**4. Security Classification of Document**
	AGARD-AG-303	ISBN 92-835-0492-5	UNCLASSIFIED

5. Originator Advisory Group for Aerospace Research and Development
North Atlantic Treaty Organization
7 rue Ancelle, 92200 Neuilly sur Seine, France

6. Title REYNOLDS NUMBER EFFECTS IN TRANSONIC FLOW

7. Presented at

8. Author(s)/Editor(s) Various

9. Date December 1988

10. Author's/Editor's Address Various

11. Pages 92

12. Distribution Statement This document is distributed in accordance with AGARD policies and regulations, which are outlined on the Outside Back Covers of all AGARD publications.

13. Keywords/Descriptors

Reynolds number
Transonic flow
Wind tunnels
Airfoils
Fuselages
Missile airframes
Afterbodies

14. Abstract

Reynolds number effects in transonic flow are critically reviewed. This review, which may be considered a supplement to AR 224 'Boundary Layer Simulation and Control in Wind Tunnels', is mainly concerned with a discussion of viscous effects actually observed on realistic configurations.

The following geometries are considered: Airfoils and high aspect ratio wings typical of transport aircraft, fighter-type low aspect ratio delta wings, two- and three-dimensional bodies characteristic of missiles and combat aircraft fuselages, and afterbodies. "Pseudo"-Reynolds number effects are identified which may arise, for instance, due to the influence of the Reynolds number on the wind tunnel environment and in turn affect the flow about a model. As an introduction, a brief retrospect of the "history" of Reynolds number effect is presented.

This AGARDograph has been produced at the request of the Fluid Dynamics Panel of AGARD.

AGARDograph No.303 Advisory Group for Aerospace Research and Development, NATO REYNOLDS NUMBER EFFECTS IN TRANSONIC FLOW Published December 1988 92 pages Reynolds number effects in transonic flow are critically reviewed. This review, which may be considered a supplement to AR 224 'Boundary Layer Simulation and Control in Wind Tunnels', is mainly concerned with a discussion of viscous effects actually observed on realistic configurations. The following geometries are considered: Airfoils and high P.T.O.	AGARD-AG-303 Reynolds number Transonic flow Wind tunnels Airfoils Fuselages Missile airframes Afterbodies	AGARDograph No.303 Advisory Group for Aerospace Research and Development, NATO REYNOLDS NUMBER EFFECTS IN TRANSONIC FLOW Published December 1988 92 pages Reynolds number effects in transonic flow are critically reviewed. This review, which may be considered a supplement to AR 224 'Boundary Layer Simulation and Control in Wind Tunnels', is mainly concerned with a discussion of viscous effects actually observed on realistic configurations. The following geometries are considered: Airfoils and high P.T.O.	AGARD-AG-303 Reynolds number Transonic flow Wind tunnels Airfoils Fuselages Missile airframes Afterbodies
AGARDograph No.303 Advisory Group for Aerospace Research and Development, NATO REYNOLDS NUMBER EFFECTS IN TRANSONIC FLOW Published December 1988 92 pages Reynolds number effects in transonic flow are critically reviewed. This review, which may be considered a supplement to AR 224 'Boundary Layer Simulation and Control in Wind Tunnels', is mainly concerned with a discussion of viscous effects actually observed on realistic configurations. The following geometries are considered: Airfoils and high P.T.O.	AGARD-AG-303 Reynolds number Transonic flow Wind tunnels Airfoils Fuselages Missile airframes Afterbodies	AGARDograph No.303 Advisory Group for Aerospace Research and Development, NATO REYNOLDS NUMBER EFFECTS IN TRANSONIC FLOW Published December 1988 92 pages Reynolds number effects in transonic flow are critically reviewed. This review, which may be considered a supplement to AR 224 'Boundary Layer Simulation and Control in Wind Tunnels', is mainly concerned with a discussion of viscous effects actually observed on realistic configurations. The following geometries are considered: Airfoils and high P.T.O.	AGARD-AG-303 Reynolds number Transonic flow Wind tunnels Airfoils Fuselages Missile airframes Afterbodies

aspect ratio wings typical of transport aircraft, fighter-type low aspect ratio delta wings, two- and three-dimensional bodies characteristic of missiles and combat aircraft fuselages, and afterbodies. "Pseudo"-Reynolds number effects are identified which may arise, for instance due to the influence of the Reynolds number on the wind tunnel environment and in turn affect the flow about a model. As an introduction, a brief retrospect of the "history" of Reynolds number effect is presented.

This AGARDograph has been produced at the request of the Fluid Dynamics Panel of AGARD.

ISBN 92-835-0492-5

aspect ratio wings typical of transport aircraft, fighter-type low aspect ratio delta wings, two- and three-dimensional bodies characteristic of missiles and combat aircraft fuselages, and afterbodies. "Pseudo"-Reynolds number effects are identified which may arise, for instance due to the influence of the Reynolds number on the wind tunnel environment and in turn affect the flow about a model. As an introduction, a brief retrospect of the "history" of Reynolds number effect is presented.

This AGARDograph has been produced at the request of the Fluid Dynamics Panel of AGARD.

ISBN 92-835-0492-5

aspect ratio wings typical of transport aircraft, fighter-type low aspect ratio delta wings, two- and three-dimensional bodies characteristic of missiles and combat aircraft fuselages, and afterbodies. "Pseudo"-Reynolds number effects are identified which may arise, for instance due to the influence of the Reynolds number on the wind tunnel environment and in turn affect the flow about a model. As an introduction, a brief retrospect of the "history" of Reynolds number effect is presented.

This AGARDograph has been produced at the request of the Fluid Dynamics Panel of AGARD.

ISBN 92-835-0492-5

aspect ratio wings typical of transport aircraft, fighter-type low aspect ratio delta wings, two- and three-dimensional bodies characteristic of missiles and combat aircraft fuselages, and afterbodies. "Pseudo"-Reynolds number effects are identified which may arise, for instance due to the influence of the Reynolds number on the wind tunnel environment and in turn affect the flow about a model. As an introduction, a brief retrospect of the "history" of Reynolds number effect is presented.

This AGARDograph has been produced at the request of the Fluid Dynamics Panel of AGARD.

ISBN 92-835-0492-5